STUDIES ON SOLID-LIQUID SEPARATION OF O/W EMULSION

CAO Daqi

NAGOYA UNIVERSITY

Doctoral Dissertation in Chemical Engineering
Department of Chemical Engineering

July, 2014

Contents

Preface

In today's world, science and technology have been progressing with each passing day. Advanced solid-liquid separation technologies have become indispensable in many fields such as environmental protection and new-product development. Physical solid-liquid separation is one of the most significant methods because no chemical additives are needed to avoid secondary pollution. Particularly, the separation of deformable and/or multicomponent materials has become significant. The current research involves the solid-liquid separation of oil-in-water (O/W) emulsion. This dissertation is composed of 5 parts. Chapter 1 gives general introduction about theory and literature review, in which mechanical separation theories, evaluation of filtration characteristics, nonlinear filtration behaviours, separation of O/W emulsion and separation of binary suspensions were introduced.

In Chapter 2, downward and upward membrane filtration experiments under constant pressure conditions were conducted for O/W emulsion using a dead-end filter and their filtration behaviors were compared. In downward filtration, the Ruth plot, in which the reciprocal filtration rate was plotted against the filtrate volume per unit membrane area, was obtained as an upward convex curve, while it showed a linear relationship in upward filtration in accordance with the Ruth filtration rate equation. In view of the difference in the filtration behaviors of both filtration methods and the density contrast between the oil droplet and continuous phase, it was anticipated that the filter cake exfoliation occurred in downward filtration. The infinite average specific cake resistance was calculated from the experimental results of flux decline behaviors, assuming that the solid mass of filter cake is increased in direct proportion to the filtrate volume. The specific resistance in downward filtration became smaller with the progress of filtration due to the exfoliation of filter cake. In contrast, the specific

resistance in upward filtration was maintained virtually constant and considerably larger than that in downward filtration. The value obtained in upward filtration was considered to be the true value that was uninfluenced by the exfoliation of filter cake. It was therefore concluded that the upward dead-end filtration test is quite effective for the evaluation of filtration properties in membrane filtration of O/W emulsion.

In Chapter 3, upward dead-end filtration tests accompanied with a sudden reduction in the cake surface area during the course of filtration were proposed in order to determine the properties of the filter cake formed during microfiltration of O/W emulsion. Both upward and downward dead-end filtration tests were conducted under constant pressure conditions by using a filter having a sudden reduction in its filtration area, and the filtration characteristics between the two were compared. Consequently, it was found that the filtration rate in downward filtration was much higher than that in upward filtration as a result of cake exfoliation which occurred in downward filtration, leading to lower specific cake resistance. Moreover, when the average cake porosity was evaluated on the basis of an overall mass balance of dead-end filtration on the assumption that the cake was not exfoliated, the cake porosity in downward filtration became much lower than that in upward filtration for a similar reason. It was revealed that the correct values of cake properties were obtained from the data of upward dead-end filtration in which the exfoliation of the cake did not occur. It was necessary to consider the influence of the cake porosity in the calculation of the average specific cake resistance when an O/W emulsion was not dilute. On the basis of upward dead-end filtration tests, the power law relationship was applicable in order to represent the effects of the applied pressure on both the average volume fraction of oil droplets and the average specific resistance of the cake comprised of oil droplets. It was found that the cake formed during filtration of O/W emulsion was highly compressible due to the deformability of oil droplets. Moreover, the average volume fraction of oil droplets and

the average specific cake resistance were kept constant throughout the course of filtration.

In chapter 4, the centrifugal separation characteristics of emulsion-slurry which contained both oil droplets and colloidal SiO_2 particles were investigated using the microprocessor controlled analytical photocentrifuge, LUMiFuge, in this study. It was clarified that oil droplets and SiO_2 particles in emulsion-slurry were separated completely after centrifugation, due to flotation of oil droplets and sedimentation of SiO_2 particles resulting from the density difference. The flotation velocity of oil droplets and the settling velocity of SiO_2 particles through emulsion-slurry became larger than those of the single dispersions (O/W emulsion and SiO_2 suspension) with the corresponding volume fraction. The acceleration effects of flotation and sedimentation through emulsion-slurry were examined by using the flotation and sedimentation coefficients in which the effect of centrifugal acceleration on the flotation and sedimentation velocities was cancelled. Both the flotation and sedimentation coefficients increased with increasing volume fraction of SiO_2 particles or oil droplets in emulsion-slurry, and the acceleration effect of the flotation coefficient was noteworthy due to the marked increase in the density difference between oil droplets and emulsion-slurry with increasing volume fraction of SiO_2 particles. The flotation and sedimentation coefficients through emulsion-slurry were experimentally described by using two types of void functions and well described the acceleration effect in centrifugal separation of emulsion-slurry.

Finally, Chapter 5 gives the summary of the main results obtained from the studies.

Chapter 1 Theory and Literature Review

1.1 Introduction

Solid-Liquid separation is a major unit operation that exists in almost every flowscheme related to the chemical process industries, ore beneficiation, pharmaceutics, food or water and waste treatment. Advanced solid-liquid separation technologies have become indispensable in many fields such as environmental protection and new-product development. Particularly, the physical solid-liquid separation method is one of the most significant methods because no chemical additives are needed to avoid secondary pollution. There have been attracted widely, for example, membrane separation (Shannon *et al.*, 2008; Ho and Li, 2013), centrifugal sedimentation (Rickwood, D., 1984, Iritani *et al.*, 2007b), consolidation (Iritani *et al.*, 2010b), freeze concentration (Iritani *et al*., 2013) and so on.

Oil-in-water (O/W) emulsions are widely produced in various industrial applications including petrochemical, metallurgical, transportation, cosmetics, domestic sewage, textile, etc.. Therefore, the separations of O/W emulsions have been an area of considerable interest over the past years. **Figure 1-1** shows the publication trend on the separation of O/W emulsion obtained by the Web of Science using the following search words: “oil”, “water”, “emulsion”, and “separation” in the period 1994-2013. From the figure, it may be understood that studies on the separation of O/W emulsion have increasingly been focused over the past two decades.

The mechanical solid-liquid separation, which is commonly used to describe the separation of solid particles and liquid and the same term is employed from the viewpoint of oil droplets as soft colloid particles in this study, may be an efficient method of treatment for O/W emulsion due to various advantages such as the elimination of chemical, lower capital cost, higher separation factors and so on. The first

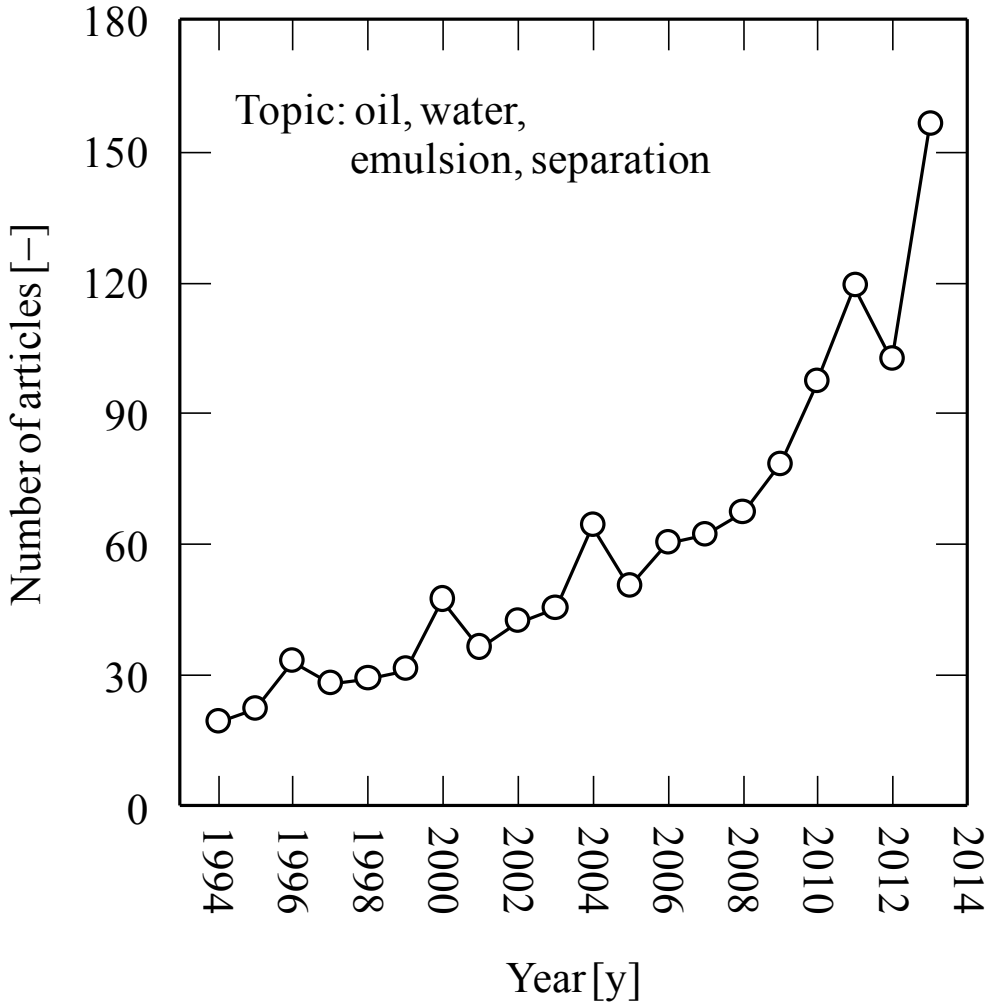

Fig. 1-1 Publication trend on the separation of O/W emulsion

of this chapter outlines the mechanical separation theories covering cake filtration and sedimentation, which are the main research methods in this study. And then evaluation of filtration characteristics and various nonlinear filtration behaviours which often occur in filtration are discussed. In addition, various separation methods for O/W emulsion and separation of binary suspensions often encountered in practical cases are also summarized through investigating some typical literatures.

1.2 Mechanical Separation Theories

1.2.1 Cake Filtration

Ruth's cake filtration theory (Ruth, 1935, 1946) can be still applied to most of the filter materials at present. The relationship between the reciprocal filtration rate ($\mathrm{d}\theta/\mathrm{d}v$) and the cumulative filtrate volume v collected per unit effective membrane area, where θ is the filtration time, is expressed as

$$\frac{\mathrm{d}\theta}{\mathrm{d}v} = \frac{2}{K_\mathrm{v}}\left(v + v_\mathrm{m}\right) \tag{1-1}$$

where v_m is the fictitious filtrate volume per unit membrane area, equivalent to the flow resistance of the membrane, and K_v is the Ruth filtration coefficient, which is defined by

$$K_\mathrm{v} = \frac{2p\left(1 - ms\right)}{\mu\rho s\alpha_\mathrm{av}} \tag{1-2}$$

where p is the applied filtration pressure, s is the mass fraction of solid in dispersions, μ is the viscosity of the filtrate, ρ is the density of the filtrate, and α_av is the average specific cake resistance and m is the ratio of mass of wet cake to mass of dry cake which is related to the average porosity ε_av of filter cake by

$$m = 1 + \frac{\rho\varepsilon_\mathrm{av}}{\rho_\mathrm{s}\left(1 - \varepsilon_\mathrm{av}\right)} \tag{1-3}$$

where ρ_s is the density of solid in dispersions.

Generally, for compressible materials the relationship between the average specific cake resistance and the applied filtration pressure accords with the power law

relationship given by (Sperry, 1921)

$$\alpha_{av} = \alpha_1 p^n \tag{1-4}$$

where α_1 and n are empirical constants, and n is specifically called the compressibility coefficient. Also, the average volume fraction ($1 - \varepsilon_{av}$) is logarithmically plotted as a function of the applied filtration pressure p in the following form (Tiller and Cooper, 1962):

$$1 - \varepsilon_{av} = Bp^{\beta} \tag{1-5}$$

where B and β are the empirical constants.

1.2.2 Sedimentation

At Reynolds numbers, $du\rho/\mu < 0.6$, a solid sphere in an infinite expanse of fluid falls at a uniform velocity given by the Stokes law (Robinson, 1926; Steinour, 1944):

$$u_0 = \frac{(\rho_s - \rho)ad^2}{18\mu} \tag{1-6}$$

where, a is the gravitational acceleration, g under the action of gravity or the centrifugal acceleration, $r\Omega^2$ under the action of centrifugal force where r is radial distance from center of rotation, Ω is angular velocity of rotor, and d is the diameter of suspended sphere. Within the given range of Reynolds numbers, the flow around a sphere is laminar, or streamline, and inertial effects are negligible.

It is well known that settling velocity of a single solid particle in fluid is most often higher than the settling velocity of a suspension consisted of many such particles. In other words, settling velocity, u is influenced by both direct and indirect (*i. e.* hydrodynamic) interactions between the particles. In general, the settling velocity of particles in a suspension is expressed by the following formula:

$$u = u_0 F(\varepsilon) \tag{1-7}$$

where ε is porosity, F is void function which is often given by the following forms.

Kozeny-Carman equation (Carman, 1937):

$$F(\varepsilon) = \frac{\varepsilon^3}{10(1-\varepsilon)} \tag{1-8}$$

Steinour equation (Steinour, 1944):

$$F(\varepsilon) = \varepsilon^2 10^{-1.82(1-\varepsilon)} \tag{1-9}$$

Happel equation (Happel, 1958):

$$F(\varepsilon) = \frac{6 - 9(1-\varepsilon)^{1/3} + 9(1-\varepsilon)^{5/3} - 6(1-\varepsilon)^2}{6 + 4(1-\varepsilon)^{5/3}} \tag{1-10}$$

Richardson-Zaki equation (Richardson and Zaki, 1954):

$$F(\varepsilon) = \varepsilon^N \tag{1-11}$$

Eq. (1-11) is one of the most popular expressions due to its simple form, where the exponent N varies with the particles Reynolds number; for low Reynolds number, it is usually between 4.65 and 6.55 (Heitkam *et al.*, 2013).

1.3 Evaluation of Filtration Characteristics

The essential parameters of solid-liquid filtration separation such as filtration resistance and porosity of cake must be obtained in order to evaluate the filtration characteristics of each material. The accurate determination of characteristics of solid-liquid separation based on simple and precise laboratory tests has been a key factor in the design of new equipment and the analysis of commercial separation operations. In the chapter 1.2.1, the most basic filtration test, namely, Ruth filtration test has been introduced. Other several filtration tests which have so far been utilized, are summarized in the following contents.

1) Constant pressure filtration based sudden reduction in filtration area

In general, the average specific cake resistance α_{av} is calculated by using both the

constant pressure filtration coefficient K_v determined from the slope of the Ruth plots and the *m*-value. The value of *m* has almost invariably been determined by weighing the filter cake before and after the cake dryness. However, visual determination of the end of filtration often leads to erroneous values for *m* and also α_{av} because of the indistinct interface between the cake surface and the slurry.

A method, which utilized the sudden reduction in filtration area of the cake surface, has been developed for evaluating rigorously the properties of the filter cake such as the average porosity ε_{av} and the average specific cake resistance α_{av} (Murase, *et al.*, 1987). The specially designed apparatus is schematically shown in **Figure 1-2**. A close-fitting cylinder with an inner diameter *D* and a height *h* is inserted in the cylindrical brass filter. A disk with a hole having a diameter D_h is placed on top of the inserted cylinder and the part below this constitutes the filter chamber.

Filter cake steadily builds up on the filter medium as soon as the filtration process starts. The surface area of the growing filter cake equals *D* exactly, as shown in **Figure 1-2(a)**. Once the filter cake builds up to the underside of the disk, the subsequent filter cake can form only inside the hole in the disk, as shown in **Figure 1-2(b)**. Consequently, the filtration area of the cake surface is reduced suddenly, and the filtration rate decreases markedly. After the filtrate volume *v* is beyond the critical volume v_t at the transition point, the reciprocal filtration rate $d\theta/dv$ vs. *v* deviates remarkably from the relation represented by Eq. (1-1). From the value of v_t, the average porosity ε_{av} of the filter cake can be calculated using an overall mass balance of dead-end filtration, to give (Murase, *et al.*, 1987; Iritani, *et al.*, 1991a)

$$\varepsilon_{av} = \frac{\rho_s h(1-s) - \rho s v_t}{\rho_s h(1-s) + \rho s h} \tag{1-12}$$

Thus, the average specific cake resistance α_{av} can be evaluated accurately from Eqs. (1-2), (1-3) and (1-12) by using the slope of the plot of $d\theta/dv$ against *v* and the value of v_t.

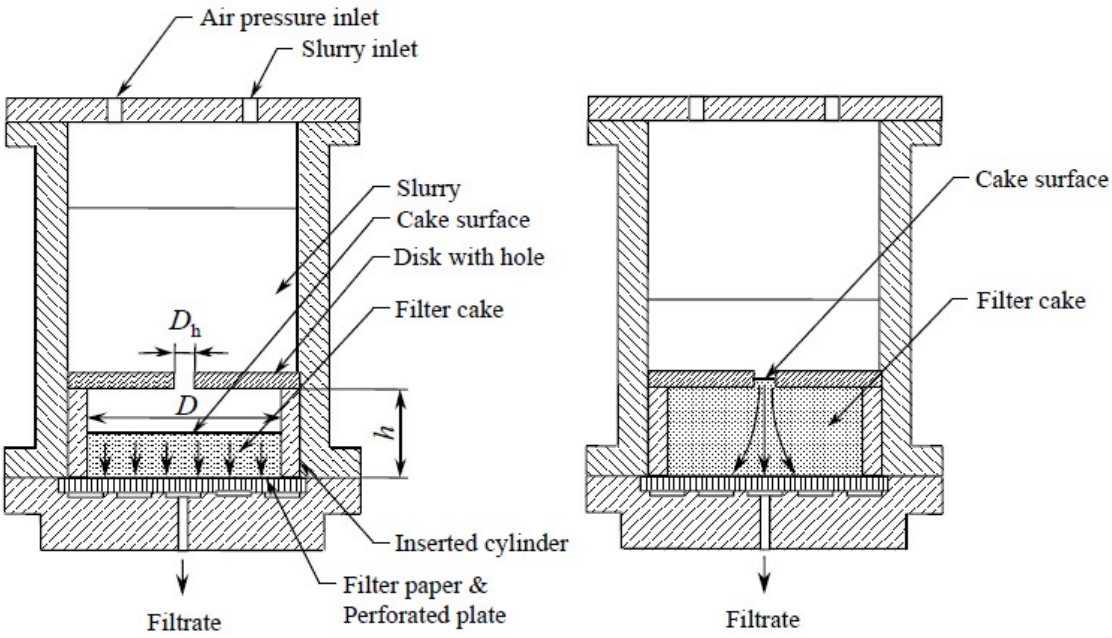

(a) Constant filtration area

(b) Sudden reduction in filtration area

Fig. 1-2 Principle of sudden reduction in filtration area

2) Constant rate filtration

Through constant pressure filtration, the constant pressure filtration coefficient or average specific cake resistance can be obtained only for a certain pressure in each filtration experiment. However, the information of the varieties of filtration characteristics can be obtained with the changes of the filtration pressure in constant rate filtration in which filtration rate remains constant. The pressure vs. time relations can be presented as an equation for conditions of constant cake resistance of the form (Tiller, 1955; Shirato, *et al.*, 1968)

$$p - p_{\mathrm{m}} = \frac{\mu \alpha_{\mathrm{av}} \rho s q_1^2}{1 - ms} \theta \tag{1-13}$$

When the specific resistance is assumed to be a power function of the pressure drop ($p - p_{\mathrm{m}}$) across the cake as shown in Eq. (1-4), Eq. (1-13) becomes

$$(p - p_{\mathrm{m}})^{1-n} = \frac{\mu \alpha_1 \rho s q_1^2}{1 - ms} \theta \tag{1-14}$$

Therefore, the relationship of ($p - p_{\mathrm{m}}$) vs. θ will represent a linear in the double logarithm coordinate when the variation of ($1 - ms$) is negligible due to the small concentration s of slurry and the values of the compressibility coefficient n and α_1 can be determined according to the graphic method. In addition, the values of α_{av} in various pressure drops ($p - p_{\mathrm{m}}$) can be also obtained immediately using Eq. (1-13) according to the plots of ($p - p_{\mathrm{m}}$) vs. θ when the dependence of m on filtration pressure is known or in the case that ($1 - ms$) = 1. It is notable that the pressure drops p_{m} of filter medium is constant in constant rate filtration and can be calculated using the following formula:

$$p_{\mathrm{m}} = \mu q_1 R_{\mathrm{m}} \tag{1-15}$$

where R_{m} is resistance of filter medium.

3) Variable-pressure-variable-rate filtration

In variable-pressure-variable-rate filtration, the filtration rate ($\mathrm{d}v/\mathrm{d}\theta$) and the

pressure drop ($p - p_m$) of filter cake changes continually with the process of filtration. Generally, the value of ($dv/d\theta$) decreases and the value of ($p - p_m$) increases with filtration time θ. In this case, filtration equation is represented as (Tiller, 1958; Shirato, *et al.*, 1969)

$$\frac{\mu\alpha_{av}\rho s}{1-ms}v = (p - p_m)\left(\frac{d\theta}{dv}\right) \tag{1-16}$$

Therefore, α_{av} can be calculated according to the known value of m by using the measured filtration rate ($dv/d\theta$) and pressure drop ($p - p_m$) of cake filter for arbitrary value of v, and then the relationship between α_{av} and ($p - p_m$) can be obtained. Besides, the pressure drop ($p - p_m$) of filter cake is different from that in constant rate filtration and can be calculated from the following form

$$p_m = \mu\left(\frac{dv}{d\theta}\right)R_m \tag{1-17}$$

4) Step-up pressure filtration

In step-up pressure filtration, filtration pressure p is increased in stages in the course of filtration. When the appropriate values of the step-up pressure are selected, the pressure dependence of α_{av} in the wide pressure range can be evaluated using the data of ($d\theta/dv$) vs. v in each pressure, as well as constant pressure filtration under various constant pressures (Murase, *et al.*, 1989).

5) Capillary suction method

The Capillary Suction Time apparatus (CST) was proposed originally by Baskerville and Gale (Baskerville and Gale, 1968). A sample is placed in a small reservoir whose open base rests on a disc of filter paper. Moisture is removed from the sample by capillary suction in the paper. The time taken for the moisture front to cover a given distance is a measure of filterability and can be observed or measured electrically by an automated apparatus. However, it is suitable only for high resistance sludges or slurries where capillary suction time often correlates well with specific cake resistance

α_{av} (Tarleton and Wakeman, 2008).

6) Single constant pressure filtration

When constant pressure filtration is conducted with considerably large values of filter medium resistance, the pressure drop ($p - p_m$) across the cake gradually increases from 0 at the start of filtration and tend to approach the limiting value p. Consequently, variable-pressure-variable-rate filtration can be virtually realized by applying a constant filtration pressure. As a result, the pressure dependence of permeability characteristics such as the average specific cake resistance α_{av} is easily available without monitoring the variation of the pressure drop across the cake with time. When the concentration s of samples is sufficiently small, the average specific cake resistance α_{av} and the pressure drop ($p - p_m$) across the cake can be calculated for arbitrary plot of ($d\theta/dv$) vs. v using the following formulas.

$$\frac{d\theta}{dv} = \frac{\mu \alpha_{av} \rho s}{p} v + \left(\frac{d\theta}{dv}\right)_m \tag{1-18}$$

$$p - p_m = p \left\{ \left(\frac{dv}{d\theta}\right) - \left(\frac{dv}{d\theta}\right)_m \right\} \Big/ \left(\frac{dv}{d\theta}\right) \tag{1-19}$$

The variation in the specific cake resistance during the initial period of filtration conducted with considerably large values of the filter medium resistance causes a marked deviation from straight-line plots of ($d\theta/dv$) vs. v. Accordingly, by carrying out a single constant pressure filtration experiment, one may obtain α_{av} vs. ($p - p_m$) data over a wide range of pressures by using Eqs. (1-18) and (1-19) (Iritani *et al.*, 2011, 2012a).

1.4 Nonlinear Filtration Behaviours

Conventional filtration theory (Ruth cake filtration theory) demonstrates that the Ruth plots depicted as the reciprocal filtration rate ($d\theta/dv$) vs. the cumulative filtrate volume v collected per unit effective membrane area, should show a linear relationship as shown in **Figure. 1-3(a)** (Terleton and Wakeman, 2007; Tanaka *et al.*, 2011). This is not

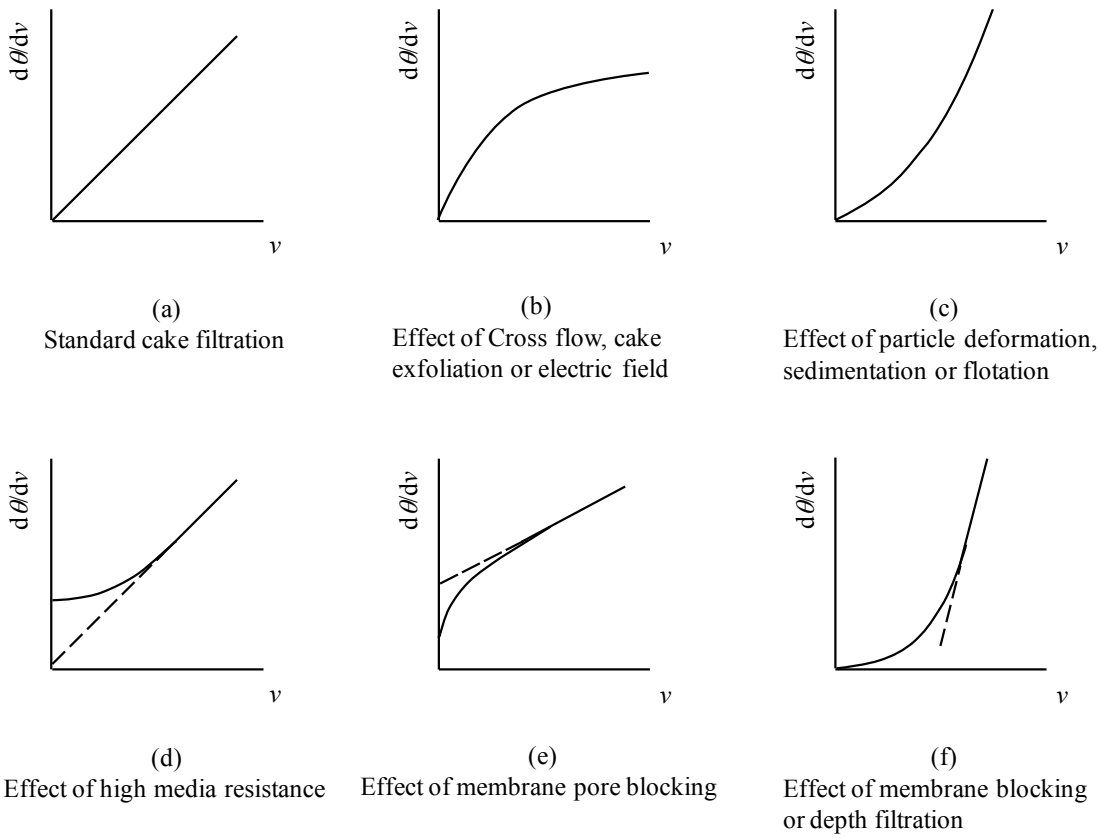

Fig. 1-3 Schematic diagram of various filtration modes

always observed, however, for the possible cases illustrated in **Figure. 1-3(b-f)**.

Figure 1-3(b) shows an upward convex curve, namely, the variation of flux decline decreases with progress of filtration. This phenomenon is because cake formation is prevented due to an external force. For example, in crossflow filtration which keeps the motion of a fluid parallel to the filter medium, the cake formed on the filter medium is swept continually by the shear stress acting on the surface of the filter medium (Lu and Ju, 1989; Iritani *et al.*, 1991b; Field *et al.*, 1995; Tien and Ramarao, 2013). In electro-ultrafiltration, the accumulation of particles/solutes on the membrane surface is limited by electrophoretic migration and therefore the filtration rate is significantly increased (Iritani *et al.*, 1992b, 2000). Furthermore, in inclined filtration the filter cake growing in the course of filtration slips down due to the gravity acting on cake and therefore the filtration resistance is decreased (Iritani *et al.*, 1991c, 2002b, 2012b; Zeng *et al.*, 1998).

Figure 1-3(c) shows a downward convex curve, namely, the variation of flux decline increases with progress of filtration. For example, in conventional downward filtration concomitant with sedimentation for suspensions in which the density ρ_s of particles is larger than that of water, the experimental cake resistances will be larger than the theoretical values due to the effect of particles settling (Sambuichi *et al*., 1982; Christensen and Dick, 1985; Tiller *et al.*, 1995; Iritani *et al*., 1999) and the same results can be speculated for O/W emulsions in which the density ρ_o of oil droplets is smaller than that of water due to the effect of oil droplets floating. On the other hand, in filtration of the soft materials such filtration behavior may occur due to the effect of particle deformation (Lu *et al*., 2001; Christensen *et al*., 2011).

Figure 1-3(d) shows a downward convex curve, which has an intercept when filtration just starts because of the high filter medium resistance (Vorobiev, 2006; Iritani *et al.,* 2011, 2012a, 2014a). In this case, the pressure drop across the cake gradually

increases from 0 at the initial stage of filtration and tends to approach the applied filtration pressure. Consequently, filtration rate is smaller than that obtained using a medium having negligibly small resistance and the slope of the straight line in the latter part of the plots is in remarkable agreement with that of the straight line obtained with a medium having negligibly small resistance.

Figure 1-3(e) shows an upward convex curve, which represents a complex filtration process where the pore blocking in which particles are rejected completely and the cake formation occurred simultaneously (Matsumoto *et al.*, 1992; Iritani *et al.*, 2005). The clogged membrane resistance by sealing the membrane pores is very large at the initial stage of filtration and increases gradually until constant value is reached as filtration progresses, and therefore Ruth plots have a intercept at $v = 0$ and the slope of the latter linear becomes constant as standard cake filtration.

Figure 1-3(f) shows a downward convex curve, where the flux decline behavior can be evaluated by considering the transition from depth to cake filtration (Grace, 1956; Iritani *et al.*, 2007c, 2010a, 2014b). The particles are captured inside a porous filter medium at the initial stage of filtration and eventually the membrane pore blocking finishes, thereby cake filtration starts in consideration of the constant slope of the latter linear as shown in Figure 1-3(f).

1.5 Separation of O/W Emulsion

The separation of difficult filterability materials having high compressibility and/ or great specific surface area, such as deformable particles, nano-particles and biological substances have become a hotspot in solid-liquid filtration separation field, as industrial products become more fine and environmental protection becomes more stringent. O/W emulsion as the research object is a difficult filterability material due to deformability of oil droplets. The following content will describe the various separation methods of O/W emulsion, mainly focusing on the related methods to this study.

Separation processes related to membranes have been extensively studied (Ho and Li, 2013). Correspondingly, membrane filtration for separation of O/W emulsion as the major research method in this study has also attracted considerable attention. Through consulting literatures, the surveys about membrane filtration of O/W emulsion are mainly summarised in **Table 1-1**. In addition, several techniques have also been proposed except membrane filtration, as shown in **Table 1-2**.

Tab. 1-1 Representative surveys about membrane filtration of O/W emulsion in recent years

Research subjects	Research literatures
cake properties	Matsumoto *et al.*, 1999; Iritani *et al*., 2003, 2008a; Headen *et al.*, 2006; Montel *et al.*, 2008; Cao *et al.*, 2012, 2013
modelling of membrane fouling	Koltuniewicz *et al.*, 1995; Mohammadi *et al.*, 2003; Peng and Tremblay, 2008
slotted pore membrane	Ullah *et al.*, 2011; Ullah *et al.*, 2012
membrane surface modification	Mueller et *al.*, 1997; Faibish and Cohen, 2001
dynamic membrane	Zhao *et al.*, 2005; Yang *et al.*, 2011; Pan *et al.*, 2012
ceramic membrane	Matos *et al.*, 2008; Nandi *et al.*, 2010; Chen *et al.*, 2012
operating conditions	Koltuniewicz and Field, 1996; Murase *et al.*, 1996; Hesampour *et al.*, 2008; Li *et al.*, 2009; Falahati and Tremblay, 2011
treatment of industrial waste emulsion	Chakrabarty *et al.*, 2010; Gutiérrez *et al.*, 2011

Tab. 1-2 Representative separation methods except membrane filtration for O/W emulsion in recent years

Separation methods	Research literatures
chemical destabilization	Gray, *et al.*, 1997; Ríos, *et al.*, 1998
dissolved air flotation	Feng and Aldrich, 2000; Al-Shamrani, *et al.*, 2002
flotation	Pal and Masliyah, 1990; Chen *et al.*, 1993; Maruyama, *et al.*, 2012
depletion flocculation	Chanamai and McClements, 2000; Shields, *et al.*, 2001
microwave heating	Binner, *et al.*, 2013
centrifugation	Iritani, *et al.*, 2007a, 2007b; Cao, *et al.*, 2014

1.6 Separation of Binary suspensions

There is scarce study on the effects of physico-chemical interactions on separation of binary suspensions, although the need to separate such suspensions often arises in industry. Many researches have been reported about filtration separation behaviors of binary suspensions in literatures, in which the samples for filtration separation include mainly clay-slurry (Shirato, *et al.*, 1963), glass bead or calcite (Abe, *et al.*, 1979), PMMA (Iritani, *et al.*, 1996), protein (Iritani, *et al.*, 1995a, 1995b), titanium dioxide/silicon dioxide (Iritani, *et al.*, 2002a), PMMA/oil droplets (Iritani, *et al.*, 2008a), fibre/titania (rutile) (Chellappah, *et al.*, 2010), BSA/dextran (Hwang and Sz, 2011), polystyrene latexes (Iritani, *et al.*, 2014b) and so on.

On the other hand, a large number of reports have been revealed that the bidisperse suspensions with two different types of solid particles dispersed uniformly in fluid can be

generally separated through the gravity sedimentation method (Smith, 1965, 1997; Lockett and Al-Habbooby, 1973, 1974; Al-Naafa and Selim, 1992; Hoyos, *et al.*, 1994; Cheung, *et al.*, 1996; Krishnamoorthy, *et al.*, 2007; Dorrell and Hogg, 2010). Particularly, based on the difference of density and size of two types of particles, it has been reported that the settling velocities of both solid phases were significantly enhanced (Whitmore, 1955; Weiland and McPherson, 1979; Fessas and Weiland, 1981, 1984). Furthermore, it has also been reported that the O/W emulsion containing big solid particle can be separated under the action of gravity (Yan and Masliyah, 1993; Beydoun *et al.*, 1998).

Chapter 2 Filtration Properties in Membrane Filtration of O/W Emulsion

2.1 Introduction

For the separation of stable oil-in-water (O/W) emulsions, membrane filtration, e.g., microfiltration, which is a mechanical separation method, has become particularly significant because no chemical additives are needed. A major problem preventing the application of membrane filtration is membrane fouling, and the most predominant factor responsible for membrane fouling is considered to be the formation of filter cake comprised of oil droplets formed on the membrane surface during filtration. In filtration process of O/W emulsion, compared with the generic materials the most remarkable difference is that the oil droplets accumulated on membrane deform extremely due to the compressive pressure applied to the cake and the distorted oil droplets cause the porosity of filter cake decreasing greatly, which increases the filtration resistance and then reflects a low filtration rate.

Therefore, it is essential to accurately obtain the relationship between cake properties and the applied filtration pressure in designing new and operating existing equipment employed in dead-end membrane filtration of O/W emulsions. Consequently, the development of more accurate experimental and analytical methods for evaluating cake properties is worthy of increased research efforts, which is the focus of the present study. On the other hand, in crossflow filtration which has been widely adopted in practical industries, the same cake as that of dead-end filtration forms on the membrane surface until the filtration rate approaches a certain value. Therefore, it is considered that an understanding of filter cake properties in dead-end filtration serves as a basis for clarifying the mechanism of crossflow filtration (Iritani *et al.*, 1991a).

At present, the outstanding issue is that the relationship between the reciprocal filtration rate and the cumulative filtrate volume collected per unit effective membrane area (referred to as Ruth plots) occasionally exhibits anomalous non-linear behaviors (Hoshino *et al.*, 1984; Lipp *et al.*, 1988; Nandi *et al.*, 2009) in downward dead-end filtration of O/W emulsion, although the fundamental filtration characteristics are generally obtained from downward dead-end filtration data collected under constant pressure conditions (Tarleton and Wakeman, 2007; Tanaka *et al.*, 2011).

In this chapter, a more correct method to determine the filtration characteristic values in membrane filtration of O/W emulsion was suggested (Cao *et al.*, 2012). In the process of investigating the causes of non-linear Ruth plot in membrane filtration of O/W emulsion, quite different result compared to the conventional downward filtration, was found in upward dead-end constant pressure filtration test and on the basis of this result the evaluation of filtration properties in membrane filtration of O/W emulsion based on upward dead-end constant pressure filtration was discussed.

2.2 Experimental

2.2.1 Materials and Dispersion Preparation

The oil used as the dispersed phase in O/W emulsion was kerosene (Wako Pure Chemical Industries, Ltd.), having a density ρ_s of 787 kg/m^3. An anionic surfactant, sodium dodecyl sulphate (SDS, Sigma-Aldrich Japan Corp.), having a critical micelle concentration (CMC) of 8×10^{-3} M (0.23 wt%), was employed to stabilize the O/W emulsion. All of the chemicals were used as received. Ultrapure, de-ionized (DI) water was obtained by purifying tap water through ultrapure water systems of both Elix-UV20 and Milli-Q Advantage System for laboratory use (Millipore Corp.).

Prior to emulsification, the surfactant was first dissolved in the ultrapure, DI water, and the aqueous solution of the surfactant was prepared with emulsifier concentration of 2% (w/w dispersed phase). The O/W emulsion was prepared with the weight

concentration of the dispersed oil phase *s* of 0.2, through ultrasound generation using an ultrasonic homogenizer (UP-200S, Dr. Hielscher GmbH) after addition of the oil to the surfactant solution. The intermittent irradiation method was used during ultrasound generation, namely, in which two cycles were conducted for 30 s interval in which one cycle was 5 s for 0.5 s irradiation and 0.5 s pause when amplitude was 100%. The O/W emulsion was degassed under vacuum for 30 min before use. The size distribution of oil droplets was measured by using a laser diffraction particle size analyzer (SALD-2200, Shimadzu Corp.) before each filtration and was consistent basically, as shown in **Figure 2-1** and the mean specific surface area size d_s was 1.88 μm in the O/W emulsion obtained. The O/W emulsion for all experiments was found to be stable and did not separate completely by gravity floatation over the course of several days.

2.2.2 Experimental Apparatus and Technique

A schematic layout of the experimental setup for conventional downward filtration is shown in **Figure 2-2(a)**. An unstirred batch filtration cell was utilized. Dead-end microfiltration experiments were performed under conditions of constant pressure ranging from 49 to 490 kPa controlled by an electronic pressure regulator by applying compressed nitrogen gas after the emulsions were poured into the filter. Hydrophilic mixed cellulose ester microfiltration membranes with a nominal pore size of 0.1 μm, supplied by Advantec Toyo Corp., were used for all microfiltration experiments to ensure almost complete rejection of oil droplets. A fresh membrane was used for each experiment. The filtrate was collected in a reservoir placed on an electronic balance connected to a personal computer to collect and record the mass versus time data. The weights were converted to volumes using density correlations. The filtration rate was obtained by numerical differentiation of the volume versus time data. Filtrate samples were taken for absorbance determination. It was recognized that the mass of oil droplets was negligible in filtrate samples. The experiments were carried out at 25 ^{o}C in a

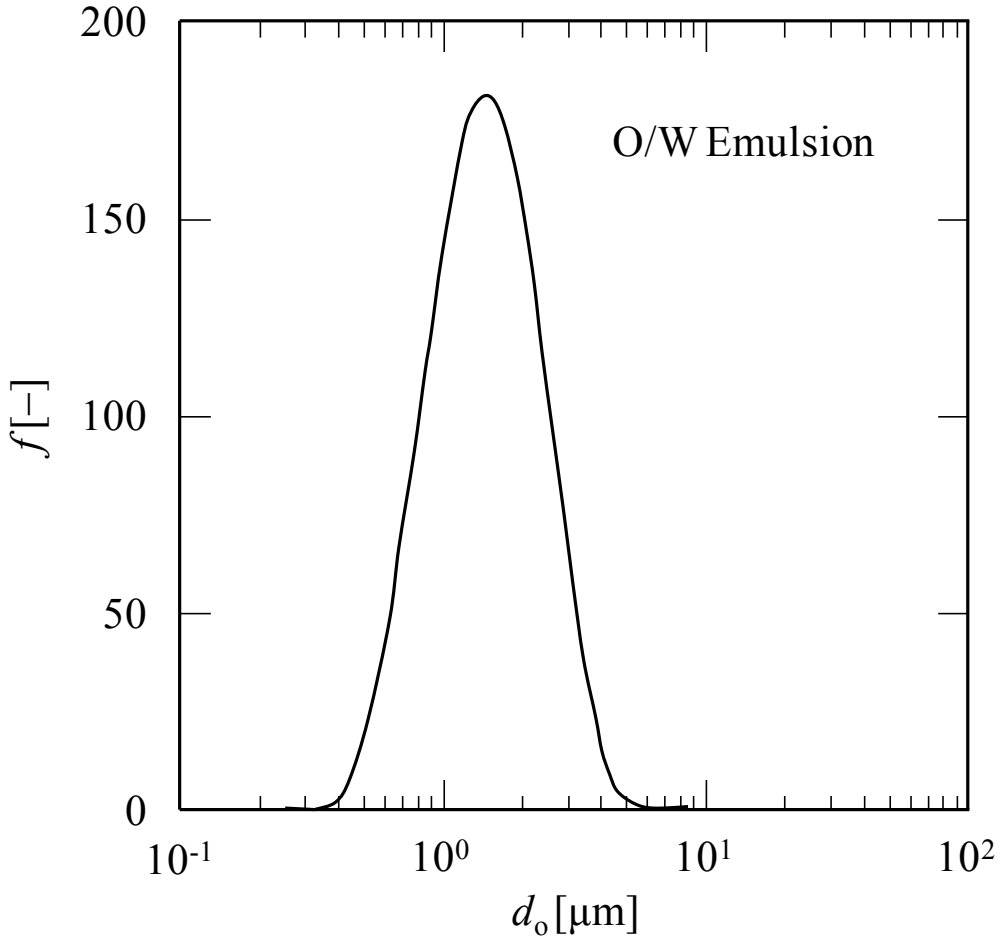

Fig. 2-1 Size distribution of oil droplets in O/W emulsion

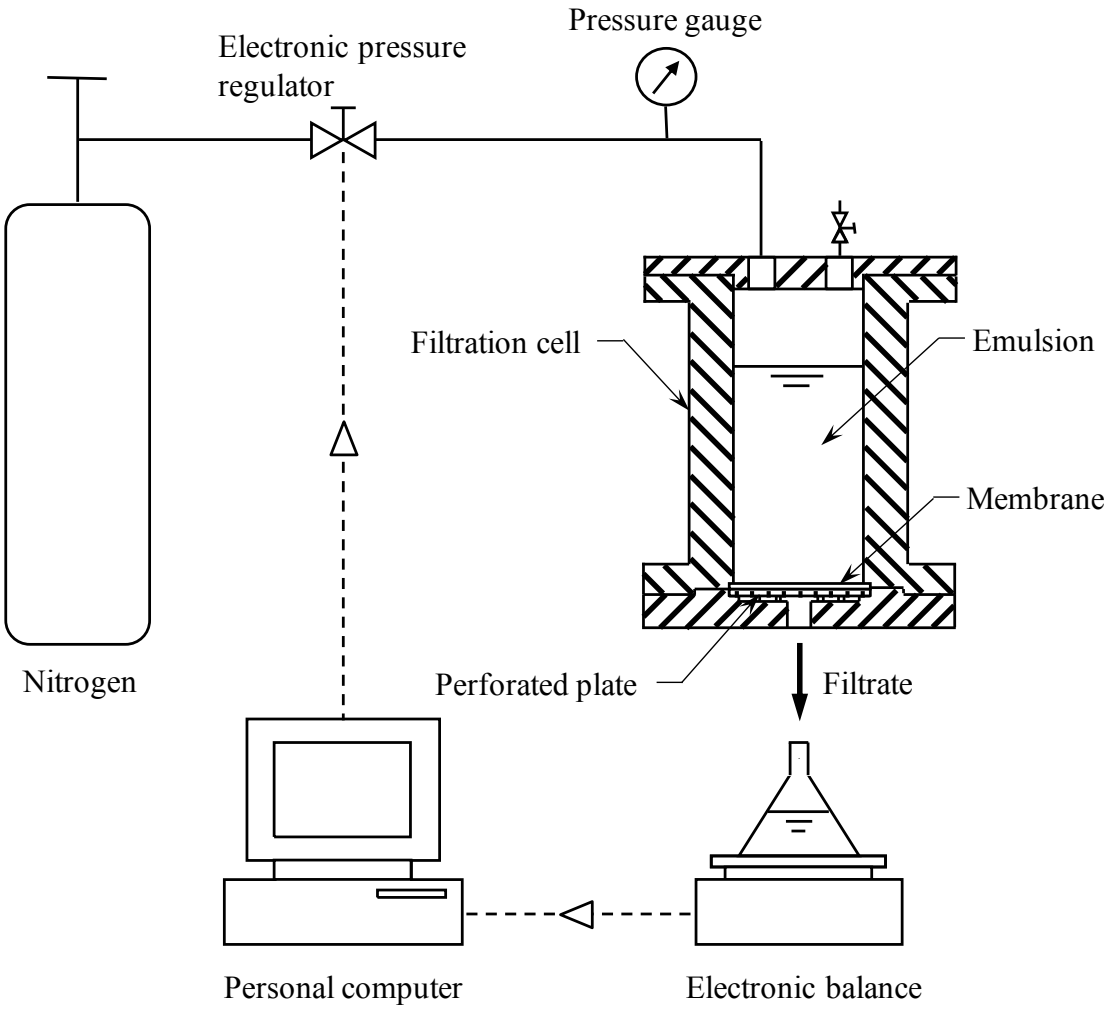

Fig. 2-2 (a) Schematic diagram of downward filtration apparatus

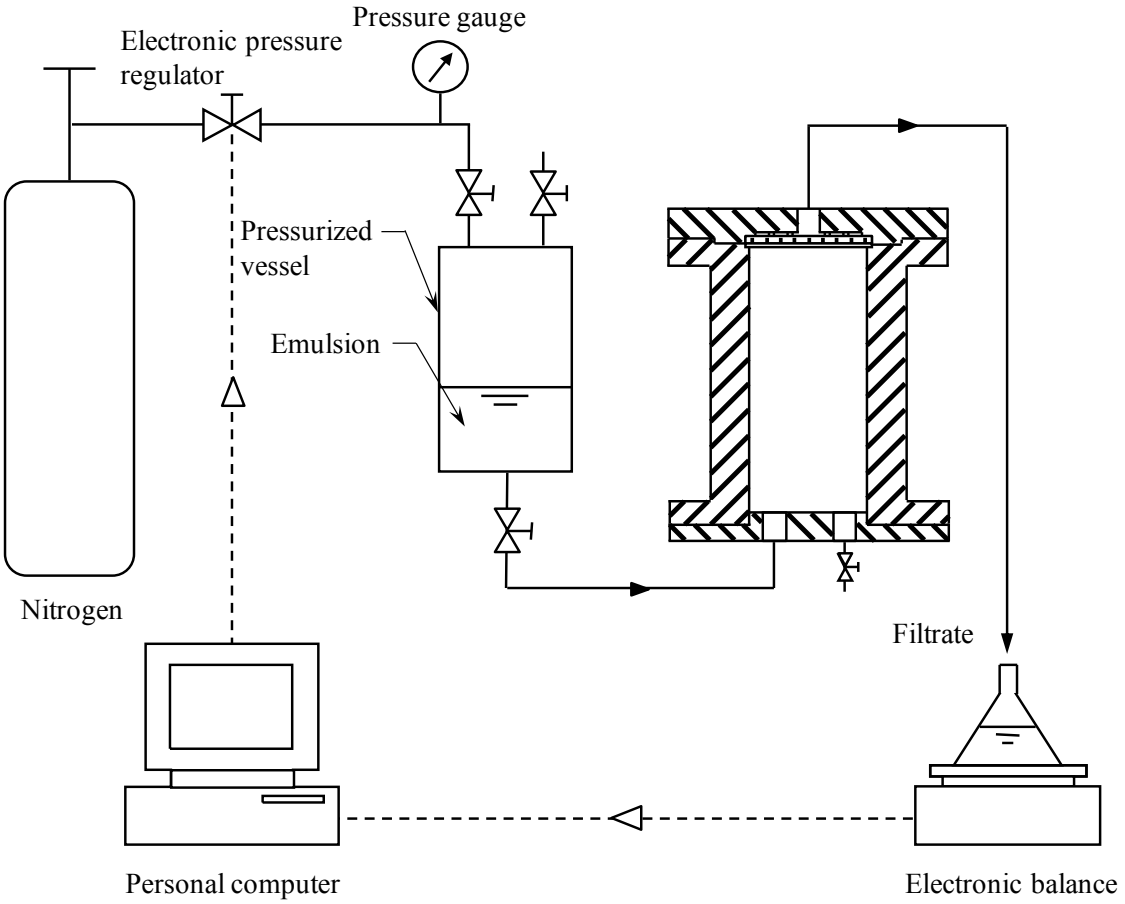

Fig. 2-2 (b) Schematic diagram of upward filtration apparatus

constant temperature room and the practical temperatures also were measured every 1 ~ 2 h through measuring the temperatures of water in a conical flask beside the filter when filtration was processing.

A schematic layout of the experimental setup for novel upward filtration is shown in **Figure 2-2(b)**. In contrast to the above, the filter was connected to a feed reservoir after O/W emulsion was poured into an unstirred batch filtration cell. In addition, the experiments that the filtration mode changes into upward from downward filtration were also conducted to examine that cake exfoliation did not occur in upward filtration.

2.3 Flux Decline Behaviours of Downward and Upward Filtration

In **Figure 2-3**, typical data during long-term operation of upward and downward microfiltration of an O/W emulsion are shown as the reciprocal filtration rate ($\mathrm{d}\theta/\mathrm{d}v$) vs. the cumulative filtrate volume v collected per unit effective membrane area in the case where the filtration area is kept constant throughout filtration, where θ is the filtration time. For upward filtration, the filtration rate declines gradually as filtration proceeds. The Ruth plots depicted as ($\mathrm{d}\theta/\mathrm{d}v$) vs. v show a linear relationship in accordance with the Ruth filtration rate equation given by (Ruth, 1935, 1946)

$$\frac{\mathrm{d}\theta}{\mathrm{d}v} = \frac{2}{K_\mathrm{v}}\left(v + v_\mathrm{m}\right) \tag{1-1}$$

where v_m is the fictitious filtrate volume per unit membrane area, equivalent to the flow resistance of the membrane, and K_v is the Ruth filtration coefficient, which is defined by

$$K_\mathrm{v} = \frac{2p\left(1 - ms\right)}{\mu\rho s\alpha_\mathrm{av}} \tag{1-2}$$

where p is the applied filtration pressure, s is the mass fraction of oil droplets in the O/W emulsion, μ is the viscosity of the filtrate, ρ is the density of the filtrate, and α_av is the average specific resistance of the emulsion cake. The ratio m of mass of wet cake to mass of oil droplets in cake in Eq. (1-2) is related to the average porosity ε_av of the filter cake by

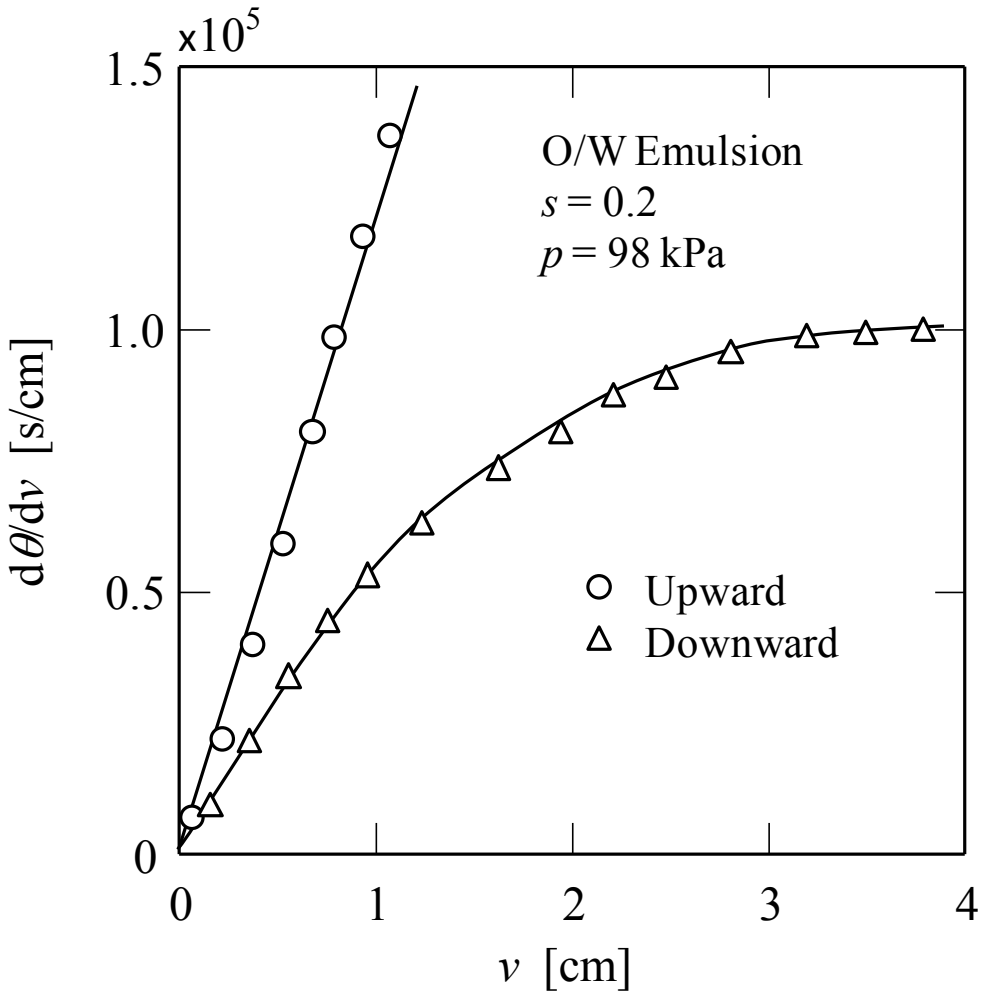

Fig. 2-3 Comparison of flux decline behaviors between upward and downward filtration in case where filtration area is constant

$$m = 1 + \frac{\rho \varepsilon_{av}}{\rho_s (1 - \varepsilon_{av})} \tag{1-3}$$

where ρ_s is the density of oil droplets. Thus, the flux decline can be analyzed on the basis of the dead-end cake filtration model.

In contrast, the Ruth plots for downward filtration show a non-linear relationship, i.e., an upward convex curve, and the filtration rate in downward filtration is much higher than that in upward filtration at an equivalent volume of the filtrate. It is anticipated that filter cake exfoliation occurred in downward filtration of the O/W emulsion due to the density difference between the oil droplet and continuous phase. A possible reason will be briefly explained subsequently.

In constant pressure filtration, the effects of sedimentation of a particle having a density greater than that of continuous phase on the overall filtration performance have been studied in detail by several researchers (Sambuichi *et al.*, 1982; Christensen and Dick, 1985; Tiller *et al.*, 1995; Iritani *et al.*, 1999). The filtration rate in upward filtration becomes much higher than that in downward filtration as the particles settle. On the other hand, Iritani *et al.* (1991c, 1992a, 1995b) found a noteworthy phenomenon of cake exfoliation in the upward filtration progress of a BSA solution, and thus it is recognized that a dynamically balanced rate of filtration was reached where the filtration rate approached a plateau due to cake exfoliation, as the data of the downward filtration shown in Fig. 2-3.

Similarly, the filtration progress of the O/W emulsion was examined. In that case, it is emphasized that the density of the dispersed phase, oil droplet, is less than that of the continuous phase. Two possible patterns of flux decline behaviors in the filtration of an O/W emulsion are illustrated in **Figure 2-4**. Figure 2-4(a) represents a significant flotation impact. In upward filtration, the decrease in the filtration rate becomes notable with the increase in the filtrate volume v, and the Ruth plots exhibit a downward convex curve because the filtration resistance markedly increases due to accelerating the increase

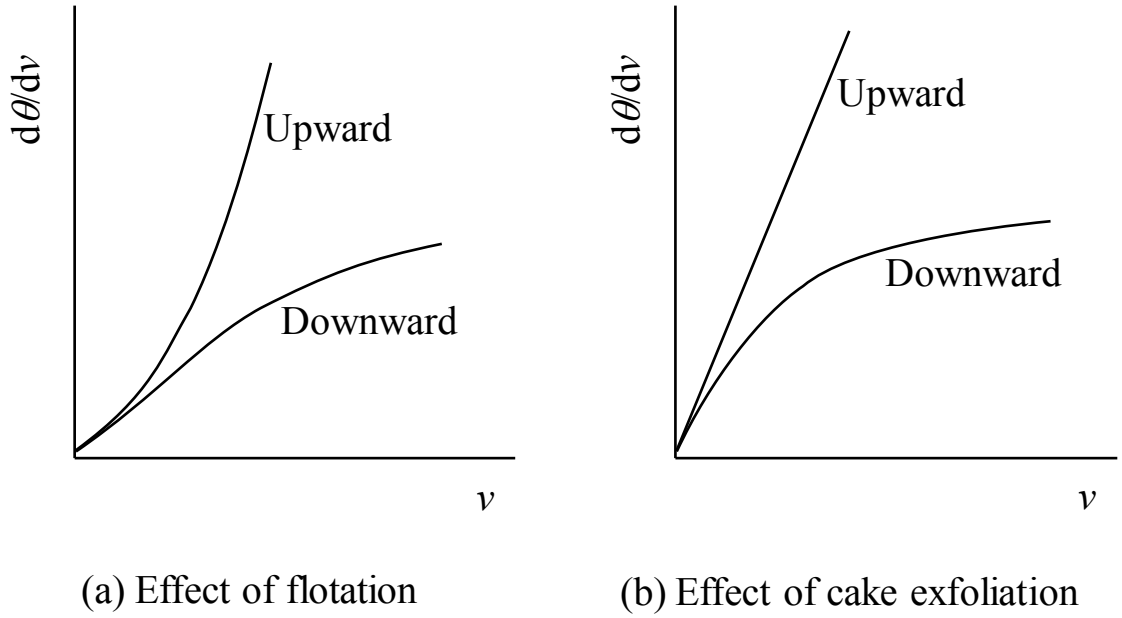

(a) Effect of flotation (b) Effect of cake exfoliation

Fig. 2-4 Two patterns of flux decline behaviors in filtration of O/W emulsion

in the thickness of the cake layer as a result of oil droplets flotation. However, in downward filtration, the decrease in the filtration rate in reverse becomes gradually slow with increasing filtrate volume v since the amount of oil droplets in the emulsion cake is suppressed under the influence of oil droplets flotation, and thus the Ruth plots show an upward convex curve.

Figure 2-4(b) represents hypothetically a case where cake exfoliation takes place for the O/W emulsion with due consideration of the density of a dispersed phase smaller than that of the continuous phase. In upward filtration, the Ruth plots show a linear relationship in accordance with Eq. (1-1), but an upward convex curve is displayed in downward filtration. This is probably because cake formation is limited by the buoyant force acting on oil droplets in the cake surface layer, and thus the surface layer of the cake overlying the membrane exfoliates continuously (Hoshino *et al.*, 1984). It should be stressed, once again, that the O/W emulsion used in the experiments did not separate completely by gravity flotation over the course of several days. On the basis of the considerations mentioned above, it is to be inferred that cake exfoliation rather than flotation of oil droplets markedly affects the filtration behaviors for O/W emulsion employed in this research since the experimental results (see Figure 2-3) are quite similar to Figure 2-4(b). It is necessary to know the size of the exfoliated cake in order to elucidate the mechanism of such phenomena.

Furthermore, for various applied filtration pressures the variations of reciprocal filtration rate with filtrate volume per unit membrane area in downward and upward dead-end filtration are also shown in **Figures 2-5 and 2-6** and it is obvious that the same results are obtained as above.

In addition, the experimental result of the filtration, in which the filter was placed upward from downward at the filtrate volume per unit effective membrane area, v = 2.1 cm, was plotted in **Figure 2-7**. It was confirmed that the cake exfoliation did not occurred

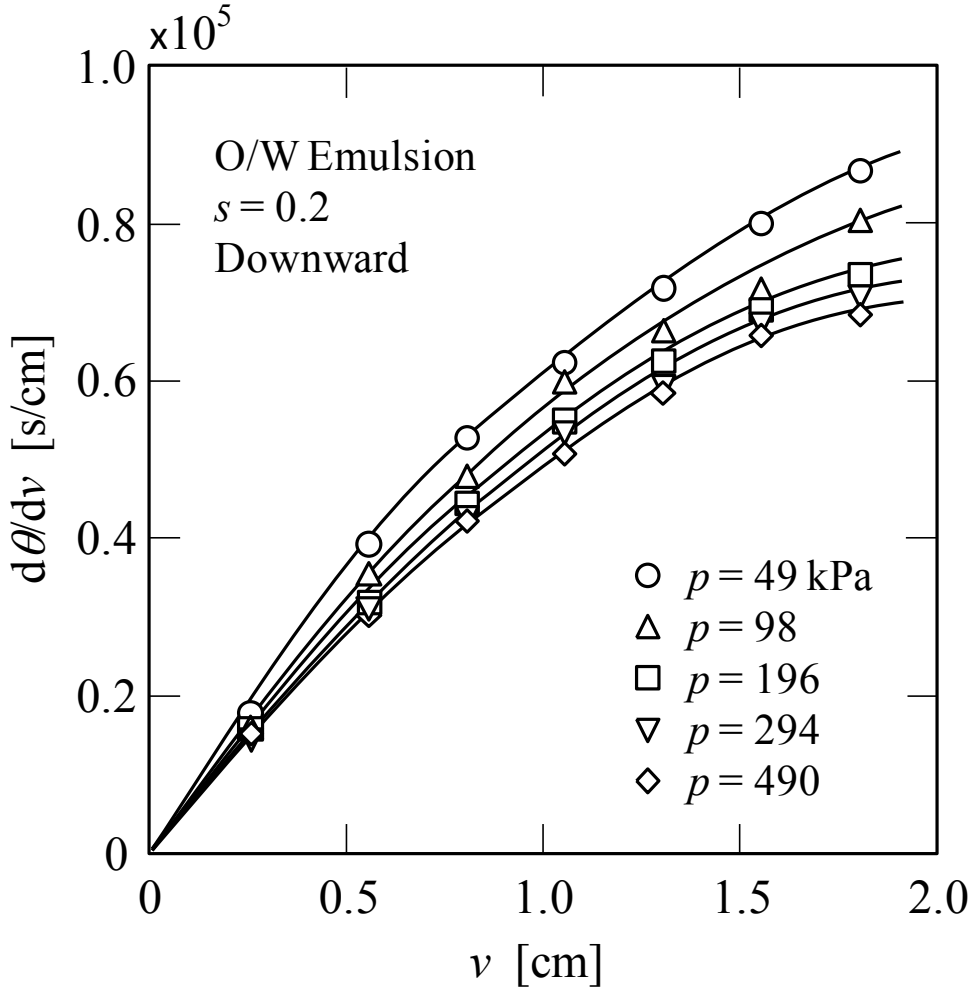

Fig. 2-5 Variation of reciprocal filtration rate with filtrate volume per unit membrane area in downward dead-end filtration

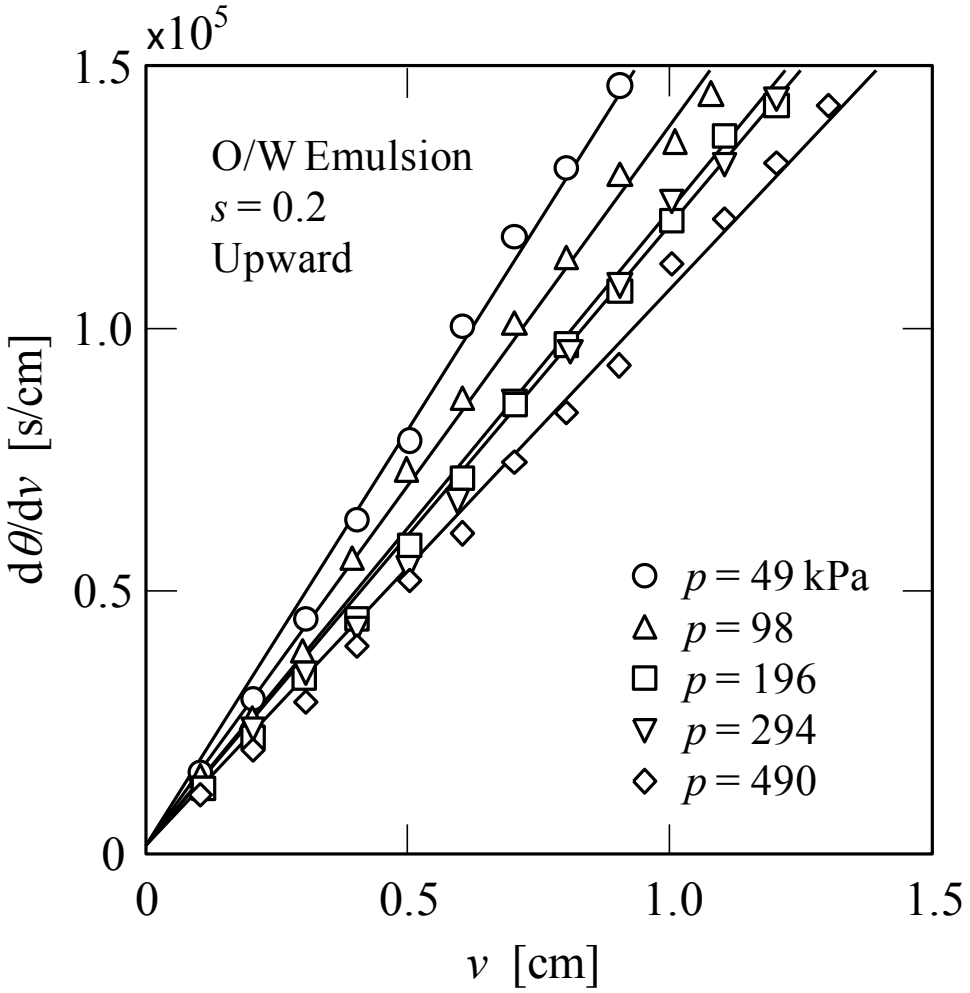

Fig. 2-6 Variation of reciprocal filtration rate with filtrate volume per unit membrane area in upward dead-end filtration

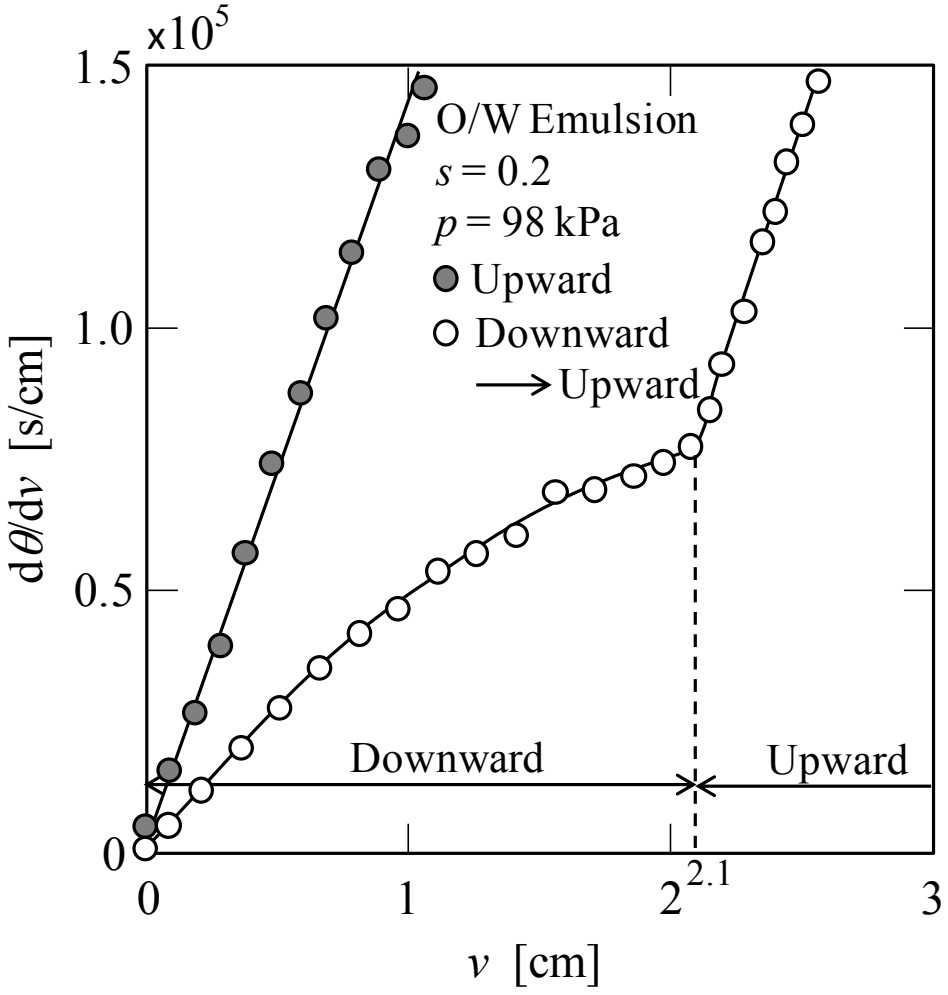

Fig. 2-7 Effect of change in filtration mode performed during part of filtration on flux decline behaviors

indeed in upward filtration since the slope (13.6×10^5 s/cm^2) of plots after v = 2.1 cm is nearly equal to the slope (13.6×10^5 s/cm^2) of the filtration behavior in filtration which is upward from beginning to end, as shown in Figure 2-7. Furthermore, from the result that the plots after v = 2.1 cm is almost parallel to the plots of the filtration behavior in filtration which is upward from beginning to end, it is demonstrated that once the cake exfoliates in downward filtration, it is not reversible to go back to the original cake through changing the filter from downward to upward, different from the inclined dead-end ultrafiltration of nano-colloids (Zeng *et al.*, 1998; Iritani *et al.*, 2002b, 2012b) and therefore the cake exfoliation occurred in downward filtration was further confirmed.

2.4 Determination of Infinite Average Specific Cake Resistance

The values of filtration properties can be calculated by using Eqs. (1-1) and (1-2) when the Ruth plots depicted as ($d\theta/dv$) vs. v show a linear relationship. However, it is impossible to treat the value K_v in Eq. (1-1) as constant because the Ruth plots represent a curve as shown in Figures (2-3) and (2-5) for downward microfiltration of the O/W emulsion. Generally, such filtration properties in which the value K_v is transformable (Iritani *et al.*, 2008a; Hwang *et al.*, 2009; Christensen *et al.*, 2011), can be evaluated by the following formula:

$$\frac{d\theta}{dv} = \frac{\mu \rho s \alpha_{av}}{p(1-ms)} v + \left(\frac{d\theta}{dv}\right)_m = \frac{\mu \rho s \alpha_{av,i}}{p} v + \left(\frac{d\theta}{dv}\right)_m \quad (2\text{-}1)$$

where $(d\theta/dv)_m$ is the value of $(d\theta/dv)$, corresponding to the flow resistance of the membrane. The value $\alpha_{av,\,i}$ (= $\alpha_{av}/(1 - ms)$) can be calculated by substituting the experimental values v and its corresponding values $(d\theta/dv)$ into Eq. (2-1). It is noteworthy that the value $\alpha_{av,\,i}$ containing the ratio m of mass of wet to mass of dry cake is used to estimate cake property because the correct average porosity of filter cake cannot be easily determined. $\alpha_{av,\,i}$ is average cake resistance when s tends to zero in this item $(1 - ms)$ and called after infinite average specific cake resistance in this study,

equivalent to the average cake resistance which can be obtained based on the following material balance equation without considering the water in cake (Iritani *et al.*, 2011; Tanaka *et al.*, 2011).

$$w = \rho s v \tag{2-2}$$

The values $\alpha_{av,\,i}$ calculated as above are shown as a function of the cumulative filtrate volume v collected per unit effective membrane area in **Figure 2-8**. From the figure, it is understood that $\alpha_{av,\,i}$ decreases gradually with the progress of filtration. It should be noted that specific cake resistance cannot be calculated actually by using Eqs. (2-1) and (2-2) because the surface filter cake exfoliates continuously, although specific cake resistance has been evaluated using this method so far.

On the other hand, similarly, for upward filtration the variation of the infinite average specific cake resistance $\alpha_{av,\,i}$ with the cumulative filtrate volume v collected per unit effective membrane area is represented in **Figure 2-9**. From the figure, it is evident that $\alpha_{av,\,i}$ remains nearly constant. The values of solid line in the figure are calculated using Eqs. (1-1) and (1-2) based on the slope of Ruth plots. Therefore, it is clear that specific cake resistance can be evaluated correctly on the basis of the slope of Ruth plots because cake exfoliation do not occur in upward filtration of O/W emulsion.

In **Figure 2-10**, the infinite average specific cake resistance $\alpha_{av,\,i}$ is logarithmically plotted against the applied filtration pressure p. For downward filtration, the plots show the experimental results when filtrate volume v collected per unit effective membrane area is 0.3, 1.0, 1.7 cm, respectively. From the figure, it is known that the values of $\alpha_{av,\,i}$ obtained in upward and downward filtration are very different and an understatement of $\alpha_{av,\,i}$ comes up due to the effect of cake exfoliation in downward filtration. As shown in the figure, the relationship between the infinite average specific cake resistance $\alpha_{av,\,i}$ and the applied filtration pressure p can be represented by the following power law relationship (Sperry, 1921):

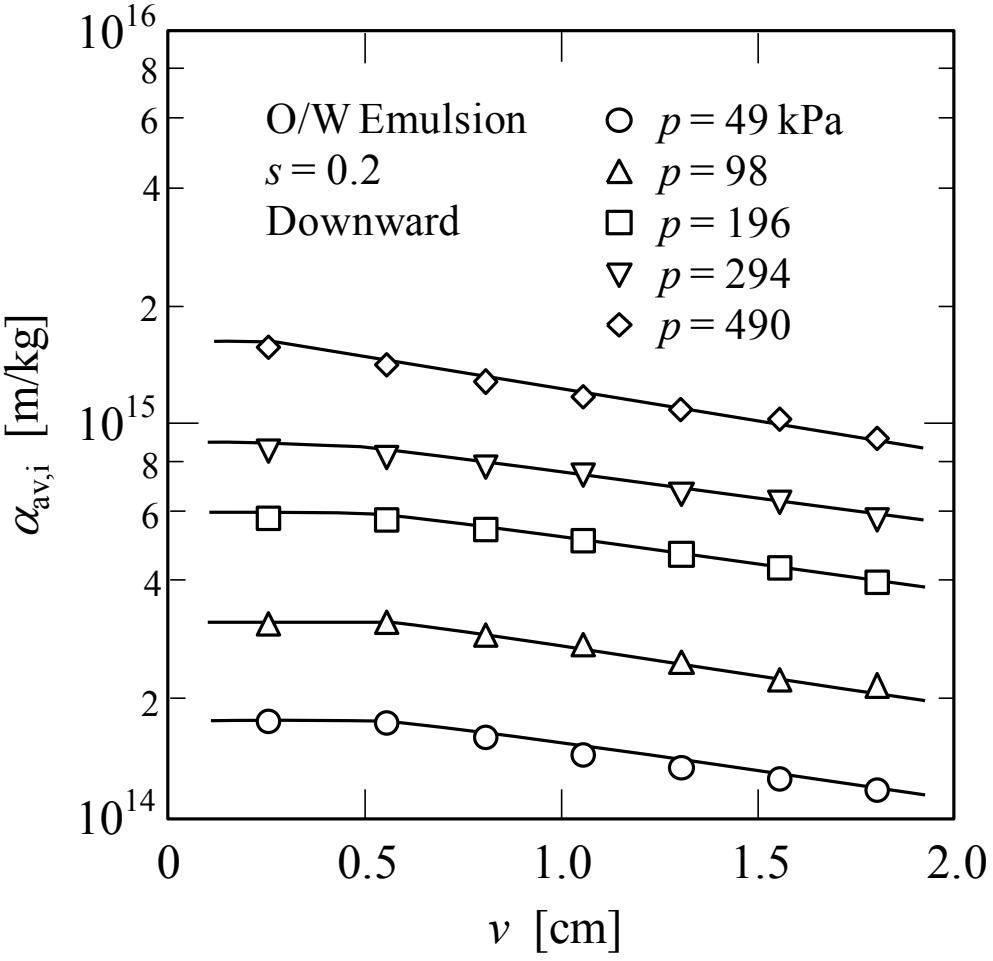

Fig. 2-8 Variation of infinite average specific cake resistance with filtrate volume per unit membrane area in downward dead-end filtration

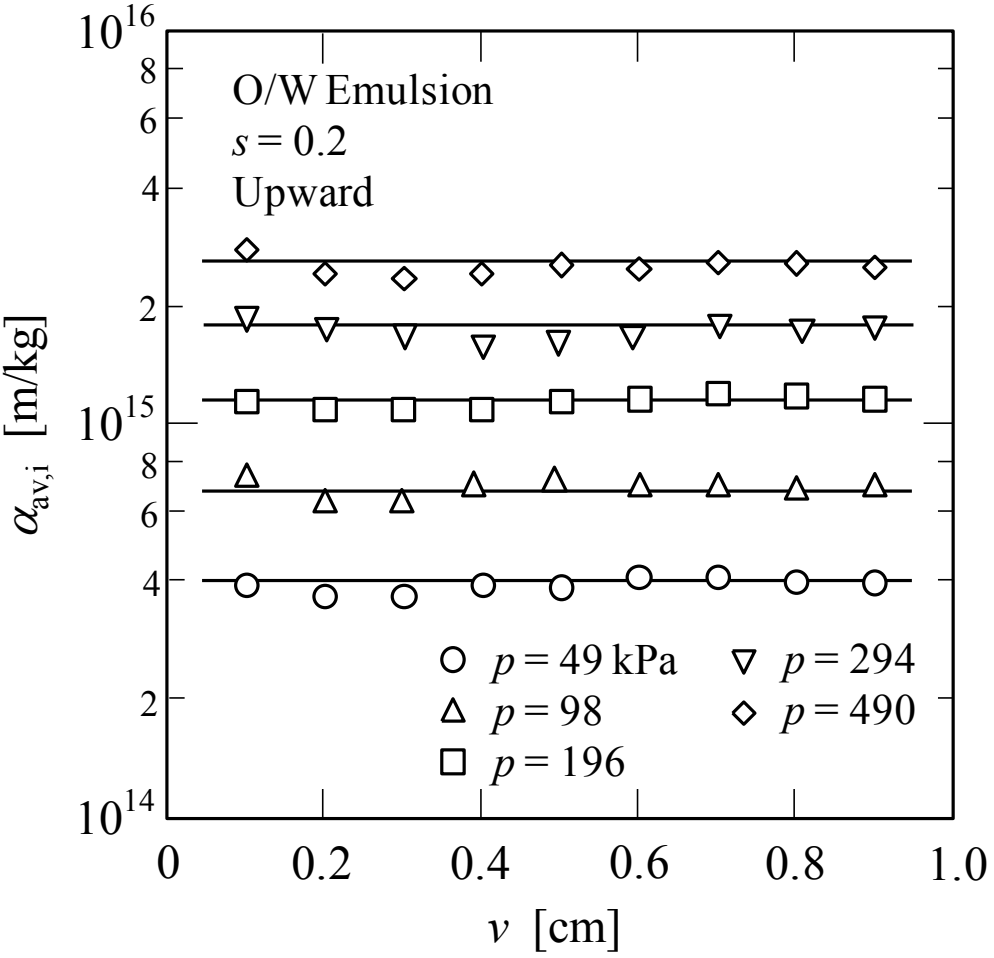

Fig. 2-9 Variation of infinite average specific cake resistance with filtrate volume per unit membrane area in upward dead-end filtration

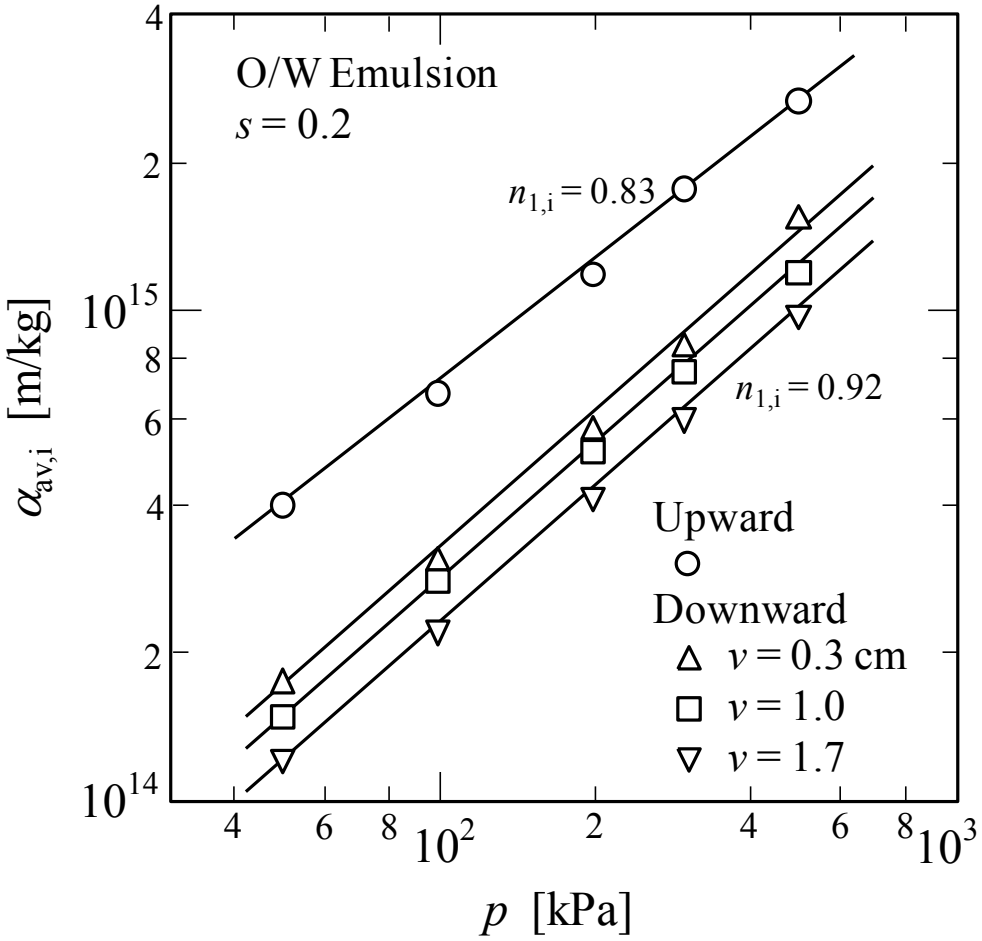

Fig. 2-10 Effect of applied filtration pressure on infinite average specific cake resistance in downward and upward dead-end filtration

$$\alpha_{\mathrm{av,i}} = \alpha_{1,\mathrm{i}} p^{n_{1,\mathrm{i}}} \tag{2-3}$$

where $\alpha_{1,\mathrm{i}}$ and $n_{1,\mathrm{i}}$ are empirical constants and $n_{1,\mathrm{i}}$ is specifically called for apparent compressibility coefficient, which is a measurement of cake compressibility. From the figure, the value of $n_{1,\mathrm{i}} = 0.83$ is obtained in upward filtration and it is obvious that a high compressibility cake forms. For downward filtration, the value of $n_{1,\mathrm{i}} = 0.92$ is obtained regardless of filtrate volume and the difference between upward and downward filtration is not apparent compared to the difference of the values of specific cake resistance.

2.5 Conclusions

Dead-end constant pressure microfiltration experiments under both modes of upward and downward were conducted in order to obtain the filtration characteristic values in membrane filtration of O/W emulsion. Ruth plots show a non-linear relationship in conventional downward filtration because cake exfoliation occurred. However, Ruth plots show a linear relationship in upward filtration because cake exfoliation did not occur. It is found that the values of the infinite average specific cake resistance obtained in both filtration modes were very different and the values of downward filtration were less than the true values. The formed cake properties can be evaluated more correctly in upward filtration because the effect of cake exfoliation was not contained in the values of specific cake resistance. Therefore, this study suggests that the upward dead-end filtration test is quite effective for evaluation of filtration properties in membrane filtration of O/W emulsion.

Chapter 3 Properties of Filter Cake Formed during Dead-End Microfiltration of O/W Emulsion

3.1 Introduction

In the preceding chapter, the determination method of filtration properties based on upward dead-end filtration, in which the filtrate flow is in the opposite direction of gravity and non-linear behaviors occurred in downward dead-end filtration is avoidable, was developed in membrane filtration of O/W emulsions. Although the infinite average specific cake resistance $\alpha_{av,i}$ was employed to evaluate cake properties, the true average specific cake resistance α_{av} and average cake porosity ε_{av}, which play the most important roles in cake filtration, were not accurately determined. In general, the value of the specific cake resistance α_{av} is calculated using both the flux decline data and the cake porosity ε_{av}, as mentioned later. Therefore, the development of a method for measuring the cake porosity ε_{av} is most crucial.

The cake porosity ε_{av} has been determined mostly by weighing the filter cake before and after drying at the end of filtration (Montel *et al.*, 2008; Hwang *et al.*, 2009, 2010). However, the filter cake is likely to experience expansion and porosity increase, especially for deformable, soft oil droplets, as soon as the system was depressurized to the atmospheric pressure at the end of filtration (Shirato *et al.*, 1963; Montel *et al.*, 2008). In another study, although Iritani *et al.* (2003) showed that the cake porosity ε_{av} was evaluated from the value of the cumulative filtrate volume at the end of filtration based on an overall mass balance of dead-end filtration through filtering the whole dispersion colloid, the method may not be applicable to upward filtration.

A technique for accurately determining the filtration characteristics on the principle

of a sudden reduction in the cake surface area during the course of filtration has been widely used in filtration of various samples, from particulate suspensions to protein solutions (Murase *et al.*, 1987, 1988; Iritani *et al.*, 1991a, 2008b; Shirato *et al.*, 1991). Both the average specific cake resistance α_{av} and the average porosity ε_{av} of the filter cake formed during filtration can be calculated only from the flux decline data with the aid of the distance h from the membrane surface to the suddenly-reduced surface.

In this chapter, we extend the work of the previous chapter and present an approach developed from a combination of dead-end upward filtration and a sudden reduction effect in the filter cake surface area in order to propose a method for determining the cake properties in filtration of O/W emulsions (Cao *et al.*, 2013). Both upward and downward filtration experiments are conducted under constant pressure conditions in order to assess the average porosity ε_{av} and the average specific resistance α_{av} of the filter cake comprised of oil droplets. The differences between upward and downward filtration data are discussed in detail. The correct values of the average volume fraction of oil droplets ($1 - \varepsilon_{av}$) and the average specific cake resistance α_{av} are related to the applied filtration pressure p.

3.2 Experimental

3.2.1 Materials and Dispersion Preparation

The experimental materials and dispersion preparation were identical with the previous chapter.

3.2.2 Experimental Apparatus and Technique

A schematic diagram of upward and downward filtration using a specially designed filter is shown in **Figure 3-1**. The filter in Figure 3-1(a) was placed upside down so that the filtrate flow was opposite to the direction of gravity. In order to rigorously evaluate such properties of the filter cake as the average porosity ε_{av} and the average specific cake

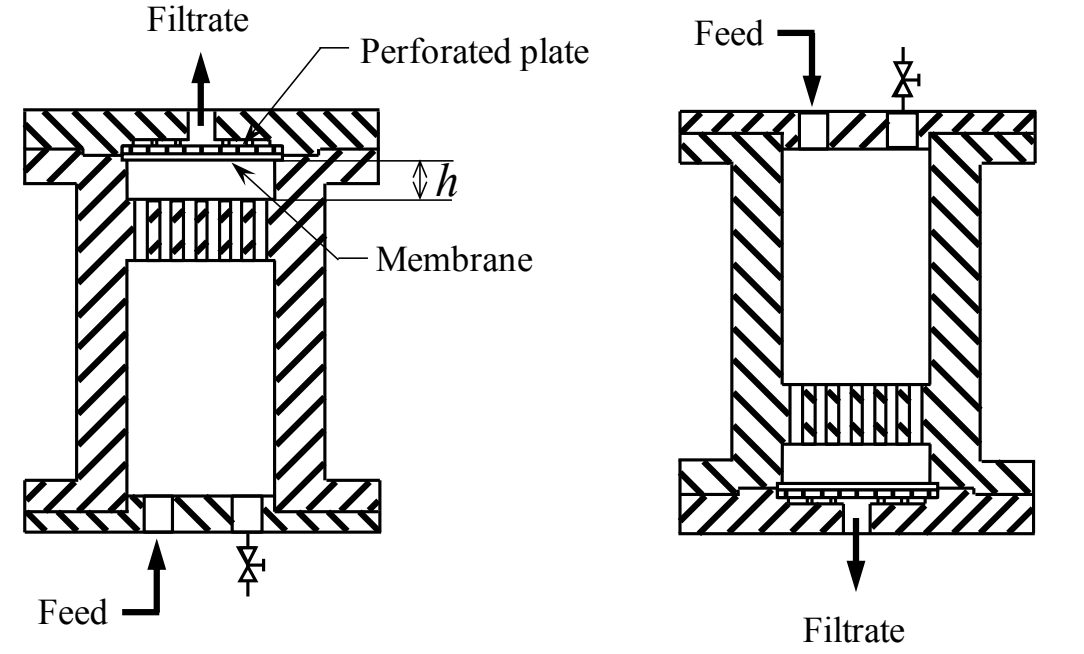

Fig. 3-1 Schematic diagram of upward and downward filtration using specially designed filter

resistance α_{av}, the filtration area was suddenly reduced at the distance h of 1.0, 1.5 and 2.0 mm from the membrane surface. Upward dead-end filtration experiments were performed under a constant pressure condition controlled by a reducing valve by applying compressed nitrogen gas. The filtrate was collected in a reservoir placed on an electronic balance connected to a personal computer to collect and record mass versus time data. The weights were converted to volumes using density correlations. The filtration rate was obtained by numerical differentiation of the volume versus time data. As soon as the filter cake grew up to reach a position where the cake surface area was reduced, the filtration rate decreased substantially. A series of constant pressure filtration experiments were performed under different filtration pressure conditions ranging from 49 to 490 kPa. Downward filtration experiments were performed using the same filter as comparative tests, as shown in Figure 3-1(b). Correspondingly, upward and downward filtration experiments were also conducted using a conventional dead-end filter in which the filtration area was kept constant.

Hydrophilic mixed cellulose ester filtration membranes (Advantec Toyo Corp.) with a nominal pore diameter of 0.1 μm were employed for all filtration experiments to ensure almost complete rejection of oil droplets. A fresh membrane was used for each experiment.

3.3 Determination of Average Cake Porosity

In order to accurately evaluate such properties of the filter cake as the average porosity ε_{av} and the average specific cake resistance α_{av}, the filtration area was suddenly reduced at the distance h from the membrane surface in upward filtration. Three kinds of filters having different h-values were used to investigate whether the cake properties change as filtration proceeds, and upward filtration experiments were carried out at a constant pressure ranging from 49 to 490 kPa. In **Figure 3-2**, typical data of upward filtration experiments with varying h carried out under a constant pressure of 98 kPa are

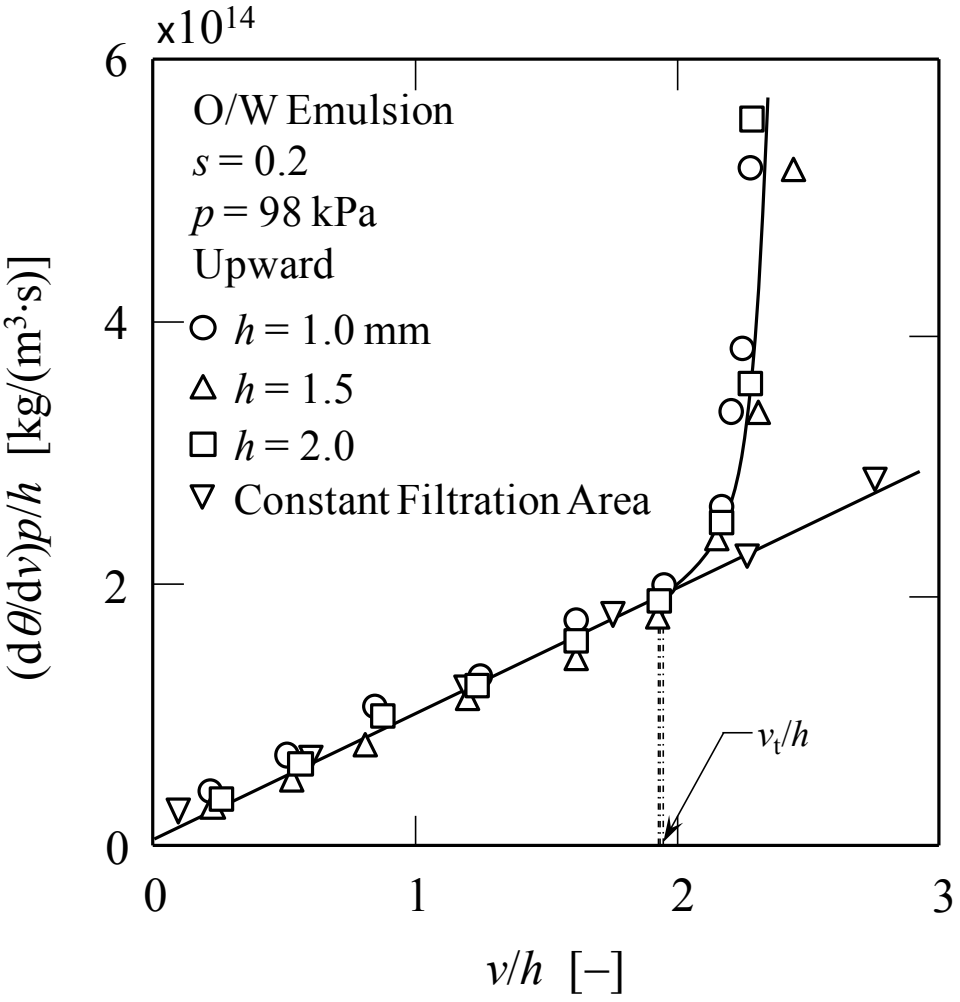

Fig. 3-2 Modified Ruth plots in upward filtration conducted using filters with and without sudden reduction in filtration area

shown as the modified Ruth plots in the form of $(d\theta/dv)p/h$ versus v/h based on

$$\frac{(d\theta/dv)p}{h} = \frac{2p}{K_v}\left(\frac{v}{h} + \frac{v_m}{h}\right) \tag{3-1}$$

The above equation is advantageously obtained by multiplying by p/h both sides of Eq. (1-1), to make it easier to compare the filtration behaviors in the case where the distance h from the membrane surface to the reduced surface is changed. Although the filtration pressure was unchanged in these experiments, such a vertical axis was employed in order to clearly perceive the effect of pressure on the filtration behaviors, as discussed later in this article.

For comparison, the experimental results of the conventional dead-end filtration in which the filtration area is kept constant throughout filtration are also included in the graph. The initial data of filtration experiments in which a sudden reduction in the filtration area is applied appear to collapse to a single straight line regardless of the values of h in accordance with Eq. (3-1) and coincide with data of the conventional filtration experiments having a constant filtration area, as indicated in the figure. However, after the values of v/h are beyond those of v_t/h, $(d\theta/dv)p/h$ increases more sharply. This is because the cake surface reaches the position of h where the filtration area is suddenly reduced. Therefore, the average porosity ε_{av} of the filter cake can be calculated from the value of v_t/h using an overall mass balance of dead-end filtration, to give (Murase *et al.*, 1987, 1988; Iritani *et al.*, 1991a, 2008b)

$$\varepsilon_{av} = \frac{\rho_s(1-s) - \rho s v_t / h}{\rho_s(1-s) + \rho s} \tag{3-2}$$

Thus, the average specific cake resistance α_{av} can be evaluated accurately from Eqs. (1-2), (1-3), (3-1) and (3-2) by using the slope of the modified Ruth plots and the value of ε_{av}. In addition, it seems that the value of the transition point v_t/h is uniform in spite of the distance h. Therefore, it is plausible that the average porosity ε_{av} of the filter cake remains unaltered regardless of the distance h, as is obvious from Eq. (3-2).

Figure 3-3 illustrates the dependence of the average volume fraction $(1 - \varepsilon_{av})$ of oil droplets and the average specific resistance α_{av} of the filter cake on the distance h for the pressure of 98 kPa. Clearly, $(1 - \varepsilon_{av})$ and α_{av} obtained at different h-values are, respectively, identical, indicating that these cake properties are independent of the cake thickness.

In order to ascertain the relationship between cake properties and the applied filtration pressure, upward filtration experiments accompanied with a sudden reduction in the cake surface area at the distance h of 1.0 mm were conducted under constant pressure conditions at a variety of pressures ranging from 49 to 490 kPa. Since the compressibility of the filter cake made of deformable oil droplets is quite high, the data represented as the form of the Ruth plots of $(d\theta/dv)$ against v for a variety of pressures overlapped (not shown as the figure). Thus, the experimental data for various pressures are shown in **Figure 3-4** in the form of the modified Ruth plots of $(d\theta/dv)p/h$ versus v/h based on Eq. (3-1) in order to clearly emphasize the effect of compressibility on the flux decline behaviors. According to these plots, as the pressure is increased, the slope of the linear relationship increases due to the cake compressibility. The plots are virtually linear in accordance with Eq. (3-1) regardless of the value of the applied pressure p before the cake surface reaches the position where the filtration area is suddenly reduced. As shown in the figure, the value of v_t/h increases with the increase in the applied pressure p. This means that the average porosity ε_{av} of the filter cake composed of deformable oil droplets decreases with increasing pressure, thereby increasing the average specific cake resistance α_{av}.

For comparison, downward filtration experiments for various constant applied pressures ranging from 49 to 490 kPa were also performed using the filter which has a sudden reduction in its filtration area. The values of ε_{av} and α_{av} were calculated using Eqs. (1-2), (1-3), (3-1) and (3-2) based on the plots shown in **Figure 3-5** on the assumption

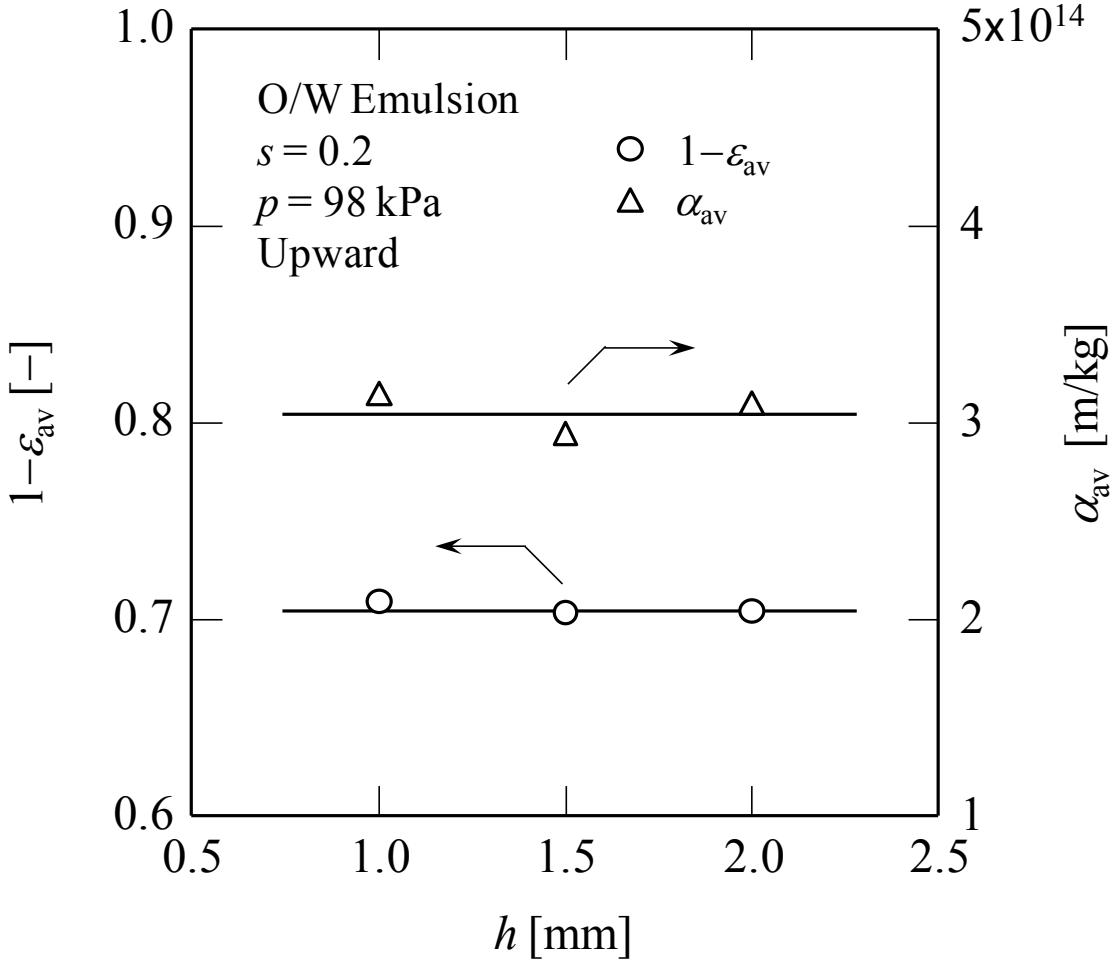

Fig. 3-3 Dependence of average solidosity (1-e_{av}) and average specific cake resistance a_{av} on distance h from membrane surface to reduced surface in upward filtration

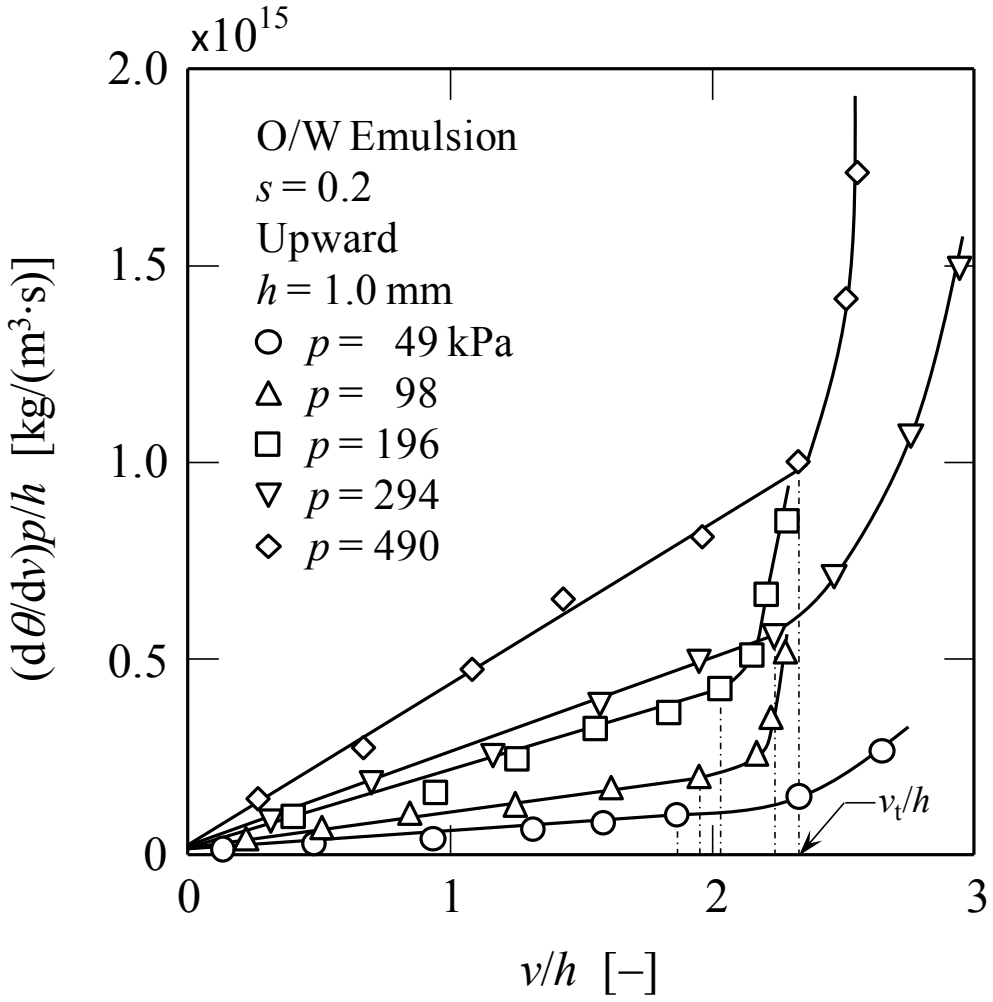

Fig. 3-4 Effect of applied filtration pressure p on modified Ruth plots in upward filtration using filter in which filtration area suddenly reduced at distance h of 1.0 mm

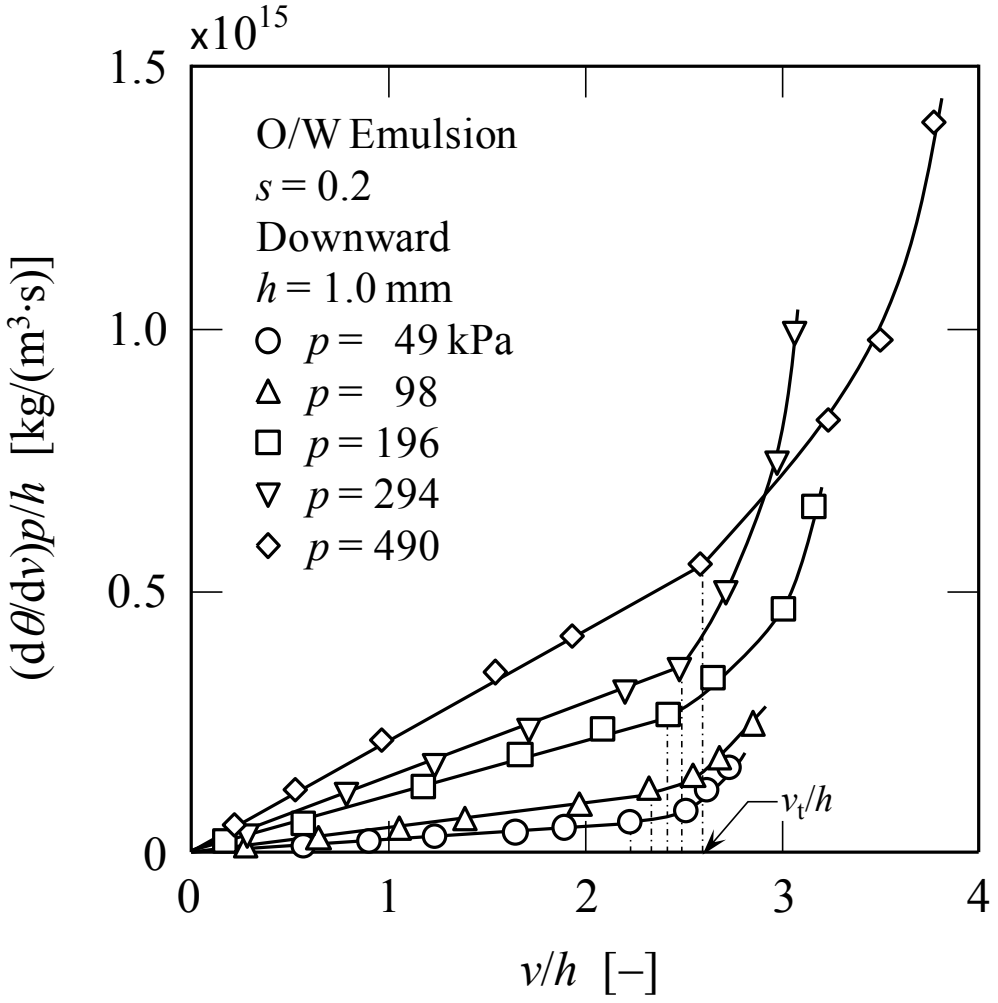

Fig. 3-5 Effect of applied filtration pressure p on modified Ruth plots in downward filtration using filter in which filtration area suddenly reduced at distance h of 1.0 mm

that all of the oil droplets transported toward the membrane accumulated in the filter cake, as in the case of upward filtration. It should be noted that the values of α_{av} were evaluated from the straight-line approximation of the modified Ruth plots for experimental data of the flux decline.

3.4 Properties of Filter Cake

The average volume fraction ($1 - \varepsilon_{av}$) of oil droplets in upward and downward filtration are logarithmically plotted in **Figure 3-6** as functions of the applied filtration pressure p. As the pressure increases, a filter cake with higher oil phase content forms, leading to the increase in the average volume fraction ($1 - \varepsilon_{av}$) of oil droplets in the cake. The plots of upward and downward filtration data exhibit, respectively, a substantially linear relationship over a wide range of data from 49 to 490 kPa in accord with the empirical power function approximation of the average volume fraction ($1 - \varepsilon_{av}$) of oil droplets in the following form (Tiller and Cooper, 1962):

$$1 - \varepsilon_{av} = Bp^{\beta} \tag{1-5}$$

where B and β are the empirical constants. However, the value of ($1 - \varepsilon_{av}$) obtained in downward filtration is substantially higher than that in upward filtration under identical pressure conditions. This is because the reduced mass of the filter cake resulting from the cake exfoliation in downward filtration is not considered in Eq. (3-2) and then the cake porosity in downward filtration is overestimated. The error bars in the figure indicate the 95% confidence interval. It is found that the data show highly reproducible results.

In **Figure 3-7**, the average specific resistance α_{av} of the filter cake is logarithmically plotted against the applied filtration pressure p in upward and downward filtration. In the previous chapter, the infinite average specific cake resistance $\alpha_{av,i}$ (= $\alpha_{av}/(1 - ms)$) was employed to evaluate the filterability because a method for measuring the average cake porosity ε_{av} (i.e., the ratio m of mass of wet cake to mass of oil droplets in cake) was not

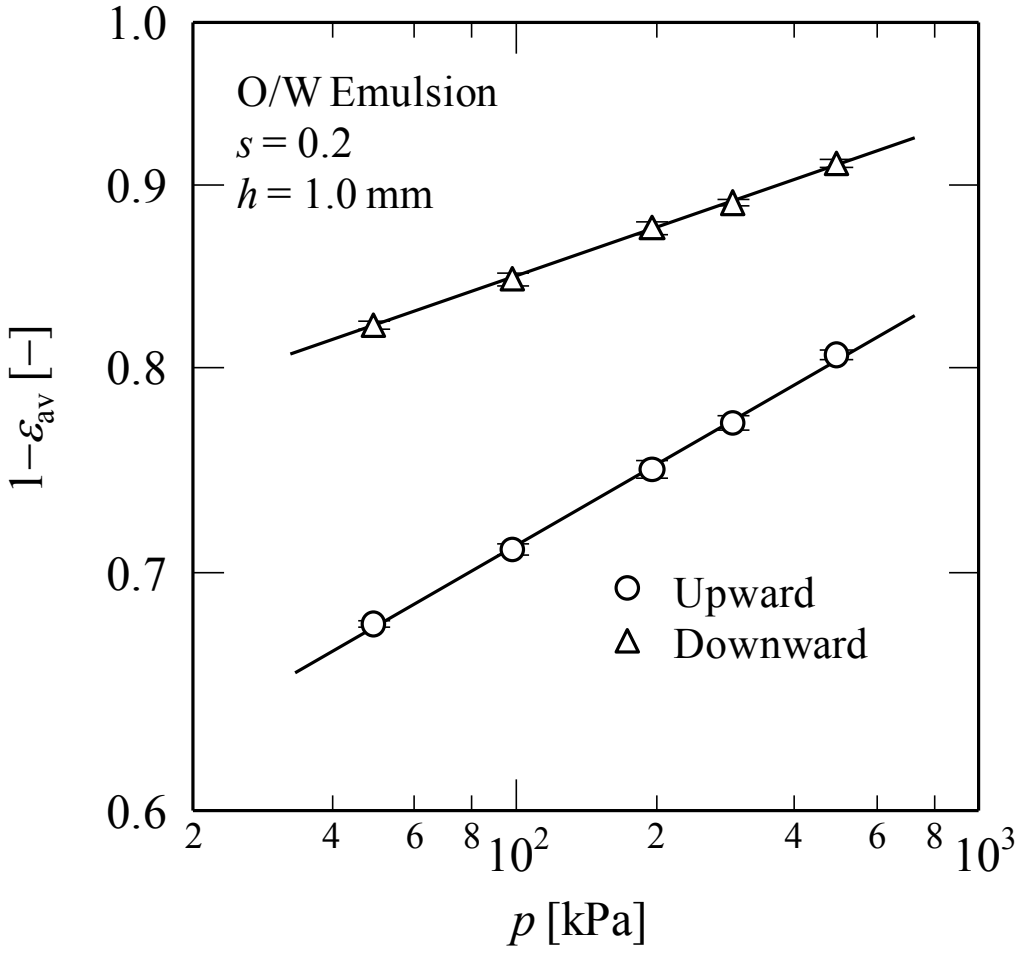

Fig. 3-6 Dependence of average solidosity ($1-\varepsilon_{av}$) of filter cake on applied filtration pressure p in upward and downward filtration

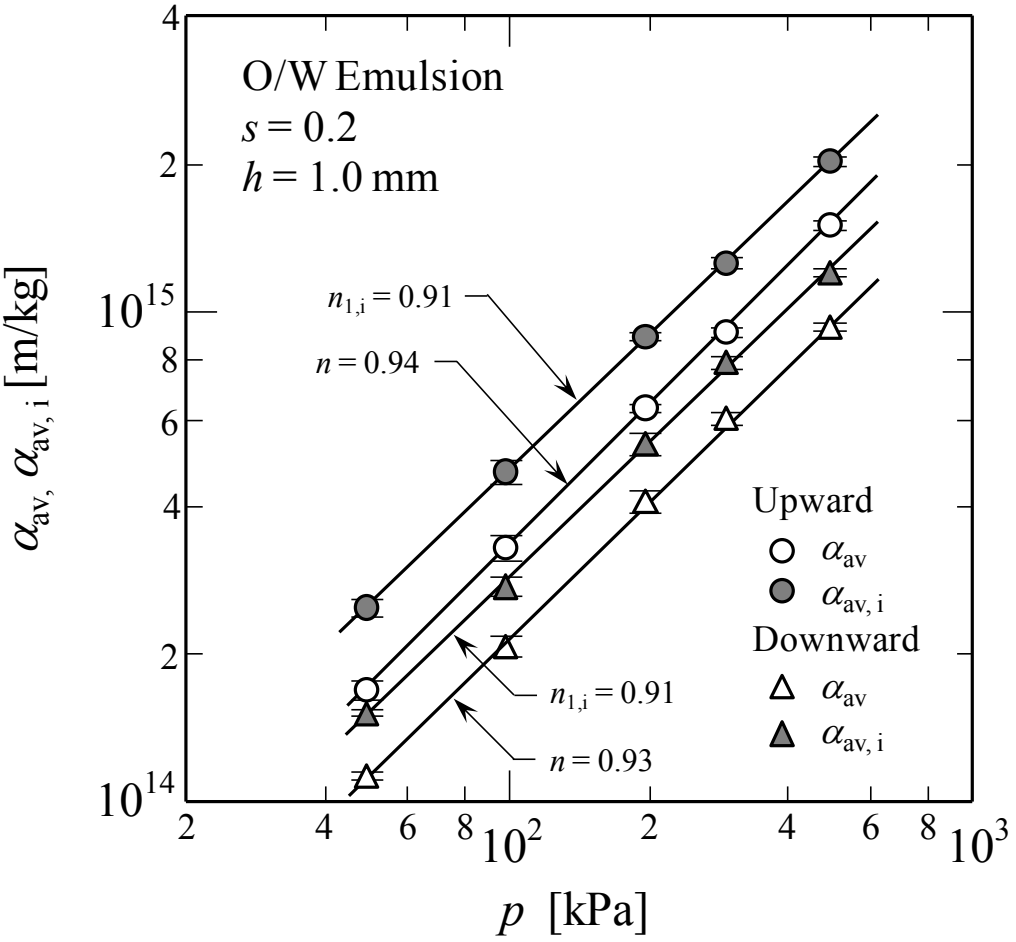

Fig. 3-7 Dependence of average specific cake resistance a_{av} and infinite average specific cake resistance $a_{av,i}$ on applied filtration pressure p in upward and downward filtration

available. The relationship between $\alpha_{av,i}$ and p is also included in the figure. The specific resistance α_{av} obtained in consideration of the value of the cake porosity ε_{av} is substantially lower than that of the infinite specific resistance $\alpha_{av,i}$ at an equivalent applied pressure in each case of upward and downward filtration. In filtration of a dilute suspension where the mass fraction s of solids in suspension is sufficiently small, the factor $(1 - ms)$ that appears in Eq. (1-2) is generally approximated by unity (Iritani *et al.*, 2011, 2012a), and then the value of $\alpha_{av,i}$ differs only negligibly from that of α_{av}. However, the value of ε_{av} is needed in the accurate estimation of the specific resistance because the mass fraction s of oil droplets in the O/W emulsion employed in this study is sufficiently large. The relationship between the specific resistance and the pressure appear to be linear over the entire range of data in upward and downward filtration in accordance with the power law relationship given by (Sperry, 1921)

$$\alpha_{av} = \alpha_1 p^n \tag{1-4}$$

$$\alpha_{av,i} = \alpha_{1,i} p^{n_{1,i}} \tag{2-3}$$

where α_1, n, $\alpha_{1,i}$, and $n_{1,i}$ are empirical constants, and n and $n_{1,i}$ are specifically called the compressibility coefficient and the apparent compressibility coefficient, respectively, which were used for evaluating the compressibility of filter cake in filtration fields.

As shown in Figure 3-7, all of the compressibility coefficients n and $n_{1,i}$ are roughly close to unity and some researchers (Matsumoto *et al.*, 1999; Iritani *et al.*, 2003; Headen *et al*, 2006; Montel *et al.*, 2008) have also reported similar results in the filtration of O/W emulsions. This suggests that the filter cake formed during filtration of an O/W emulsion is classified as highly compressible because oil droplets in the cake are easily deformed under compressive forces. It is, therefore, important to note that the increase in the applied pressure is not necessarily relevant to the improvement in the filtration performance.

It is obvious from the figure that the values of α_{av} in downward filtration are much

lower than those in upward filtration at an equivalent applied pressure. As previously mentioned, the reason for which such results are obtained is that the influence of cake exfoliation occurred in downward filtration of the O/W emulsion is not taken into account. This leads to an understatement of the oil droplets deposited in the filter cake and causes serious errors in calculated values of the average specific cake resistance α_{av}. Therefore, constant pressure upward filtration tests accompanied with a sudden reduction in the cake surface area was shown to be suitable as the method for accurately evaluating the cake properties in membrane filtration of an O/W emulsion.

In addition, **Figure 3-8** shows an interesting result that the filtration rate ($d\theta/dv$ = 1.31 x 10^4 s/cm^2) in downward filtration is more larger than that ($d\theta/dv$ = 2.04 x 10^4 s/cm^2) in upward filtration at the same filtration pressure p = 98 kPa and thickness h = 1.0 mm of filter cake. This maybe indicates that the filter cake formed in downward filtration is more looser than that in upward filtration because cake exfoliation occurred continuously in downward filtration. About this, further research will be needed.

3.5 Conclusions

Upward filtration tests accompanied with a sudden reduction in the cake surface area were conducted under constant pressure conditions, in order to accurately evaluate cake properties as reflected by the average porosity ε_{av} and the average specific cake resistance α_{av}. For comparison, downward filtration tests were also conducted. The calculated values of the average specific cake resistance α_{av} became lower in downward filtration although the calculated values of the average volume fraction ($1 - \varepsilon_{av}$) of oil droplets obtained based on a dead-end filtration mechanism were higher in downward filtration. This is because the influence of the cake exfoliation cannot be ruled out in downward filtration. It is found that the determination of cake properties based on downward filtration may lead to erroneous results. Therefore, this study suggests that the upward dead-end filtration test accompanied with a sudden reduction in the cake surface

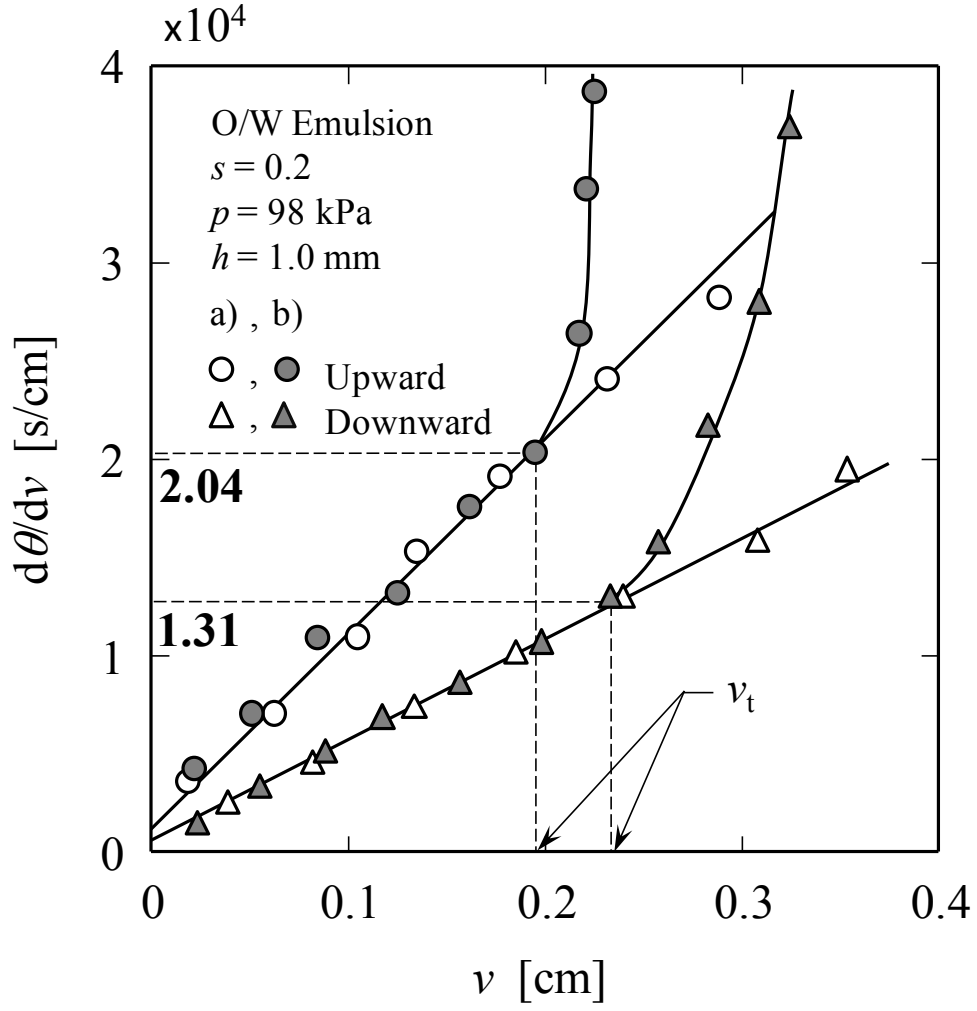

Fig. 3-8 Comparison of Ruth plots between upward and downward filtration

(a) Filtration area is constant.

(b) Filtration area is suddenly reduced at distance h = 1.0 mm from membrane surface to reduced surface.

area is particularly suitable for evaluating cake properties in membrane filtration of O/W emulsions.

Chapter 4 Flotation and Sedimentation Properties in Centrifugal Separation of Emulsion-Slurry

4.1 Introduction

O/W emulsion can be separated using a variety of mechanical separation methods such as membrane filtration (Iritani *et al.*, 2003; Cao *et. al*, 2012, 2013) and centrifugal flotation (Iritani *et al.*, 2007a, 2007b). So far, the characteristics of filtration and centrifugation for O/W emulsion have been extensively studied. However, very little work has been done on the separation and/or stability of O/W emulsion containing solid particles, which can be seen as bidisperse suspensions, whilst O/W emulsion containing solid particles is encountered in wastewater treatment of industries producing cosmetics, pharmaceuticals, agrochemical and paints.

The bidisperse suspensions in which two different types of solid particles are dispersed uniformly in fluid can be generally separated through the gravity sedimentation method, based on the difference of density and size of two types of particles, and it was reported that the settling velocities of both solid phases were significantly enhanced (Whitmore, 1955; Weiland and McPherson, 1979; Fessas and Weiland, 1981, 1984). The O/W emulsion containing the large solid particles such as particles ranging from 29 to 157 μm (Yan and Masliyah, 1993) and millimeter-size particles (1.50 – 2.38 mm) (Beydoun *et al.*, 1998) can be also separated under the action of gravity.

However, the outstanding issue is that the separation of O/W emulsion containing the fine particles which can be regarded as colloidal particles is infeasible under the action of gravity due to its high stability. Particularly, it is well known that solid particles can serve as emulsifying agents by adsorbing to the oil-water interface (Yan and Masliyah, 1997; Binks and Lumsdon, 1999; Binks, 2002; Aveyard *et al.*, 2003) and there exists the

interaction between oil droplets and solid particles (Tadros *et al.*, 1998). Membrane filtration (Iritani *et al.*, 2008) and centrifugal separation methods are expected to serve as potential separation methods for such dispersed system as with the case of O/W emulsion. Recently, an introduced analytical photocentrifuge allowing the study of the movement of the phase boundary in centrifugation has been used as a powerful tool to analyze the mechanism of centrifugal separation because it can monitor the position of phase boundary readily and accurately without stopping the rotation (Lerche, 2002; Sobisch, *et al.*, 2006; Lerche and Sobisch, 2007, 2011; Loginov *et al.*, 2012, 2013).

In this chapter, centrifugal separation experiments of emulsion-slurry which is a mixture of O/W emulsion and particulate slurry are conducted using the analytical photocentrifuge (Cao *et al.*, 2014). The interactions between oil droplets and solid particles in emulsion-slurry are experimentally investigated from the viewpoint of the acceleration effects of the flotation velocity of oil droplets and the settling velocity of solid particles. The flotation coefficient of oil droplets floating and the sedimentation coefficient of solid particles settling through emulsion-slurry are employed to examine the effect of each dispersed phase volume fraction. An attempt is made to develop the expressions for the flotation and sedimentation coefficients in order to describe the centrifugal separation behaviors of emulsion-slurry.

4.2 Experimental

4.2.1 Materials and Dispersion Preparation

The oil employed as the dispersed phase in O/W emulsion was kerosene (Wako Pure Chemical Industries, Ltd.), having a density ρ_o of 787 kg/m^3. An anionic surfactant, sodium dodecyl sulphate (SDS, Sigma-Aldrich Japan Corp.), having a critical micelle concentration (CMC) of 8×10^{-3} M (0.23 wt%), was employed to stabilize the O/W emulsion. The solid particles used as the dispersed phase in particulate slurry were silicon dioxide (SiO_2) (Yukijirushi SP-3, Marugamakamado Toryo Corp.) with irregular shapes,

having a density ρ_p of 2580 kg/m^3. All of the chemicals were used as received. Ultrapure, de-ionized (DI) water (ρ_l = 997 kg/m^3) was prepared by purifying tap water through ultrapure water systems of both Elix-UV20 and Milli-Q Advantage System for laboratory use (Millipore Corp.).

The surfactant solution was prepared by dissolving SDS in the ultrapure, DI water. The O/W emulsion was prepared with the volume concentration of the dispersed oil phase of 0.652 and the SDS mass concentration of 0.3 % (w/w total quantity), by shear mixing under the mixing speed of 20,000 rpm for a period of 90 s using a homogenizer (SilentCrusher M, Heidolph Instruments GmbH) after addition of the oil to the surfactant solution. The SiO_2 suspension was prepared with the volume concentration of the dispersed phase of 0.321 and the SDS mass concentration of 0.3 % (w/w total quantity), through ultrasound dispersion. The emulsion-slurry with the predetermined concentrations of oil droplets and SiO_2 particles was prepared by mixing O/W emulsion, particulate slurry, and the surfactant solution of the SDS mass concentration of 0.3 % (w/w total quantity), with the stirring rate of 250 rpm for 10 min.

The size distributions of oil droplets and SiO_2 particles were measured by a laser diffraction particle size analyzer (SALD-2200, Shimadzu Corp.) and shown in **Figure 4-1**. The mean specific surface area sizes, d_o and d_p, of the oil droplets in O/W emulsion and the SiO_2 particles in particulate slurry were 2.21 and 1.07 μm, respectively. Through the measurements after the centrifugal separation experiments, it was confirmed that the size distributions of oil droplets contained in the creaming layer and particles consisted in the sediment remained unchanged.

4.2.2 Experimental Apparatus and Procedure

Centrifugation experiments were carried out at different constant rotor speeds ranging from 1500 to 2500 rpm (the angular velocities Ω of the rotor ranging from 157.1 to 261.8 rad/s) corresponding to centrifugal accelerations of 274 - 760 × g with reference

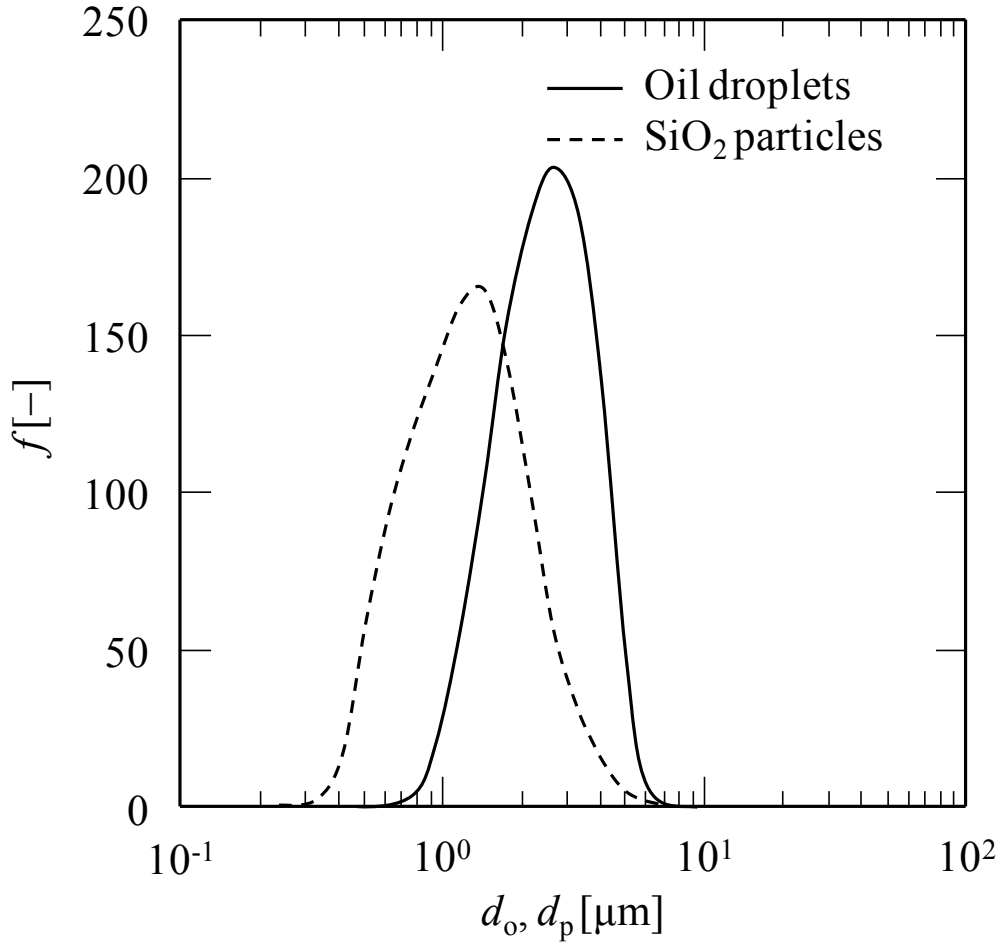

Fig. 4-1 Size distributions of oil droplets in O/W emulsion and SiO_2 particles in SiO_2 suspension

to the base of the cell, using the microprocessor controlled analytical photocentrifuge (LUMiFuge 116, L.U.M. GmbH) (Lerche, 2002; Sobisch, *et al.*, 2006; Lerche and Sobisch, 2007, 2011), where g is the gravitational acceleration. The precision spectroscopic rectangular glass cells with an optical path length of 1 mm were used, and the cells charged with the sample were positioned in the radial direction on the rotor. The instrument non-invasively traced the local and temporal variations of the intensity of transmitted NIR light at 880 nm over the total length of the sample cell containing the dispersion, even while centrifugation was in progress. Particle migration due to the centrifugal force causes a variation of the local particle concentration and correspondingly local and temporal variations of transmission. The transmission profile of the sample during the course of centrifugation was continuously recorded by the CCD-line sensor, displayed as the temporal sequence on the computer screen, and stored on a PC. The data was available to determine the time course of the position of the interface of the dispersion and the clear liquid, as described later.

4.3 Centrifugal Separation Characteristics of Emulsion-Slurry

Various values of NIR light transmission were used to determine the interface between dispersion and transparent in the available literatures; e.g. 50% (Iritani *et al.*, 2007a, 2007b), 30% (Sobisch *et al.*, 2006), 20% (Loginov *et al.*, 2013), 15% (Loginov *et al.*, 2012). **Figure 4-2** shows the relationship between NIR light transmission T and each volume fraction ϕ_o, ϕ_p of oil droplets in O/W emulsion and SiO_2 particles in SiO_2 suspension. In general, the concentration of a thick dispersion should change sharply at the interface of the hindered flotation or sedimentation. Therefore, the transmission T of 20 % was employed to determine the interface of centrifugal separation in this study, as shown subsequently.

Figure 4-3 illustrates the typical result of the change with time in NIR light transmission T expressed in percentage over the entire sample height for centrifugal

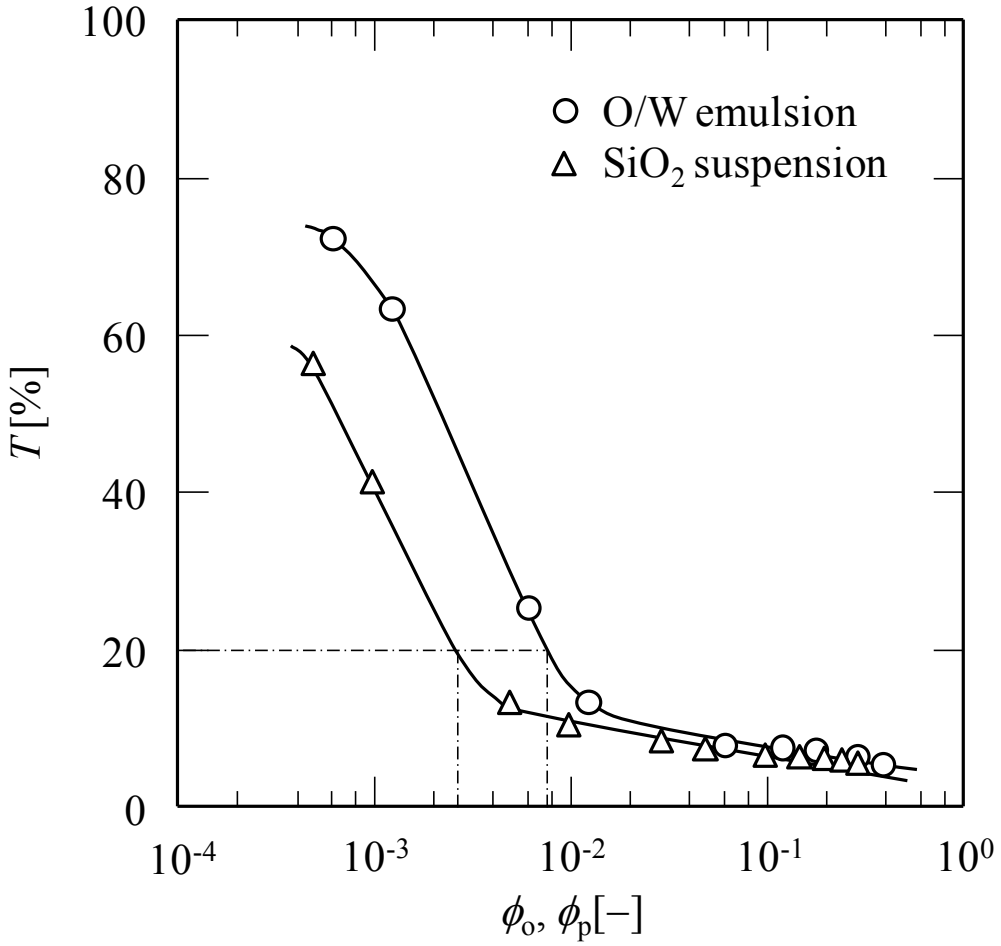

Fig. 4-2 Relation between NIR light transmission and volume fractions of oil droplet in O/W emulsion and SiO_2 particles in SiO_2 Suspension

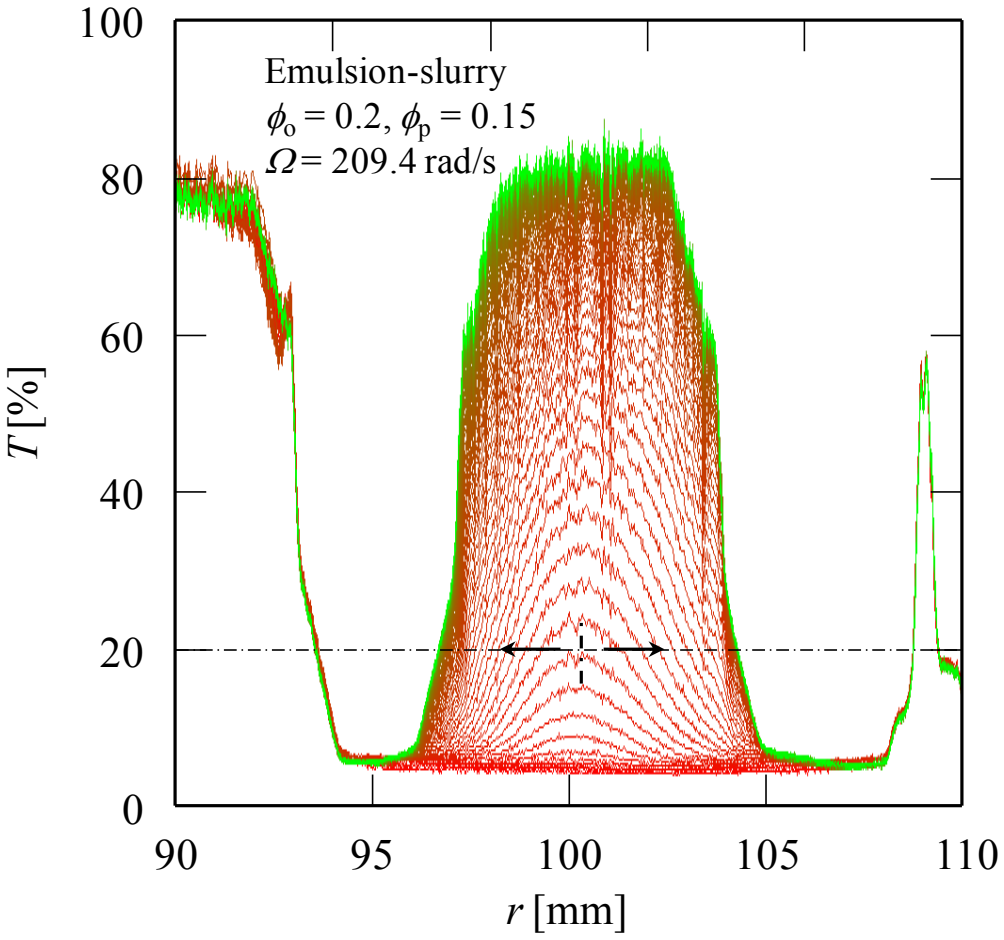

Fig. 4-3 Typical result of change with time in NIR light transmission

flotation and sedimentation of emulsion-slurry, where the volume fractions of oil droplets and SiO_2 particles, ϕ_o and ϕ_p, based on the total volume of emulsion-slurry are 0.2 and 0.15, respectively. In this figure, r is the radial distance of an arbitrary position from the center of rotation. The transmission profiles are taken every 20 s. The evolution of the time dependent transmission profiles progresses from the middle to both ends of sample contained in the test cell. The overlay of profiles at the left and right sides documents that the flotation and sedimentation process came to terminate.

Figure 4-4 shows the variations with centrifugal time t of the interfaces determined, as mentioned above, for centrifugal flotation and sedimentation of emulsion-slurry, where r_i is the radial distance from the center of rotation to the interface of dispersion and clear liquid, and r_1 and r_2 are the radial distances from the center of rotation to the bottom and top of sample filled in cell, respectively. In the figure, r_c is defined as the radial distance from the center of rotation to the critical interface where flotation and sedimentation interfaces arise for the first time simultaneously, and t_c is the critical time when r_c appears. The vertical coordinate is represented as the logarithmic form, as used in the previous paper (Iritani *et al.*, 2007b). On the basis of the result shown in Figure 4-4, the schematic diagram of centrifugal flotation and sedimentation of emulsion-slurry is shown in **Figure 4-5**. As shown in the figure, there are three layers such as creaming, emulsion-slurry layer and sediment before the critical time, and after that the clear liquid layer appears and the emulsion-slurry layer disappears gradually. Finally, the consolidated equilibrium is reached and three layers such as creaming, clear liquid layer and sediment are represented. As shown in Figures 4-4 and 4-5, it is clarified that the flotation of oil droplets and the sedimentation of SiO_2 particles synchronized in the centrifugal separation of emulsion-slurry, and the interfaces can be observed after the critical time t_c and approach to balance as the centrifugal time t goes on. The results for single dispersion having a volume fraction equal to that of each dispersed phase in emulsion-slurry are also

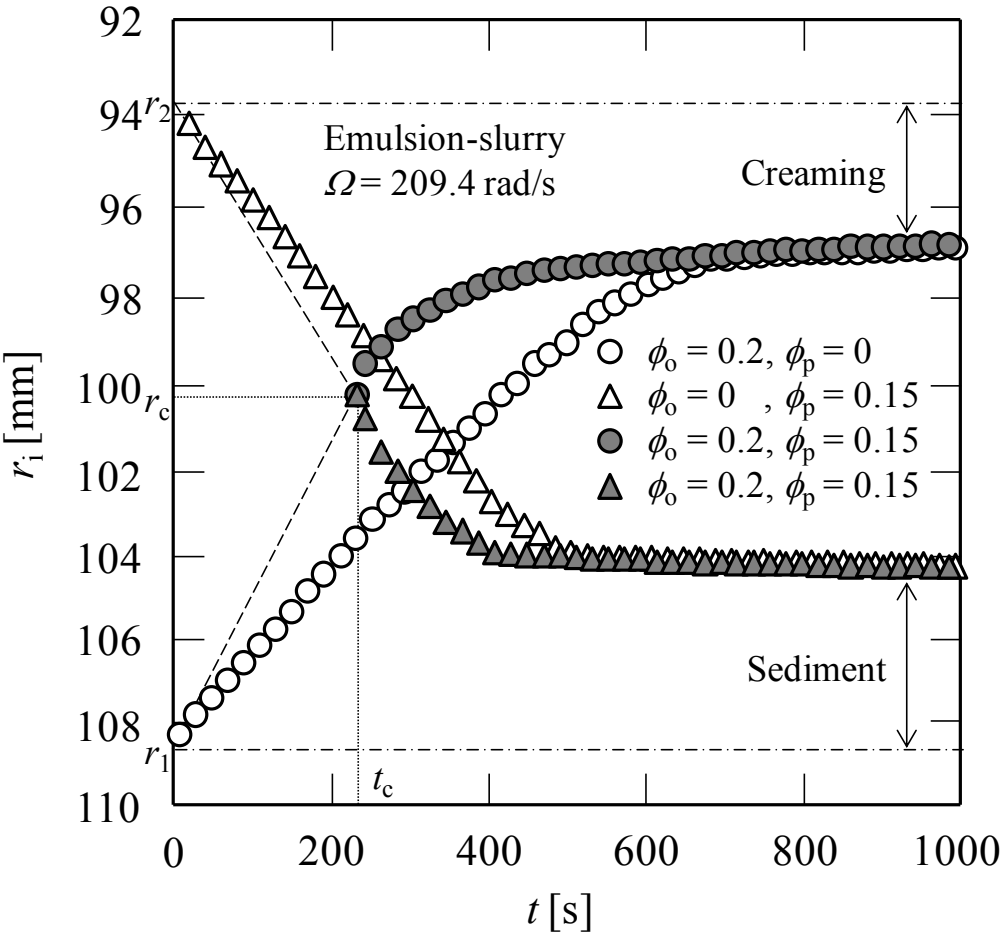

Fig. 4-4 Flotation curve of oil droplets and sedimentation curve of SiO_2 particles in centrifugal separation of emulsion-slurry, O/W emulsion, and SiO_2 suspension

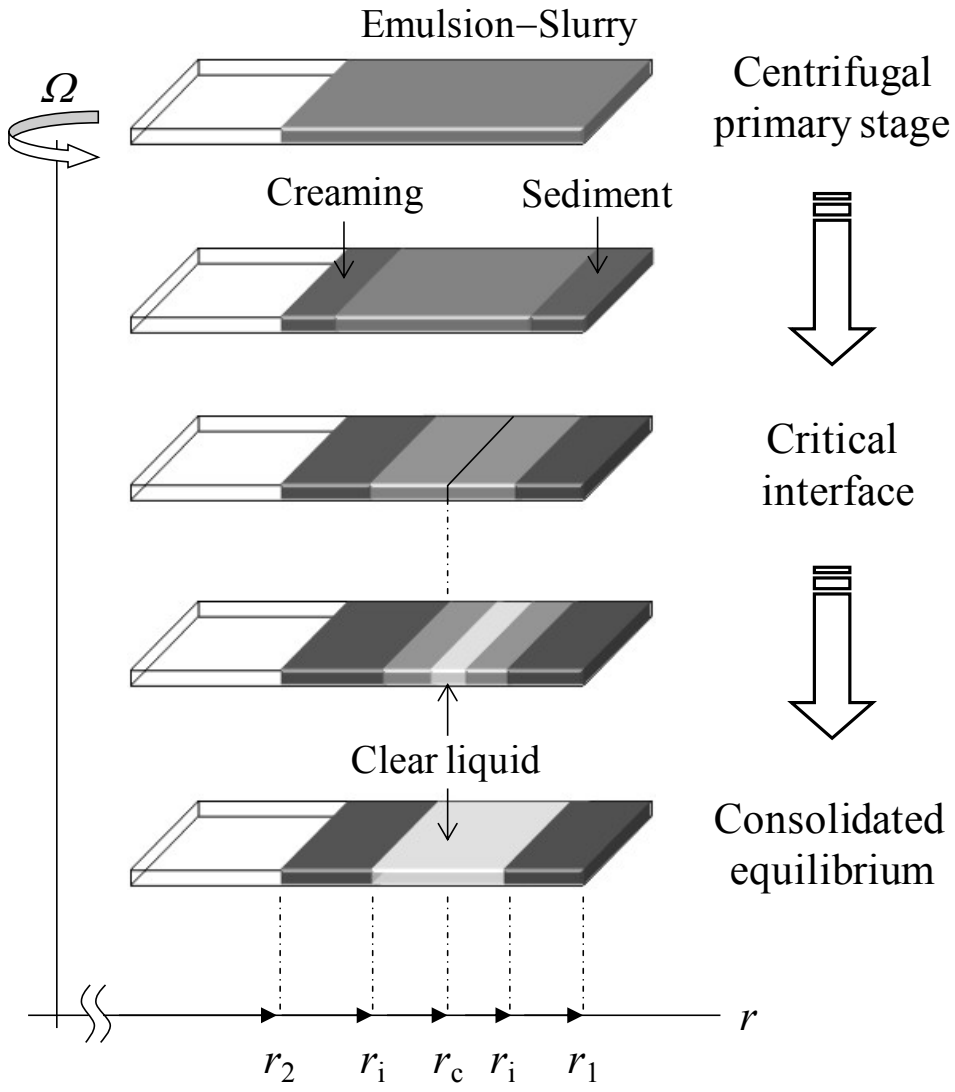

Fig. 4-5 Schematic diagram of centrifugal flotation and sedimentation of emulsion-slurry

included in the Figure 4-4. Comparing the results for emulsion-slurry with those for single dispersion, it seems obvious that the flotation rate of oil droplets and the settling rate of SiO_2 particles for binary dispersion are faster than the rates for single dispersion. This may be attributed to the larger density difference between oil droplets (or SiO_2 particles) and dispersion.

It can be also seen from Figure 4-4 that the equilibrium interfaces for emulsion-slurry are consistent with those of single dispersion. To investigate the result in more detail, the ratios, R_c and R_s, of the creaming and sediment heights for emulsion-slurry and single dispersions to the initial height of the dispersions are plotted in **Figure 4-6** against the volume fraction of oil droplets and the volume fraction of SiO_2 particles, ϕ_o and ϕ_p. It is revealed that the creaming and sediment heights of binary dispersion are identical to those of single dispersion in spite of the values of ϕ_o and ϕ_p. Whilst it is well known that solid colloidal particles sometimes adsorb to the oil-water interface for O/W emulsion (Yan and Masliyah, 1997; Binks and Lumsdon, 1999; Binks, 2002; Aveyard *et al.*, 2003), it can be concluded from the figure that little SiO_2 particles are contained in the equilibrium creaming layer after centrifugation. This is probably because oil droplets were stabilized by surfactants in advance.

4.4 Centrifugal Flotation Behaviours of Oil Droplets in Emulsion-Slurry

In order to normalize the dependence of the flotation and the settling rates on the centrifugal acceleration $r_i\Omega^2$ (Iritani *et al.*, 1993 and 2007b), the flotation coefficient S_o of oil droplets floating and the sedimentation coefficient S_p of SiO_2 particles settling through emulsion-slurry are defined by

$$S = \frac{1}{\Omega^2}\frac{\Delta \ln r_i}{t_c} \tag{4-1}$$

where $S = S_o$ and $\Delta \ln r_i = \ln (r_1/r_c)$ for centrifugal flotation, and $S = S_p$ and $\Delta \ln r_i = \ln (r_c/r_2)$

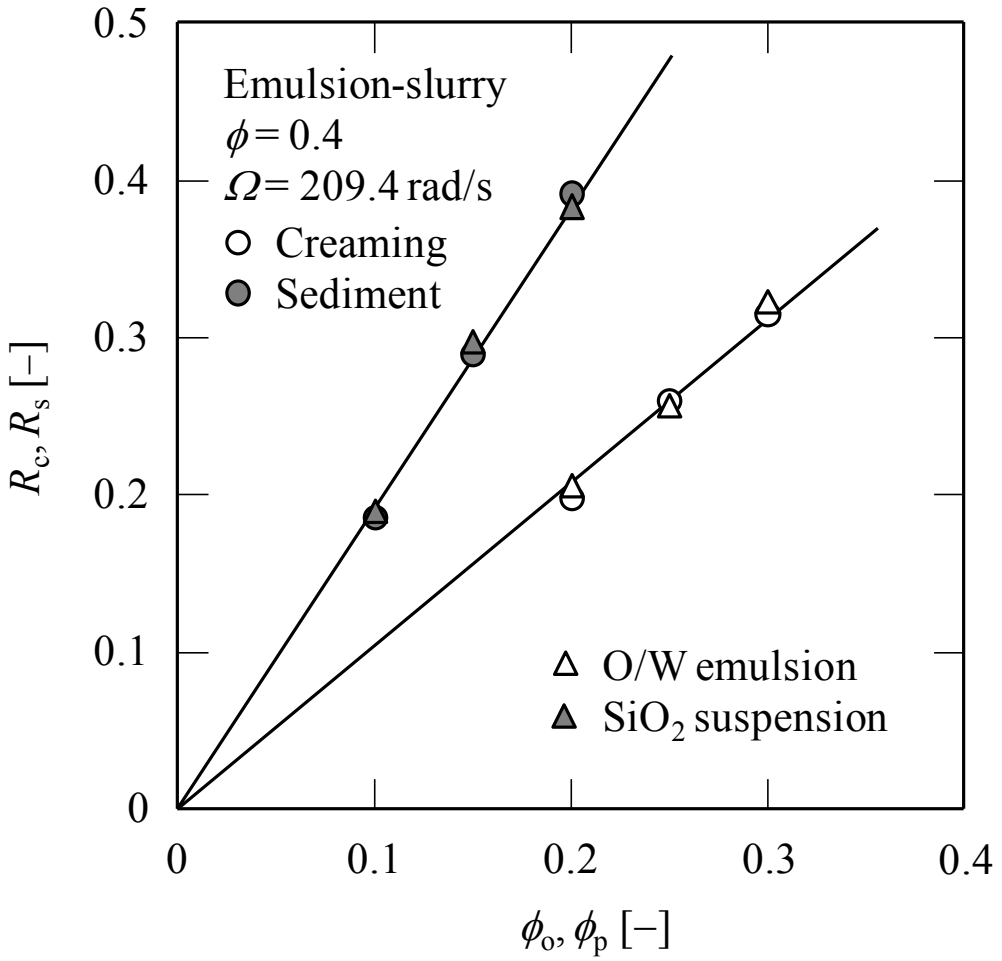

Fig. 4-6 Dependence of creaming and sediment heights of emulsion-slurry and single dispersion on volume fractions of oil droplets and SiO_2 particles after centrifugal equilibrium

for centrifugal sedimentation. The flotation or sedimentation coefficient S is a characteristic constant having the unit of time for the emulsion-slurry of a certain concentration and means the flotation or sedimentation rate for a unit centrifugal acceleration (Moore, 1972).

In **Figure 4-7**, the profiles of the flotation coefficient S_o of oil droplets floating through emulsion-slurry are illustrated against the volume fraction ϕ_p of SiO_2 particles with the volume fraction ϕ_o of oil droplets as the parameter. It should be noted that the flotation coefficient S_o increases with increasing volume fraction ϕ_p when ϕ_o remains constant. This may be explained by the increase in the density difference between the oil droplets and SiO_2 suspension on the oil free basis, resulting from the increase in the volume fraction ϕ_p of SiO_2 particles (Robinson, 1926; Steinour, 1944; Felice, 2000). Besides, the results at different values of the angular velocity Ω were included in the figure under the condition of ϕ_o of 0.20, and it is confirmed that the flotation coefficients is independent of Ω.

In order to analyze the acceleration effect of flotation coefficient S_o caused by the increase in SiO_2 concentration, the decrease in S_o with increasing ϕ_o was examined based on experiments when φ_p is kept constant, where φ_p is the volume fraction of SiO_2 particles on the oil free basis defined as

$$\varphi_p = \frac{\phi_p}{1-\phi_o} \tag{4-2}$$

In **Figure 4-8**, the flotation coefficient S_o of oil droplets are logarithmically plotted against the void $(1 - \phi_o)$ relative to oil droplets for different values of φ_p. It is found from the figure that S_o is related to $(1 - \phi_o)$ by (Richardson and Zaki, 1954; Maude and Whitmore, 1958; Yan and Masliyah, 1997)

$$S_o = S_{o1}(1-\phi_o)^{n_1} \tag{4-3}$$

where S_{o1} and n_1 are experimental constants. An outstanding result is found from the

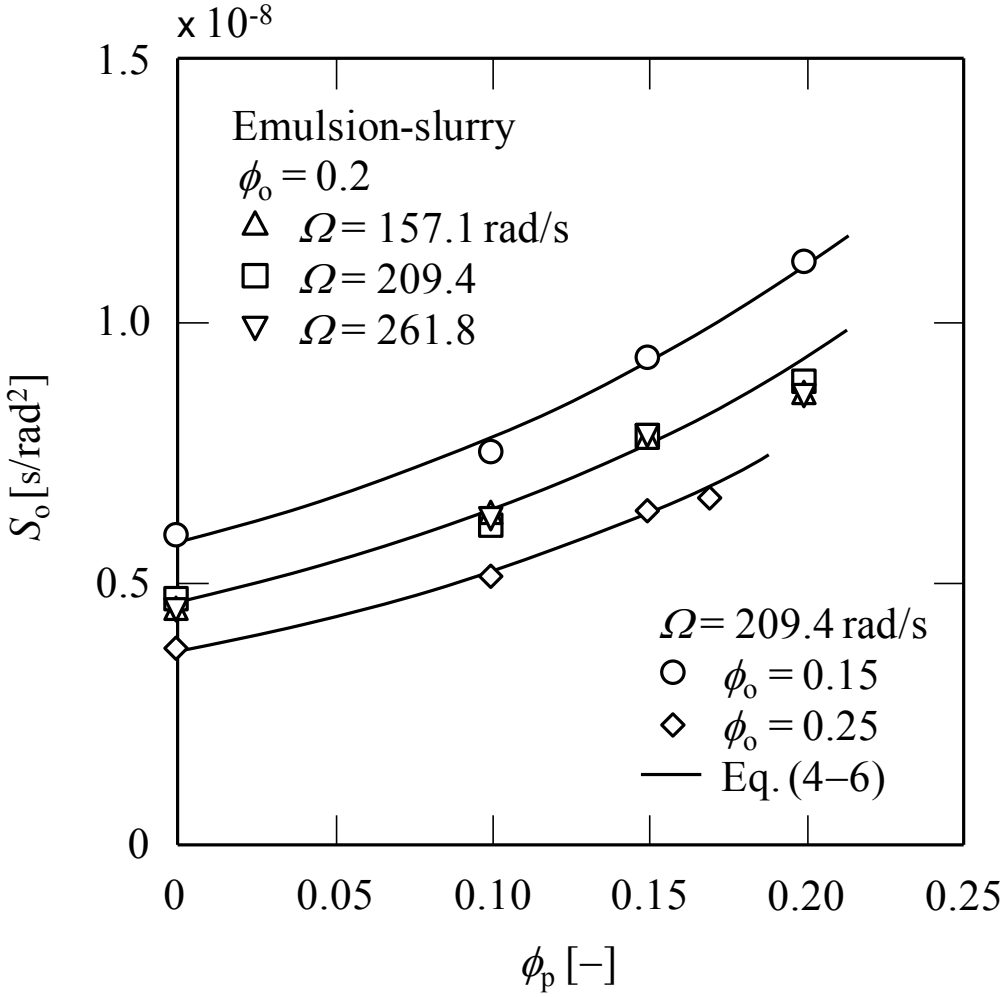

Fig. 4-7 Effect of volume fraction of SiO_2 particles on flotation coefficient of oil droplets in emulsion-slurry at different values of volume fraction of oil droplets

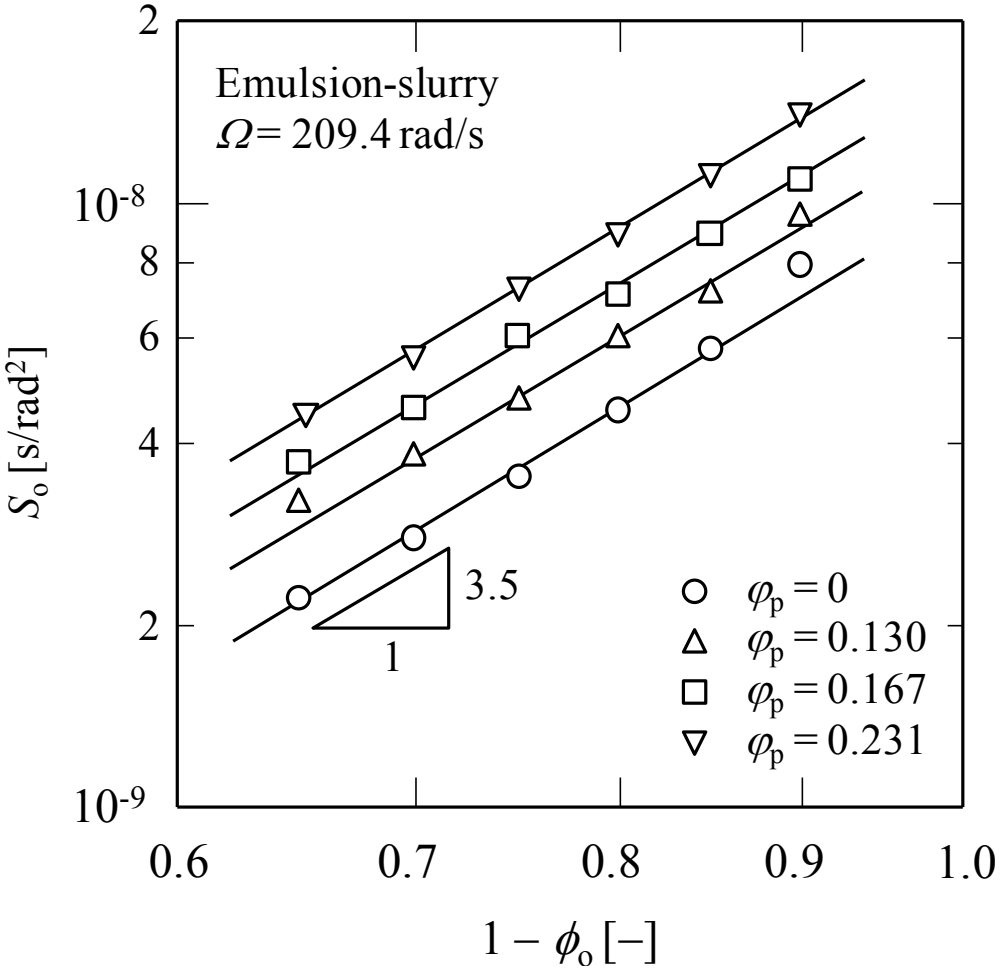

Fig. 4-8 Relation between flotation coefficient of oil droplets and void relative to oil droplets in emulsion-slurry at different values of volume fraction of SiO_2 particles on oil free basis

figure that the slopes n_1 of plots are unaltered regardless of the values of φ_p.

It is expected that S_{o1} should be the function of φ_p by considering the flotation of oil droplets rising through the particulate slurry which can be treated as a continuum fluid. In **Figure 4-9**, S_{o1} is plotted logarithmically against $(1-\varphi_p)$. Plots can be approximated by a linear relationship in the range tested, in accordance with

$$S_{o1} = S_{p0}(1-\varphi_p)^{m_1} \tag{4-4}$$

where S_{p0} and m_1 are experimental constants. Substituting Eq. (4-4) into Eq. (4-3), one obtains

$$S_o = S_{p0}(1-\varphi_p)^{m_1}(1-\phi_o)^{n_1} \tag{4-5}$$

With the aid of Eq. (4-2), Eq. (4-5) reduces to

$$S_o = S_{p0}(1-\phi_o-\phi_p)^{m_1}(1-\phi_o)^{n_1-m_1} \tag{4-6}$$

It is interesting to note that S_o is represented by two types of void functions, $(1-\phi_o-\phi_p)^{m_1}$ and $(1-\phi_o)^{n_1-m_1}$. In this study, $S_{p0} = 1.03\times10^{-8}$ s·rad^{-2}, $m_1 = -2.41$, $n_1 = 3.50$. The solid lines shown in Figure 4-7 are the calculations obtained from Eq. (4-6) by using these values and are in relatively good agreement with the experimental data.

Subsequently, the effect of particles added in O/W emulsion of a certain volume concentration on the flotation coefficient of oil droplets was investigated with varying the volume fraction of particles, keeping φ_o constant, where φ_o is the volume fraction of oil droplets on the particles free basis defined as

$$\varphi_o = \frac{\phi_o}{1-\phi_p} \tag{4-7}$$

Figure 4-10 shows the variations of the flotation coefficient S_o of oil droplets with the volume fraction ϕ_p of SiO_2 particles for different values of φ_o. The lines are the calculations obtained on the basis of Eqs. (4-6) and (4-7) and are in fairly good agreement

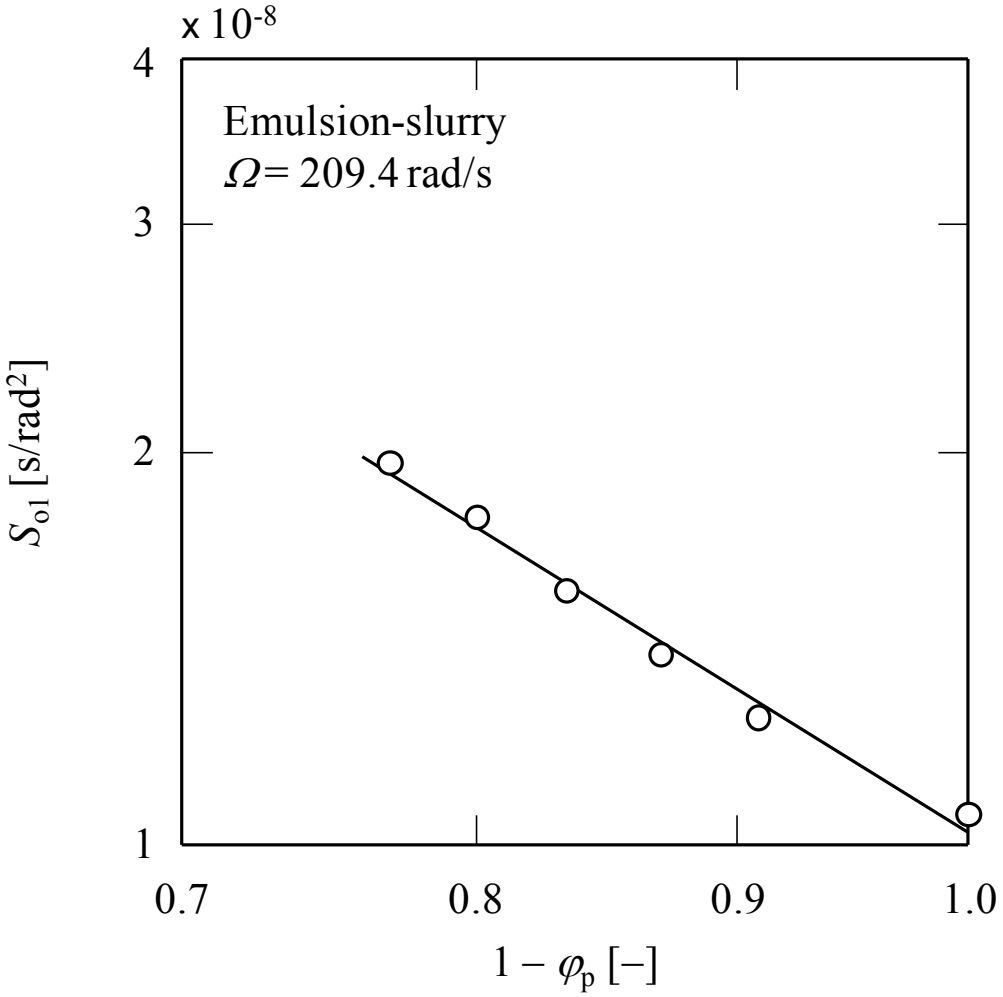

Fig. 4-9 Relation between S_{o1} in Eq. (4-3) and volume fraction of SiO_2 particles on oil free basis

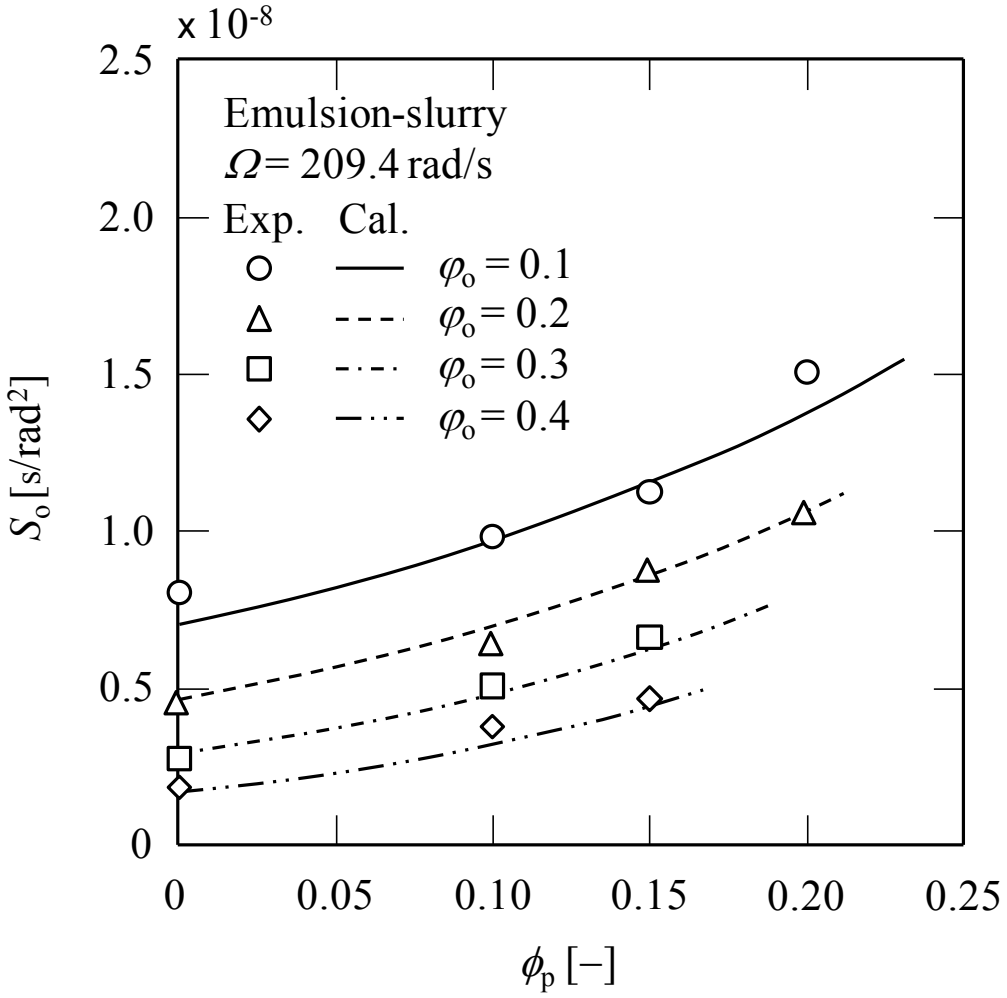

Fig. 4-10 Variation of flotation coefficient of oil droplets with volume fraction of SiO_2 particles for different values of volume fraction of oil droplets defined by Eq. (4-7)

with the experimental data except the individual points, indicating that Eq. (4-6) accurately describes the centrifugal flotation behavior of oil droplets in emulsion-slurry. It is found from the figure that the flotation coefficient S_o of oil droplets increased with the increase in the additive amount of SiO_2 particles in O/W emulsion.

4.5 Centrifugal Sedimentation Behaviours of Particles in Emulsion-Slurry

Figure 4-11 shows the effect of the volume fraction ϕ_o of oil droplets on the sedimentation coefficient S_p of SiO_2 particles settling through emulsion-slurry for different values of volume fractions ϕ_p of SiO_2 particles. Similar to the results shown in Figure 4-7, the more concentrated the volume fraction ϕ_o of oil droplets is, the greater the sedimentation coefficient S_p of SiO_2 particles is, due to the presence of oil droplets, and S_p is not influenced by the angular velocity. However, such acceleration effect is more remarkable in the case of the flotation coefficient S_o (Figure 4-7) compared to that of the sedimentation coefficient S_p (Figure 4-11). This is because the increase in the density difference between oil droplets and emulsion-slurry with increasing volume fraction ϕ_p of SiO_2 particles, influencing the flotation of oil droplets, is larger than that of the density difference between SiO_2 particles and emulsion-slurry with increasing volume fraction ϕ_o of oil droplets, influencing the sedimentation of SiO_2 particles, in our experimental system (Robinson, 1926; Steinour, 1944).

Similar to Eq. (4-5) derived for the flotation coefficient S_o, the sedimentation coefficient S_p of SiO_2 particles are logarithmically plotted against the void $(1 - \phi_p)$ relative to SiO_2 particles for different values of φ_o, in **Figure 4-12**. It is found from the figure that S_p is related to $(1 - \phi_p)$ by

$$S_p = S_{p1}(1-\phi_p)^{n_2} \tag{4-8}$$

And the relationship between S_{p1} and $(1 - \varphi_o)$ can be represented by

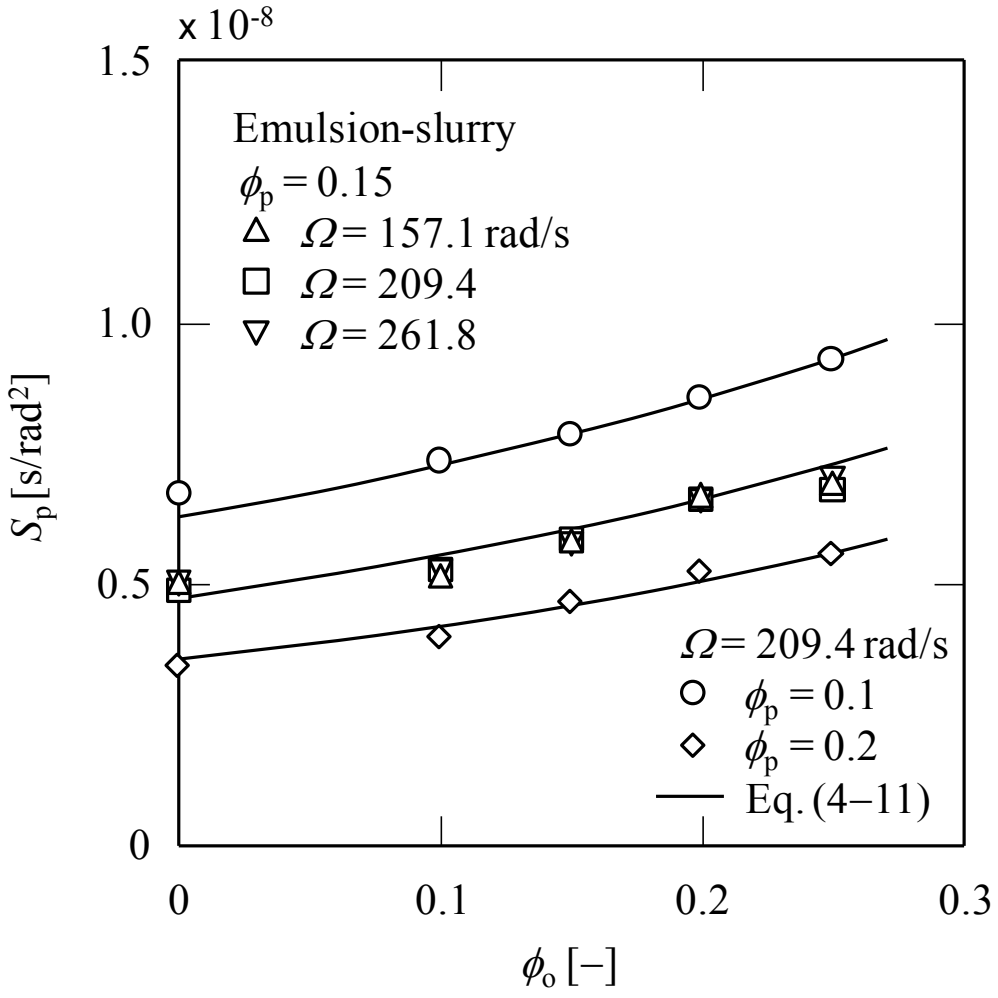

Fig. 4-11 Effect of volume fraction of oil droplets on sedimentation coefficient of SiO_2 particles in emulsion-slurry at different values of volume fraction of SiO_2 particles

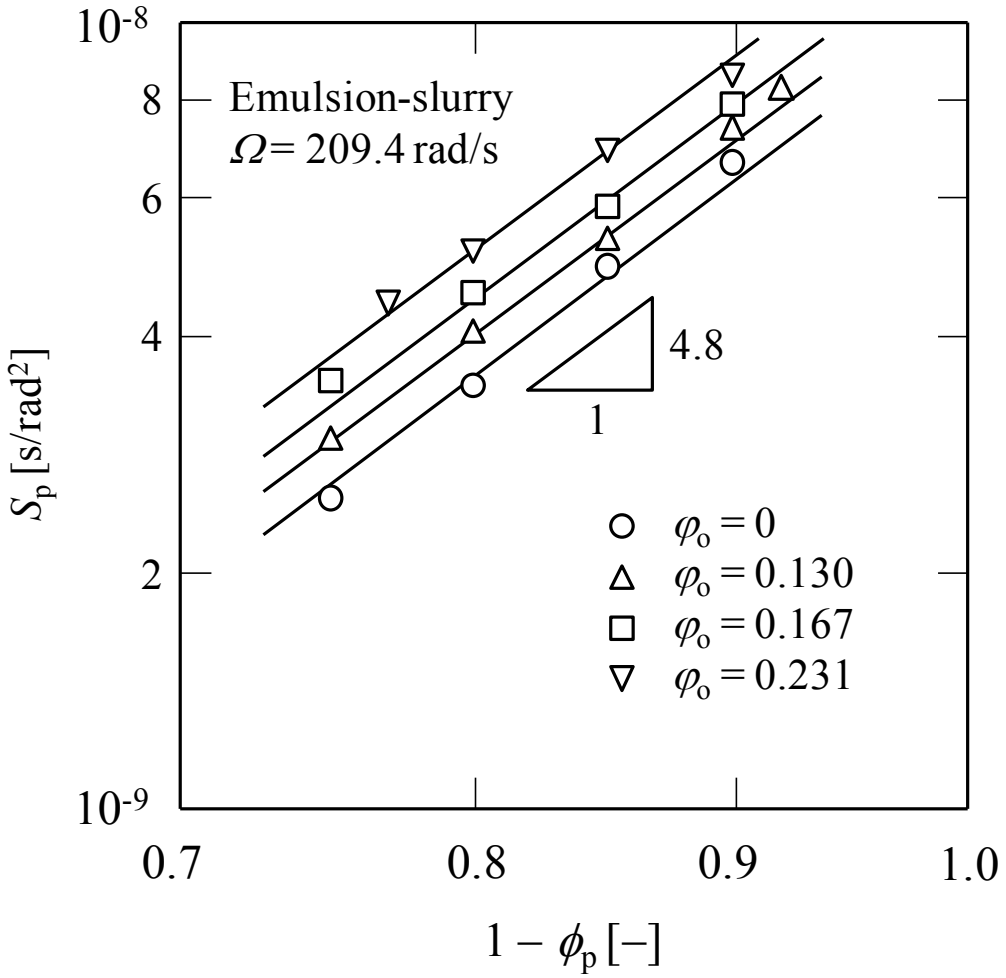

Fig. 4-12 Relation between flotation coefficient of SiO_2 particles and void relative to SiO_2 particles in emulsion-slurry at different values of volume fraction of oil droplets on particle free basis

$$S_{p1} = S_{o0}(1-\varphi_o)^{m_2} \tag{4-9}$$

as shown in **Figure 4-13**. Therefore, the sedimentation coefficient S_p of SiO_2 particles in emulsion-slurry were expressed as

$$S_p = S_{o0}(1-\varphi_o)^{m_2}(1-\phi_p)^{n_2} \tag{4-10}$$

where S_{o0}, m_2 and n_2 are experimental constants and are 1.05×10^{-8} s·rad^{-2}, –1.20, 4.80 in this study, respectively. The following expression can be obtained by substituting Eq. (4-7) into Eq. (4-10).

$$S_p = S_{o0}(1-\phi_o-\phi_p)^{m_2}(1-\phi_p)^{n_2-m_2} \tag{4-11}$$

The solid curves in Figure 4-11 are the calculations obtained using Eq. (4-11). The experimental results are in fairly good agreement with the calculations over the range tested except the individual points, indicating that Eq. (4-11) is available to describe the centrifugal sedimentation behavior of SiO_2 particles in emulsion-slurry.

4.6 Conclusions

In this chapter, the centrifugation experiments of emulsion-slurry which was the mixture of O/W emulsion and SiO_2 suspension were conducted under different experimental conditions by means of an analytical centrifuge with a NIR light source, and each of O/W emulsion and SiO_2 suspension were also employed in experiments for comparison. As a result, it was confirmed that the oil droplets and SiO_2 particles in emulsion-slurry were separated completely after centrifugation. The flotation and sedimentation coefficients in centrifugal separation of emulsion-slurry were uninfluenced by the centrifugal acceleration. The acceleration effect is more remarkable in the case of the flotation coefficient although the flotation and sedimentation coefficients are both increased with increasing volume fraction of SiO_2 particles or oil droplets in emulsion-slurry. The flotation and sedimentation coefficients were represented by using

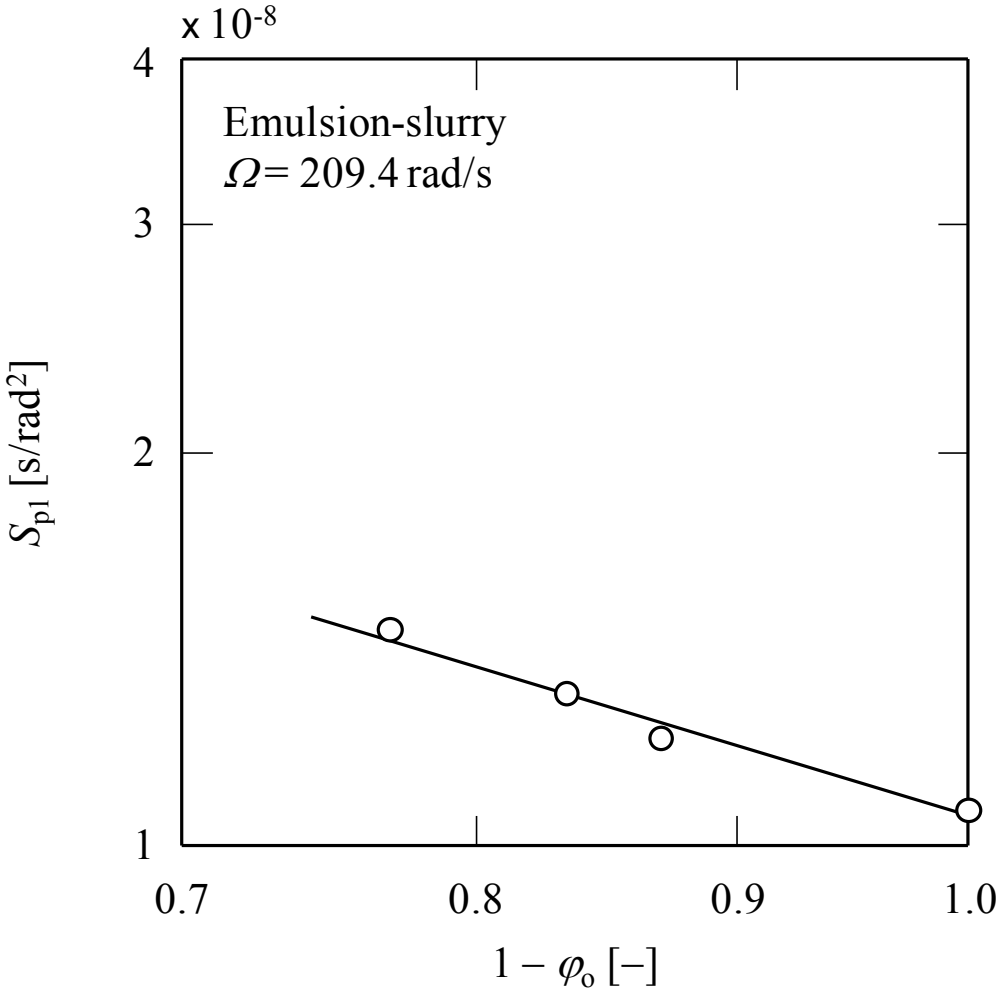

Fig. 4-13 Relation between S_{p1} in Eq. (4-8) and volume fraction of oil droplets on particle free basis

two types of void functions and were shown to account correctly for the acceleration effect in centrifugal separation of emulsion-slurry. The obtained results indicated that the centrifugation is effective for the separation of O/W emulsion containing solid particles which is often encountered in wastewater treatment of industries producing cosmetics, pharmaceuticals, agrochemicals and paints due to the smaller density of oil droplets and the larger density of solid particles than the continuous phase.

Chapter 5 Conclusions

In this study, the mechanical solid-liquid separations related to O/W emulsion were investigated. First, the evaluation of filtration properties and properties of filter cake in membrane filtration of O/W emulsion were revealed. Second, flotation and sedimentation properties in centrifugal separation of O/W emulsion containing solid particles were discussed. The following results were obtained from the studies:

1) Dead-end constant pressure microfiltration experiments under both modes of upward and downward were conducted in order to obtain the filtration characteristic values in membrane filtration of O/W emulsion. Ruth plots showed a non-linear relationship in conventional downward filtration because cake exfoliation occurred. However, Ruth plots showed a linear relationship in upward filtration because cake exfoliation did not occur. It was found that the values of the infinite average specific cake resistance obtained in both filtration modes were very different and the values of downward filtration were less than the true values. The formed cake properties was able to be evaluated more correctly in upward filtration because the effect of cake exfoliation was not contained in the values of specific cake resistance calculated, and therefore it was concluded that the upward dead-end filtration test was quite effective for evaluation of filtration properties in membrane filtration of O/W emulsion (Chapter 2).

2) Upward filtration tests accompanied with a sudden reduction in the cake surface area were conducted under constant pressure conditions, in order to accurately evaluate cake properties as reflected by the average porosity ε_{av} and the average specific cake resistance α_{av}. For comparison, downward filtration tests were also conducted. The calculated values of the average specific cake resistance α_{av} became lower in downward filtration although the calculated values of the average volume fraction $(1 - \varepsilon_{av})$ of oil droplets obtained based on a dead-end filtration mechanism were higher in downward

filtration. This was because the influence of the cake exfoliation was not able to be ruled out in downward filtration. It was found that the determination of cake properties based on downward filtration may lead to erroneous results. Therefore, it is suggested that the upward dead-end filtration test accompanied with a sudden reduction in the cake surface area is particularly suitable for evaluating cake properties in membrane filtration of O/W emulsions (Chapter 3).

3) The centrifugation experiments of emulsion-slurry which was the mixture of O/W emulsion and SiO_2 suspension were conducted under different experimental conditions by means of an analytical centrifuge with a NIR light source, and each of O/W emulsion and SiO_2 suspension were also employed in experiments for comparison. As a result, it was confirmed that the oil droplets and SiO_2 particles in emulsion-slurry were separated completely after centrifugation. The flotation and sedimentation coefficients in centrifugal separation of emulsion-slurry were uninfluenced by the centrifugal acceleration. The acceleration effect is more remarkable in the case of the flotation coefficient although the flotation and sedimentation coefficients are both increased with increasing volume fraction of SiO_2 particles or oil droplets in emulsion-slurry. The flotation and sedimentation coefficients were represented by using two types of void functions and were shown to account correctly for the acceleration effect in centrifugal separation of emulsion-slurry (Chapter 4).

Author expects that the present research results about the mechanical solid-liquid separations of O/W emulsion can give some contribution for separation of O/W emulsion. As the extension of this study, ultrafiltration, centrifugation and compression experiments will be carried out using various O/W emulsions such as surfactant-stabilized O/W emulsion and nanoparticle-stabilized O/W emulsion (Pickering O/W emulsion), which has been a completely unexplored research field.

Nomenclature

a	=	gravitational or centrifugal acceleration	[m/s^2]
B	=	empirical constant defined in Eq. (1-5)	[kg$^{-\beta}$·m$^{\beta}$·s$^{2\beta}$]
d	=	diameter of sphere	[m]
D	=	inner diameter of inserted cylinder	[m]
D_h	=	diameter of hole	[m]
d_o	=	mean specific surface area size of oil droplets	[m]
d_p	=	mean specific surface area size of SiO_2 particles	[m]
g	=	gravitational acceleration	[m/s^2]
h	=	distance from membrane surface to suddenly-reduced surface	[m]
K_v	=	Ruth filtration coefficient defined by Eq. (1-2)	[m^2/s]
m	=	ratio of mass of wet to mass of dry cake	[–]
m_1	=	experimental constant defined in Eq.(4-4)	[–]
m_2	=	experimental constant defined in Eq.(4-9)	[–]
N	=	exponent defined in Eq. (1-11)	[–]
n	=	compressibility coefficient defined in Eq. (1-4)	[–]
n_1	=	experimental constant defined in Eq.(4-3)	[–]
$n_{1,i}$	=	apparent compressibility coefficient defined in Eq. (2-3)	[–]
n_2	=	experimental constant defined in Eq.(4-8)	[–]
p	=	applied filtration pressure	[Pa]
p_m	=	pressure drop across filter medium	[Pa]
q_1	=	filtration rate	[m/s]
R_c	=	ratio of creaming height for emulsion-slurry and emulsion to initial height of dispersions	[–]
R_m	=	resistance of filter medium	[m^{-1}]

R_s	=	ratio of sediment height for emulsion-slurry and SiO_2 suspension to initial height of dispersions	[–]
r	=	radial distance of an arbitrary position from center of rotation	[m]
r_1	=	radial distance from center of rotation to bottom of sample filled in cell	[m]
r_2	=	radial distance from center of rotation to the top of sample filled in cell	[m]
r_c	=	radial distance from center of rotation to critical interface where flotation and sedimentation interfaces arise for the first time simultaneously	[m]
r_i	=	radial distance from center of rotation to interface of dispersion and clear liquid	[m]
s	=	mass fraction of oil droplets in emulsion	[–]
S	=	flotation or sedimentation coefficient	[s/rad^2]
S_o	=	flotation coefficient	[s/rad^2]
S_{o0}	=	empirical constant defined in Eq. (4-9)	[s/rad^2]
S_{o1}	=	empirical constant defined in Eq. (4-3)	[s/rad^2]
S_p	=	sedimentation coefficient	[s/rad^2]
S_{p0}	=	empirical constant defined in Eq. (4-4)	[s/rad^2]
S_{p1}	=	empirical constant defined in Eq. (4-8)	[s/rad^2]
t	=	centrifugal time	[s]
t_c	=	critical time when flotation and sedimentation interfaces arise for the first time simultaneously	[s]
T	=	NIR light transmission	[–]
v	=	cumulative filtrate volume collected per unit effective membrane area	[m]

v_m	=	fictitious filtrate volume per unit effective membrane area, equivalent to flow resistance of membrane	[m]
v_t	=	cumulative filtrate volume per unit effective membrane area collected until filter cake surface reaches reduced surface	[m]
w	=	net solid mass of entire filter cake per unit effective membrane area	[kg/m^2]

Greek letters

α_l	=	empirical constant defined in Eq. (1-4)	[kg^{-1-n}·m^{1+n}·s^{2n}]
$\alpha_{l,i}$	=	empirical constant defined in Eq. (2-3)	[kg$^{-1-n_{l,i}}$·m$^{1+n_{l,i}}$·s$^{2n_{l,i}}$]
α_{av}	=	average specific cake resistance	[m/kg]
$\alpha_{av,i}$	=	infinite average specific cake resistance in Eq. (2-1)	[m/kg]
β	=	empirical constant defined in Eq. (1-5)	[–]
ε_{av}	=	average porosity of filter cake	[–]
θ	=	filtration time	[s]
μ	=	viscosity of filtrate	[Pa·s]
ρ	=	density of filtrate	[kg/m^3]
ρ_l	=	density of water	[kg/m^3]
ρ_o	=	density of oil droplets	[kg/m^3]
ρ_p	=	density of SiO_2 particles	[kg/m^3]
ϕ	=	total volume fraction of oil droplets and SiO_2 particles in emulsion-slurry	[–]
ϕ_o	=	volume fraction of oil droplets in emulsion-slurry	[–]
ϕ_p	=	volume fraction of SiO_2 particles in emulsion-slurry	[–]
φ_o	=	volume fraction of oil droplets on particle free basis	[–]
φ_p	=	volume fraction of SiO_2 particles on oil free basis	[–]
Ω	=	angular velocity of rotor	[rad/s]

Subscript

m = filter medium

References

Abe, E., H. Hirosue and K. Yokota; "Pressure Drop through a Packed Bed of Binary Mixture," *J. Chem. Eng. Japan*, **12**, 302-306 (1979)

Al-Naafa, M. A. and M. S. Selim; "Sedimentation of Monodisperse and Bidisperse Hard-Sphere Colloidal Suspensions," *AIChE J.*, **38**, 1618-1630 (1992)

Al-Shamrani, A. A., A. James and H. Xiao; "Destabilisation of Oil-Water Emulsions and Separation by Dissolved Air Flotation," *Water Res.*, **36**, 1503-1512 (2002)

Aveyard, R., B. P. Binks and J. H. Clint; "Emulsions Stabilised Solely by Colloidal Particles," *Adv. Colloid Interf. Sci.*, **100-102**, 503-546 (2003)

Beydoun, D., D. Guang, R. P. Chhabra and J. A. Raper; "Particle Settling in Oil-in-Water Emulsions," *Powder Technol.*, **97**, 72-76 (1998)

Binks, B. P. and S. O. Lumsdon; "Stability of Oil-in-Water Emulsions Stabilised by Silica Particles," *Phys. Chem. Chem. Phys.*, **1**, 3007-3016 (1999)

Binks, B. P.; "Particles as Surfactants – Similarities and Differences," *Curr. Opin. Colloid Interf. Sci.*, **7**, 21-41 (2002)

Binner, E. R., J. P. Robinson, S. W. Kingman, E. H. Lester, B. J. Azzopardi, G. Dimitrakis and J. Briggs; "Separation of Oil/Water Emulsions in Continuous Flow Using Microwave Heating," *Energy Fuels*, **27**, 3173-3178 (2013)

Carman, P. C.; "Fluid Flow through Granular Beds," *Trans. Inst. Chem. Eng.*, **15**, 150-166 (1937)

Cao, D. Q., E. Iritani and N. Katagiri; "Evaluation of Filtration Properties in Membrane Filtration of O/W Emulsion Based on Upward Dead-End Constant Pressure Filtration," *Kagaku Kogaku Ronbunshu*, **38**, 378-383 (2012)

Cao, D. Q., E. Iritani and N. Katagiri; "Properties of Filter Cake Formed during Dead-End Mirofiltration of O/W Emulsion," *J. Chem. Eng. Japan*, **46**, 593-600

(2013)

Cao, D. Q., E. Iritani and N. Katagiri; “Flotation and Sedimentation Properties in Centrifugal Separation of Emulsion-Slurry,” *J. Chem. Eng. Japan*, **47**, 392-398 (2014)

Chakrabarty, B., A. K. Ghoshal and M. K. Purkait; “Cross-Flow Ultrafiltration of Stable Oil-in-Water Emulsion Using Polysulfone Membranes,” *Chem. Eng. J.*, **165**, 447-456 (2010)

Chanamai, R. and D. J. McClements; “Creaming Stability of Flocculated Monodisperse Oil-in-Water Emulsions,” *J. Colloid Interface Sci.*, **225**, 214-218 (2000)

Chellappah, K., E. S. Tarleton and R. J. Wakeman; “Aggregation Effects in the Cake Filtration of Interacting Binary Mixtures,” *Chem. Eng. Sci.*, **65**, 6407-6414 (2010)

Chen, E. S., S. Gohtani, T. Nakashima and Y. Yamano; “Creaming Rate of O/W Emulsion,” *J. Japan. Oil Chem. Soc.* (*Yukagaku*), **42**, 972-977 (1993)

Chen, X., L. Hong, Y. Xu and Z. W. Ong; “Ceramic Pore Channels with Inducted Carbon Nanotubes for Removing Oil from Water,” *ACS Appl. Mater. Interf.*, **4**, 1909-1918 (2012)

Cheung, M. K., R. L. Powell and M. J. McCarthy; “Sedimentation of Noncolloidal Bidisperse Suspensions,” *AIChE J.*, **42**, 271-276 (1996)

Christensen, G. L. and R. I. Dick; “Specific Resistance Measurements: Nonparabolic Data,” *J. Environ. Eng. ASCE*, **111**, 243-257 (1985)

Christensen, M. L., C. Johansson, M. Sedin and K. Keiding; “Nonlinear Filtration Behavior of Soft Particle: Effect of Dynamic Cake Compression,” *Powder Technol.*, **207**, 428-436 (2011)

Dorrell, R. and A. J. Hogg; “Sedimentation of Bidisperse Suspensions,” *Int. J. Multiphase Flow*, **36**, 481-490 (2010)

Faibish, R. S. and Y. Cohen; “Fouling and Rejection Behavior of Ceramic and

Polymer-Modified Ceramic Membranes for Ultrafiltration of Oil-in-Water Emulsions and Microemulsions," *Colloid Surfaces A: Physicochem. Eng. Aspects*, **191**, 27-40 (2001)

Falahati, H. and A. Y. Tremblay; "Flux Dependent Oil Permeation in the Ultrafiltration of Highly Concentrated and Unstable Oil-in-Water Emulsions," *J. Membr. Sci.*, **371**, 239-247 (2011)

Felice, R. D.; "The Pseudo-Fluid Model Applied to Three-Phase Fluidisation," *Chem. Eng. Sci.*, **55**, 3899-3906 (2000)

Feng, D. and C. Aldrich; "Removal of Diesel from Aqueous Emulsions by Flotation," *Sep. Sci. Technol.*, **35**, 2159-2172 (2000)

Fessas, Y. P. and R. H. Weiland; "Convective Solids Settling Induced by a Buoyant Phase," *AIChE J.*, **27**, 588-592 (1981)

Fessas, Y. P. and R. H. Weiland; "The Settling of Suspensions Promoted by Rigid Buoyant Particles," *Int. J. Multiphase Flow*, **4**, 485-507 (1984)

Field, R. W., D. Wu, J. A. Howell and B. B. Gupta; "Critical Flux Concept for Microfiltration Fouling," *J. Membr. Sci.*, **100**, 259-272 (1995)

Grace H. P.; "Structure and Performance of Filter Media. II. Performance of Filter Media in Liquid Service," *AIChE J.*, **2**, 316-336 (1956)

Gray, S. R., P. J. Harbour and D. R. Dixon; "Effect of Polyelectrolyte Charge Density and Molecular Weight on the Flotation of Oil in Water Emulsions," *Colloids Surfaces A: Physicochem. Eng. Aspects*, **126**, 85-95 (1997)

Gutiérrez, G., A. Lobo, J. M. Benito, J. Coca and C. Pazos; "Treatment of a Waste Oil-in-Water Emulsion from a Copper-Rolling Process by Ultrafiltration and Vacuum Evaporation," *J. Hazard. Mater.*, **185**, 1569-1574 (2011)

Happel, J.; "Viscous Flow in Multiparticles Systems: Slow Motion of Fluids Relative to Beds of Spherical Particles," *AIChE J.*, **4**, 197-201 (1958)

Headen, T. F., S. M. Clarke, A. Perdigon, G. H. Meeten, J. D. Sherwood and M. Aston; "Filtration of Deformable Emulsion Droplets," *J. Colloid Interf. Sci.*, **304**, 562-565 (2006)

Heitkam, S., Y. Yoshitake, F. Toquet, D. Langevin and A. Salonen; "Speeding Up of Sedimentation under Confinement," *Phys. Rev. Lett.*, **110**, 178302 (2013)

Hesampour, M., A. Krzyzaniak and M. Nyström; "The Influence of Different Factors on the Stability and Ultrafiltration of Emulsified Oil in Water," *J. Membr. Sci.*, **325**, 199-208 (2008)

Ho W. W. and K. Li; "Recent Advances in Separations," *Curr. Opin. Chem. Eng.*, **2**, 1-2 (2013)

Hoshino, T., M. Kasahara and H. Yukawa; "Characteristics and Equation of Filtration of O/W Emulsion with Glass-Fiber Filter Paper under Constant Pressure," *Kagaku Kogaku Ronbunshu*, **10**, 454-460 (1984)

Hoyos, M., J. C. Bacri, J. Martin and D. Salin; "A Study of the Sedimentation of Noncolloidal Bidisperse, Concentrated Suspensions by an Acoustic Technique," *Phys. Fluids*, **6**, 3809-3817 (1994)

Hwang, K. J., Y. T. Wang, E. Iritani and N. Katagiri; "Effects of Porous Gel Particle Compression on Microfiltration Characteristics," *J. Membr. Sci.*, **341**, 286-293 (2009)

Hwang, K. J., Y. T. Wang, E. Iritani and N. Katagiri; "Effect of Gel Particles Softness on the Performance of Cross-Flow Microfiltration," *J. Membr. Sci.*, **365**, 130-137 (2010)

Hwang, K. J. an P. Y. Sz; "Membrane Fouling Mechanism and Concentration Effect in Cross-flow Microfiltration of BSA/Dextran Mixtures," *Chem. Eng. J.*, **166**, 669-677 (2011)

Iritani, E., S. Nakatsuka, H. Aoki and T. Murase; "Effect of Solution Environment on

Unstirred Dead-End Ultrafiltration Characteristics of Proteinaceous Solutions," *J. Chem. Eng. Japan*, **24**, 177-183 (1991a)

Iritani, E., T. Hayashi and T. Murase; "Analysis of Filtration Mechanism of Crossflow Upward and Downward Ultrafiltration," *J. Chem. Eng. Japan*, **24**, 39-44 (1991b)

Iritani, E., T. Watanabe and T. Murase; "Upward and Inclined Ultrafiltration under Constant Pressure by Use of Dead-End Filter," *Kagaku Kogaku Ronbunshu*, **17**, 206-209 (1991c)

Iritani, E., T. Watanabe and T. Murase; "Effects of pH and Solvent Density on Dead-End Upward Ultrafiltration," *J. Membr. Sci.*, **69**, 87-97 (1992a)

Iritani, E., K. Ohashi and T. Murase; "Analysis of Filtration Mechanism of Dead-End Electro-Ultrafiltration for Proteinaceous Solutions," *J. Chem. Eng. Japan*, **25**, 383-388 (1992b)

Iritani, E., K. Hattori and T. Murase; "Analysis of Dead-End Ultrafiltration Based on Ultracentrifugation Method," *J. Membr. Sci.*, **81**, 1-13 (1993)

Iritani, E., Y. Mukai and T. Murase; "Properties of Filter Cake in Dead-End Ultrafiltration of Binary Protein Mixtrues with Retentive Memranes," *Trans. IChemE*, **73A**, 551-558 (1995a)

Iritani, E., Y. Mukai and T. Murase; "Upward Dead-End Ultrafiltration of Binary Protein Mixtures," *Sep. Sci. Technol.*, **30**, 369-382 (1995b)

Iritani, E., H. Nagaoka and T. Murase; "Filtration Characteristics and Cake Properties in Microfiltration of Binary Mixtures of Fine Particles," *Kagaku Kogaku Ronbunshu*, **22**, 648-654 (1996)

Iritani, E., Y. Mukai and H. Yorita; "Effect of Sedimentation on Properties of Upward and Downward Cake Filtration," *Kagaku Kogaku Ronbunshu*, **25**, 742-746 (1999)

Iritani, E., Y. Mukai and Y. Kiyotomo; "Effects of Electric Field on Dynamic Behaviors of Dead-End Inclined and Downward Ultrafitration of Protein Solutions," *J. Membr.*

Sci., **164**, 51-57 (2000)

Iritani, E., Y. Mukai and Y. Toyoda; "Properties of a Filter Cake Formed in Dead-End Microfiltration of Binary Particulate Mixtures," *J. Chem. Eng. Japan*, **35**, 226-233 (2002a)

Iritani, E., Y. Mukai and E. Hagihara; "Measurements and Evaluation of Concentration Distributions in Filter Cake Formed in Dead-End Ultrafiltration of Protein Solutions," *Chem. Eng. Sci.*, **57**, 53-62 (2002b)

Iritani, E., Y. Mukai, N. Katagiri and I. Yoshii; "Formation of Gel Emulsions by Filtration-Consolidation of O/W Emulsions," *J. Chem. Eng. Japan*, **36**, 590-596 (2003)

Iritani, E., Y. Mukai, M. Furuta, T. Kawakami and N. Katagiri; "Blocking Resistance of Membrane during Cake Filtration of Dilute Suspensions," *AIChE J.*, **51**, 2609-2614 (2005)

Iritani, E., N. Katagiri, K. Aoki, M. Shimamoto and J. H. Cho; "Compression Characteristics of Consolidated Deposits Formed in Centrifugation of Soft and Hard Colloids," *Kagaku Kogaku Ronbunshu*, **33**, 553-560 (2007a)

Iritani, E., N. Katagiri, K. Aoki, M. Shimamoto and K. M. Yoo; "Determination of Permeability Characteristics from Centrifugal Flotation Velocity of Deformable Oil Droplets in O/W Emulsions," *Sep. Purif. Technol.*, **58**, 247-255 (2007b)

Iritani, E., N. Katagiri, Y. Sugiyama and K. Yagishita; "Analysis of Flux Decline Behaviors in Filtration of Very Dilute Suspensions," *AIChE*, **53**, 2275-2283 (2007c)

Iritani, E., S. Matsumoto and N. Katagiri; "Formation and Consolidation of Filter Cake in Microfiltration of Emulsion-Slurry," *J. Membr. Sci.*, **318**, 56-64 (2008a)

Iritani, E., H. Nagaoka and N. Katagiri; "Determination of Filtration Characteristics of Yeast Suspension Based upon Multistage Reduction in Cake Surface Area under Step-Up Pressure Conditions," *Sep. Purif. Technol.*, **63**, 379-385 (2008b)

Iritani, E., N. Katagiri, T. Tadama and H. Sumi; “Analysis of Clogging Behaviors of Diatomaceous Ceramic Membranes during Membrane Filtration Based upon Specific Deposit,” *AIChE J.*, **57**, 1748-1758 (2010a)

Iritani, E., T. Sato, N. Katagiri and K. J. Hwang; “Multi-Stage Creep Effect in Consolidation of Tofu and Okara as Soft Colloids,” *J. Chem. Eng. Japan*, **43**, 140-149 (2010b)

Iritani, E., N. Katagiri, Y. Takaishi and S. Kanetake; “Determination of Pressure Dependence of Premeability Characteristics from Single Constant Pressure Filtration Test,” *J. Chem. Eng. Japan*, **44**, 14-23 (2011)

Iritani, E., N. Katagiri and S. Kanetake; “Determination of Cake Filtration Characteristics of Dilute Suspension of Bentonite from Various Filtration Tests,” *Sep. Purif. Technol.*, **92**, 143-151 (2012a)

Iritani, E., N. Katagiri and D. Nakano; “Flux Decline Behaviors in Inclined Dead-End Ultrafiltration of BSA Solutions,” *Chem. Eng. J.*, **184**, 98-105 (2012b)

Iritani, E., N. Katagi, K. Okada, D. Q. Cao and K. Kawasaki; “Improvement of Concentration Performance in Shaking Type of Freeze Concentration,” *Sep. Purif. Technol.*, 120, 445-451 (2013)

Iritani, E., N. Katagiri, M. Tsukamoto and K. J. Hwang; “Determination of Cake Properties in Ultrafiltration of Nano-colloids Based on Single Step-up Pressure Filtration Test,” *AIChE J.*, **60**, 289-299 (2014a)

Iritani, E., N. Katagiri, Y. Ishikawa and D. Q. Cao; “Cake Formation and Particle Rejection in Microfiltration of Binary Mixtures of Particles with Two Different Sizes,” *Sep. Purif. Technol.*, **123**, 214-220 (2014b)

Koltuniewicz, A. B., R. W. Field and T. C. Arnot; “Cross-Flow and Dead-End Microfiltration of Oily-Water Emulsion. Part I: Experimental Study and Analysis of Flux Decline,” *J. Membr. Sci.*, **102**, 193-207 (1995)

Koltuniewicz, A. B. and R. W. Field; "Process Factors during Removal of Oil-in-Water Emulsions with Cross-Flow Microfiltration," *Desalination*, **105**, 79-89 (1996)

Krishnamoorthy, P., I. Reghupathi and T. Murugesan; "An Experimental Study and Correlation for Differential Settling of Bidisperse Suspensions," *Chem. Biochem. Eng. Q.*, **21**, 241-250 (2007)

Lerche, D.; "Dispersion Stability and Particle Characterization by Sedimentation Kinetics in a Centrifugal Field," *J. Dispersion Sci. Technol.*, **23**, 699-709 (2002)

Lerche, D. and T. Sobisch; "Consolidation of Concentrated Dispersions of Nano- and Microparticles Determined by Analytical Centrifugation," *Powder Technol.*, **174**, 46-49 (2007)

Lerche, D. and T. Sobisch; "Direct and Accelerated Characterization of Formulation Stability," *J. Dispersion Sci. Technol.*, **32**, 1799-1811 (2011)

Li, L., L. Ding, Z. Tu, Y. Wan, D. Clausse and J. L. Lanoisellé; "Recovery of Linseed Oil Dispersed within an Oil-in-Water Emulsion Using Hydrophilic Membrane by Rotating Disk Filtration System," *J. Membr. Sci.*, **342**, 70-79 (2009)

Lipp, P., C. H. Lee, A. G. Fane and C. J. D. Fell; "A Fundamental Study of the Ultrafiltration of Oil-Water Emulsions," *J. Membr. Sci.*, **36**, 161-177 (1988)

Lockett, M. J. and H. M. Al-Habbooby; "Differential Settling by Size of Two Particles Species in a Liquid," *Trans. Inst. Chem. Eng.*, **51**, 281-292 (1973)

Lockett, M. J. and H. M. Al-Habbooby; "Relative Particle Velocities in Two-Species Settling," *Powder Technol.*, **10**, 67-71 (1974)

Loginov, M., M. Citeau, N. Lebovka and E. Vorobiev; "Evaluation of Low-Pressure Compressibility and Permeability of Bentonite Sediment from Centrifugal Consolidation Data," *Sep. Purif. Technol.*, **92**, 168-173 (2012)

Loginov, M., N. Lebovka and E. Vorobiev; "Dertermination of Filtration Properties of Mineral Suspensions from Analytical Centrifugation Data," *Filtration*, **13**, 58-64

(2013)

Lu, W. M. and S. C. Ju; "Selective Particle Deposition in Crossflow Filtration," *Sep. Sci. Technol.*, **24**, 517-540 (1989)

Lu, W. M., K. L. Tung, S. M. Hung, J. S. Shiau and K. J. Hwang; "Constant Pressure Filtration of Mono-Dispersed Deformable Particle Slurry," *Sep. Sci. Technol.*, **36**, 2355-2383 (2001)

Maruyama, H., H. Seki and Y. Satoh; "Removal Kinetic Model of Oil Droplet from O/W Emulsion by Adding Methylated Milk Casein in Flotation," *Water Res.*, **46**, 3094-3100 (2012)

Matos, M., A. Lobo, E. Fernández, J. M. Benito, C. Pazos and J. Coca; "Recycling of Oily Ultrafiltration Permeates to Reformulate O/W Emulsions," *Colloids Surfaces A: Physicochem. Eng. Aspects*, **331**, 8-15 (2008)

Matsumoto K., S. Hirata and H. Ohya; "Microfiltration Model Considering Incomplete Pore Blocking and Incomplete Capture of Particles by Cake," *Kagaku Kogaku Ronbushu*, **18**, 455-462 (1992)

Matsumoto, Y., T. Kawakatsu, M. Nakajima and Y. Kikuchi; "Visualization of Filtration Phenomena of a Suspended Solution Including O/W Emulsion or Solid Particle and Membrane Separation Properties of the Solution," *Water Res.*, **33**, 929-936 (1999)

Maude, A. D. and R. L. Whitmore; "A Generalized Theory of Sedimentation," *Brit. J. Appl. Phys.*, **9**, 477-482 (1958)

Mohammadi, T., M. Kazemimoghadam and M. Saadabadi; "Modeling of Membrane Fouling and Flux Decline in Reverse Osmosis during Separation of Oil in Water Emulsions," *Desalination*, **157**, 369-375 (2003)

Montel, V., V. Lazzeri, B. Brocart and H. Zhou; "Asphaltene Cake Properties," *Energy Fuels*, **22**, 3970-3975 (2008)

Moore, W. J.; Physical Chemistry, 4th ed., pp. 938-939, Prentice-Hall, Inc., New Jersey,

USA (1972)

Mueller, J., Y. Cen and R. H. Davis; “Crossflow Microfiltration of Oily Water,” *J. Membr. Sci.*, **129**, 221-235 (1997)

Murase, T., E. Iritani, J. H. Cho, S. Nakanomori, and M. Shirato; “Determination of Filtration Characteristics Due to Sudden Reduction in Filtration Area of Filter Cake Surface,” *J. Chem. Eng. Japan*, **20**, 246-251 (1987)

Murase, T., E. Iritani, S. Nakatsuka and M. Shirato; “Experimental Analysis of Mechanism of Batch Ultrafiltration under Constant Pressure,” *Kagaku Kogaku Ronbunshu*, **14**, 241-244 (1988)

Murase, T., E. Iritani, J. H. Cho and M. Shirato; “Determination of Filtration Characteristics Based upon Filtration Tests under Step-up Pressure Conditions,” *J. Chem. Eng. Japan*, **22**, 373-378 (1989)

Murase, T., T. Ohn and K. Kamimura; “Dynamic Microfiltration of Dilute O/W Emulsion in Rotating Cylindrical Membrane Filter,” *Kagaku Kogaku Ronbunshu*, **22**, 120-126 (1996)

Nandi, B. K., R. Uppaluri and M. K. Purkait; “Treatment of Oily Waste Water Using Low-Cost Ceramic Membrane: Flux Decline Mechanism and Economic Feasibility,” *Sep. Sci. Technol.*, **44**, 2840-2869 (2009)

Nandi, B. K., A. Moparthi, R. Uppaluri and M. K. Purkait; “Treatment of Oily Wastewater Using Low Cost Ceramic Membrane: Comparative Assessment of Pore Blocking and Artificial Neural Network Models,” *Chem. Eng. Res. Des.*, **88**, 881-892 (2010)

Pal, R. and J. Masliyah; “Oil Recovery from Oil in Water Emulsion Using a Flotation Column,” *Can. J. Chem. Eng.*, **68**, 959-967 (1990)

Pan, Y., T. Wang, H. Sun and W. Wang; “Preparation and Application of Titanium Dioxide Dynamic Membranes in Microfiltration of Oil-in-Water Emulsions,” *Sep.*

Purif. Technol., **89**, 78-83 (2012)

Peng, H. and A. Y. Tremblay; "Membrane Regeneration and Filtration Modeling in Treating Oily Wastewaters," *J. Membr. Sci.*, **324**, 59-66 (2008)

Richardson, J. F. and W. N. Zaki; "Sedimentation and Fluidisation: Part I," *Trans. Inst. Chem. Eng.*, **32**, 35-53 (1954)

Rickwood D.; Centrifugation (2nd Edition), A Practical Approach. IRL Press, Oxford, Washington DC (1984)

Ríos, G., C. Pazos and J. Coca; "Destabilization of Cutting Oil Emulsions Using Inorganic Salts as Coagulants," *Colloids Surfaces A: Physicochem. Eng. Aspects*, **138**, 383-389 (1998)

Robinson, C. S.; "Some Factors Influencing Sedimentation," *Ind. Eng. Chem.*, **18**, 869-871 (1926)

Ruth, B. F.; "Studies in Filtration. III. Derivation of General Filtration Equations," *Ind. Eng. Chem.*, **27**, 708-723 (1935)

Ruth, B. F.; "Correlating Filtration Theory with Industrial Practice," *Ind. Eng. Chem.*, **38**, 564-571 (1946)

Sambuichi, M., H. Nakakura and K. Ohsasa; "The Effect of Gravity Settling on Constant Pressure Filtration," *Mem. Fac. Eng., Yamaguchi Univ.*, **33**, 65-70 (1982)

Shannon, M. A., P. W. Bohn, M. Elimelech, J. G. Georgiadis, B. Mariñas and A. M. Mayes; "Science and Technology for Water Purification in the Coming Decades," *Nature*, **452**, 301-310 (2008)

Shields M., R. Ellis and B. R. Saunders; "A Creaming Study of Weakly Flocculated and Depletion Flocculated Oil-in-Water Emulsions," *Colloids and Surfaces A: Physicochem. Eng. Aspects*, **178**, 265-276 (2001)

Shirato, M., M. Sambuichi and S. Okamura; "Filtration Behavior of a Mixture of Two Slurries," *AIChE J.*, **9**, 599-605 (1963)

Shirato, M., T. Aragaki, R. Mori and K. Sawamoto; “Predictions of Constant Pressure and Constant Rate Filtrations Based upon an Approximate Correction for Side Wall Friction in Compression Permeability Cell Data,” *J. Chem. Eng. Japan*, **1**, 86-90 (1968)

Shirato, M., T. Aragaki, R. Mori and K. Imai; “Study on Variable-Pressure-Variable-Rate Filtration,” *Kagoku Kogaku*, **33**, 576-581 (1969)

Shirato, M., T. Murase, E. Iritani and S. Nakatsuka; “Experimental Analysis of Flux Decline Mechanism of Batch Ultrafiltration (Filtration Characteristics of Gel Layer),” *Filtr. Sep.*, **28**, 104-109 (1991)

Smith, T. N.; “The Differential Sedimentation of Particles of Two Different Species,” *Trans. Inst. Chem. Eng.*, **43**, T69-T73 (1965)

Smith, T. N.; “Differential Settling of a Binary Mixture,” *Powder Technol.*, **92**, 171-178 (1997)

Sobisch, T., D. Lerche, T. Detloff, M. Beiser and A. Erk; “Tracing the Centrifugal Separation of Fine-Particle Slurries by Analytical Centrifugation,” *Filtration*, **6**, 313-321 (2006)

Sperry, D. R.; “Notes and Correspondence: A Study of the Fundamental Laws of Filtration Using Plant-Scale Equipment,” *Ind. Eng. Chem.*, **13**, 1163-1164 (1921)

Steinour, H. H.; “Rate of Sedimentation: Nonflocculated Suspensions of Uniform Spheres,” *Ind. Eng. Chem.*, **36**, 618-624 (1944)

Tadros, T., J. Cutler, R. Pons and P. Rossi; “Investigations of the Interaction Between Suspensions and Emulsions (Suspoemulsions),” Modern Aspects of Colloidal Dispersions, R. H. Ottewill and A. R. Rennie eds., pp. 247-256, Kluwer Academic Publishers, Dordrecht, The Netherlands (1998)

Tarleton, S. and R. Wakeman; Solid/Liquid Separation: Equipment Selection and Process Design, pp. 152-164, Elsevier, Amsterdam, The Netherlands (2007)

Tarleton, S. and R. Wakeman; Dictionary of Filtration and Separation, pp.36, Filtration Solutions, Exeter, UK (2008)

Tanaka, T., M. Ueno, Y. Watanabe, T. Kouya, M. Taniguchi and D. R. Lloyd; "Poly(L-lactic acids) Microfiltration Membrane Formation via Thermally Induced Phase Separation with Drying," *J. Chem. Eng. Japan*, **44**, 467-475 (2011)

Tien, C. and B. V. Ramarao; "On Analysis and Modeling of Cross-flow Membrane Filtration of Particle Suspensions," *Curr. Opin. Chem. Eng.*, **2**, 245-254 (2013)

Tiller, F. M.; "The Role of Porosity in Filtration, Part 2: Analytical Equations for Constant Rate Filtration," *Chem. Eng. Prog.*, **51**, 282-290 (1955)

Tiller, F. M.; "The Role of Porosity in Filtration, Part 3: Variable-Pressure-Variable-Rate Filtration," *AIChE J.*, **4**, 170-174 (1958)

Tiller, F. M. and H. Cooper; "The Role of Porosity in Filtration. Part V. Porosity Variation in Filter Cakes," *AIChE J.*, **8**, 445-449 (1962)

Tiller, F. M., N. B. Hsyung and D. Z. Cong; "Role of Porosity in Filtration: XII. Filtration with Sedimentation," *AIChE J.*, **41**, 1153-1164 (1995)

Ullah, A., V. M. Starov, M. Naeem and R. G. Holdich; "Microfiltration of Deforming Oil Droplets on a Slotted Pore Membrane and Sustainable Flux Rates," *J. Membr. Sci.*, **382**, 271-277 (2011)

Ullah, A., R. G. Holdich, M. Naeem and V. M. Starov; "Shear Enhanced Microfiltration and Rejection of Crude Oil Drops through a Slotted Pore Membrane Including Migration Velocities," *J. Membr. Sci.*, **421-422**, 69-74 (2012)

Vorobiev E.; "Derivation of Filtration Equations Incorporating the Effect of Pressure Redistribution on the Cake-Medium Interface: a Constant Pressure Filtration," *Chem. Eng. Sci.*, **61**, 3686-3697 (2006)

Weiland, R. H. and R. R. McPherson; "Accelerated Settling by Addition of Buoyant Particles," *Ind. Eng. Chem. Fundam.*, **18**, 45-49 (1979)

Whitmore, R. L.; "The Sedimentation of Suspensions of Spheres," *Brit. J. Appl. Phys.*, **6**, 239-245 (1955)

Yan, Y. and J. H. Masliyah; "Sedimentation of Solid Particles in Oil-in-Water Emulsions," *Int. J. Multiphase Flow*, **19**, 875-886 (1993)

Yan, N. and J. H. Masliyah; "Creaming Behavior of Solids-Stabilized Oil-in-Water Emulsions," *Ind. Eng. Chem. Res.*, **36**, 1122-1129 (1997)

Yang, T., Z. F. Ma and Q. Y. Yang; "Formation and Performance of Kaolin/MnO_2 Bi-layer Composite Dynamic Membrane for Oily Wastewater Treatment: Effect of Solution Conditions," *Desalination*, **270**, 50-56 (2011)

Zeng, W. P., E. Iritani and T. Murase; "Dynamic Behavior of BSA Cake Layer Deposited on Membrane in Dead-End Inclined Ultrafiltration," *Kagaku Kogaku Ronbunshu*, **24**, 158-160 (1998)

Zhao, Y., Y. Tan, F. S. Wong, A. G. Fane and N. Xu; "Formation of Dynamic Membranes for Oily Water Separation by Crossflow Filtration," *Sep. Purif. Technol.*, **44**, 212-220 (2005)

List of Publications

1. **Cao, D. Q.**, E. Iritani and N. Katagiri; "Evaluation of Filtration Properties in Membrane Filtration of O/W Emulsion Based on Upward Dead-End Constant Pressure Filtration," *Kagaku Kogaku Ronbunshu*, **38**, 378-383 (2012)
2. **Cao, D. Q.**, E. Iritani and N. Katagiri; "Properties of Filter Cake Formed during Dead-End Mirofiltration of O/W Emulsion," *J. Chem. Eng. Japan*, **46**, 593-600 (2013)
3. **Cao, D. Q.**, E. Iritani and N. Katagiri; "Flotation and Sedimentation Properties in Centrifugal Separation of Emulsion-Slurry," *J. Chem. Eng. Japan*, **47**, 392-398 (2014)

International Conferences

1. **Cao, D. Q.**, E. Iritani and N. Katagiri; "Determination of Cake Properties in Membrane Filtration of O/W Emulsion," Proceedings of the 9th World Congress of Chemical Engineering, Seoul (Korea), CD-ROM (2013)

Acknowledgements

I would like to express my special appreciation and thanks to my advisor Professor Dr. Eiji IRITANI, Department of Chemical Engineering, Nagoya University, you have been a tremendous mentor for me. I would like to thank you for encouraging my research and for allowing me to grow as a research scientist. Your advice on both my research as well as on my academic career, particularly for the field of solid-liquid separation, have been priceless.

I would also like to thank Professor Dr. Shinobu KODA, Department of Molecular Design and Engineering, Nagoya University, Professor Dr. Hitoki MATSUDA, Department of Energy Engineering and Science, Nagoya University and Professor Dr. Atsushi SATSUMA, Department of Molecular Design and Engineering, Nagoya University. You have made your valuable time and effort devoted to reviewing the draft carefully, and given me your useful suggestions for my future research.

I would also like to thank Assistant Professor Dr. Nobuyuki KATAGIRI, Department of Chemical Engineering, Nagoya University. I would like to thank you for giving me many suggestions and assistances in many respects, for example, specific experiment and modification of manuscript. In addition, I also want to thank all members in the Laboratory of Separation Process Engineering for their generous help and cooperation.

I would especially like to acknowledge funding from the China State-Sponsored "Post-graduate Study Abroad Program". Just based on the financial support, I am able to whole-heartedly engaged in scientific research and finish my doctoral dissertation.

I would also like to thank Professor emeritus Dr. Kazuhiro FUJISAKI, Kyushu Institute of Technology, Member of KIT Senior Academy. Precisely because of your commendation, I can study abroad in Nagoya University.

A special thanks to my family. Words cannot express how grateful I am to my mother, and father for all of the sacrifices that you've made on my behalf. I would also like to thank all of my friends who supported me in my doctoral studies, and incented me to strive towards my goal.